DRSAR/PE/N-84

PROGRAM ANALYSIS AND EVALUATION DIRECTORATE

ACTIVITIES SUMMARY

VOLUME II

APRIL 1980

Approved for public release; distribution unlimited.

US ARMY ARMAMENT MATERIEL READINESS COMMAND

PROGRAM ANALYSIS AND EVALUATION DIRECTORATE

ROCK ISLAND, ILLINOIS 61299

REPORT DOCUMENTATION PAGE		READ INSTRUCTIONS BEFORE COMPLETING FORM
1. REPORT NUMBER DRSAR/PE/N-84 Vol. II	2. GOVT ACCESSION NO.	3. RECIPIENT'S CATALOG NUMBER
4. TITLE (and Subtitle) Program Analysis and Evaluation Directorate Activities Summary		5. TYPE OF REPORT & PERIOD COVERED Note - Final
		6. PERFORMING ORG. REPORT NUMBER
7. AUTHOR(s)		8. CONTRACT OR GRANT NUMBER(s)
9. PERFORMING ORGANIZATION NAME AND ADDRESS US Army Armament Materiel Readiness Command Program Analysis and Evaluation Directorate Rock Island, IL 61299		10. PROGRAM ELEMENT, PROJECT, TASK AREA & WORK UNIT NUMBERS
11. CONTROLLING OFFICE NAME AND ADDRESS US Army Armament Materiel Readiness Command Program Analysis and Evaluation Directorate Rock Island, IL 61299		12. REPORT DATE April 1980
		13. NUMBER OF PAGES 163
14. MONITORING AGENCY NAME & ADDRESS(if different from Controlling Office)		15. SECURITY CLASS. (of this report) UNCLASSIFIED
		15a. DECLASSIFICATION/DOWNGRADING SCHEDULE

16. DISTRIBUTION STATEMENT (of this Report)

Approved for public release; distribution unlimited

17. DISTRIBUTION STATEMENT (of the abstract entered in Block 20, if different from Report)

18. SUPPLEMENTARY NOTES
Additions or deletions to/from DISTRIBUTION LIST are invited and should be forwarded to address below. Inquiries pertinent to specific items of interest may be forwarded to Commander, USA Armament Materiel Readiness Command, ATTN: DRSAR-PE, Rock Island, IL 61299, AUTOVON 793-5075/5930.

19. KEY WORDS (Continue on reverse side if necessary and identify by block number)

Data reduction	M110A2 SP howitzer	M509E1 projectile
Digital filtering	Interior ballistics	Cannon damage
Robust statistics	Propelling charge	Projectile damage
Signal processing	Temperature sensitivity	Projectile fallback
Rotary potentiometers	Artillery	M106 projectile (See reverse side)

20. ABSTRACT (Continue on reverse side if necessary and identify by block number)
This report contains five Memoranda for Record (MFRs) representing some of the activities of the Program Analysis and Evaluation Directorate, US Army Armament Materiel Readiness Command, Rock Island, IL 61299. Subjects dealt with are the systems analysis of cannon damage in the M110/M110A1 systems and an approximation for the standard cumulative production cost using learning theory.

DD FORM 1473 EDITION OF 1 NOV 65 IS OBSOLETE
1 JAN 73

19. Key Words:

M650 projectile
M422 projectile
8-inch ammunition
Production cost
Learning theory
Wholesale logistics

TABLE OF CONTENTS

<u>Memorandum for Record</u>

METHODS FOR PROCESSING SIGNALS

FROM ROTARY POTENTIOMETERS

WITH APPLICATION TO THE

REDUCTION OF M110A2 LOADER-RAMMER

TEST DATA

George Schlenker

Lanny Wells

5

MEMORANDUM FOR RECORD

SUBJECT: Methods for Processing Signals from Rotary Potentiometers with
          Application to the Reduction of M110A2 Loader-Rammer Test Data

1. Reference:

    a. MFR, DRSAR-PEL, 29 Aug 79, subject: Observations Concerning the
M110A1 Loader-Rammer Performance Test at YPG, Aug 79.

    b. Article appearing in the Journal of Geophysical Research, Vol 77,
No. 36 by W. D. Hibler III, 20 Dec 72, title: Removal of Aircraft Alti-
tude Variation from Laser Profiles of the Arctic Ice Pack.

2. Background

    The work reported in this memorandum completes one task in a project
associated with a problem experienced by the M110A2 SP howitzer system.
Cannon damage reported after fielding the M110A2 in Europe in 1978 was
found to be associated with firing the M106 projectile from an unseated
position. Some projectiles had apparently been improperly rammed and had
fallen back upon the propelling charge when the gun tube was elevated.
Because the loader-rammer (L/R) was implicated in this problem, a series
of tests were devised to explore the limits of rammer function. Certain
proposals to improve the standard loader-rammer were submitted and as a
consequence, the scope of the loader-rammer tests was expanded in order
to compare the performance of the standard configuration with the pro-
posed modification. Tests have been conducted at Yuma Proving Ground
(YPG), as reported in Reference a. An additional L/R test program was
conducted at Jefferson Proving Ground (JPG) during August 1979 using a
different M110A2 weapon. This test was considerably more modest in scope
than the Yuma tests, having been intended as a corroborative test. The
JPG tests measured only displacement of the rammer head using a rotary
potentiometer (pot) attached to the axle of the chain sprocket. From
these data it was desired to derive velocity and acceleration of the
rammer as functions of time. The velocity functions for different experi-
mental systems (or treatments) would then be compared to identify differ-
ential effects.

DRSAR-PEL
13 November 1979
SUBJECT: Methods for Processing Signals from Rotary Potentiometers with
Application to the Reduction of M110A2 Loader-Rammer Test Data

3. In practice, however, rotary potentiometer signals contain spurious
noise and end-of-cycle non-linearity. Additionally, the displacement
cycles must be smoothly pieced together, i.e., "stacked", to yield a
continuous displacement function which can be differentiated. These
effects[1] (and some others) pose analytic difficulties which must be
addressed to obtain meaningful velocity functions.

4. Purpose

There are two principal purposes in writing this MFR: to set down
the lessons learned from trying various methods of analysis and to indi-
cate what differences appear in the velocity functions estimated for
various experimental systems run at JPG. Relative to the first purpose,
the authors would be gratified if some of the techniques used in the
present analysis were applied or refined in future analyses by others
confronted with similar problems.

5. Organization

The remainder of this memorandum is organized as follows: Data reduc-
tion problems and methods of treatment are contained under Methodology.
Results of applying these methods to the present problem are presented
under Results, where some of the lessons are illustrated. Finally, the
methodological conclusions and specific inferences for the JPG loader-
rammer data are presented under Conclusions. For the reader who is not
interested in supporting evidence the final section may alone serve as
an adequate summary.

6. Methodology

The displacement of the rammer head as measured by the rotary poten-
tiometer is divided into cycles each of which represents one rotation of
the pot. The potentiometer signal rises to a maximum voltage and then
abruptly falls to its minimum value at the end of a cycle. However,
experience indicates that the potentiometer has a finite resolution.
This causes non-linearity and uncertainty in voltage at the beginning
and end of each cycle and produces a finite fall time in passing from

---

(1) In view of all of the problems encountered in obtaining a valid velo-
city function from rotary pot signals, one may ask why not use an alterna-
tive type of instrument such as a tachometer? In the present case, the
authors did not have a choice of instruments and had to use the available
data.

DRSAR-PEL   13 November 1979
SUBJECT: Methods for Processing Signals from Rotary Potentiometers with
           Application to the Reduction of M110A2 Loader-Rammer Test Data

max to min values. Generally also, the voltage swing corresponding to
one rotation of the pot is not known precisely but must be estimated from
the noisy output signal. To obtain a displacement signal one must scan
the (analog) record for max and min values -- y_{max} and y_{min} -- or some
average max and min over cycles -- $\bar{y}_{max}$ and $\bar{y}_{min}$ -- and obtain a scale
factor of displacement per volt by dividing the cycle length (24 inches
in the present case) by the voltage swing $(\bar{y}_{max} - \bar{y}_{min})$. This scheme
is implemented in the computer program provided in Annex 2.

7.   Processing of the signals will generally be performed on a digital
computer, so that an analog-to-digital (A to D) conversion of the pot
signals is required. Our experience indicates that this operation is
also a source of noise. In fact, A to D conversion seems to yield quan-
tization of the signal in which certain "favorite" numbers repeatedly
appear. Ways to minimize this effect include recording at a maximal
signal level and time sampling at a high data rate. This rate may be
limited by the available high-speed data storage but should be at least
20 times the highest significant[*] frequency seen in the signal. For
example, our analog pot signals were time-sampled at 500 hertz (2 ms
intervals) since an upper frequency limit of 25 hertz was expected. Pre-
sent experience indicates that filtering the analog signal with a 100
hertz pass band before digitizing creates more problems than it solves.
This type of filtering exaggerates the non-linearity in the end-of-cycle
pot signal and leads to stacking difficulty.

8.   To obtain a stacked displacement signal which is sufficiently smooth
to tolerate a differencing procedure requires some digital filtering.
Two types of non-recursive filters were tried -- a symmetric moving
average and a filter having exceptional discrimination and low ripple
outside the passband. The latter was designed by a method devised by
W. D. Hibler (Reference b). The modulus and squared modulus of the
transfer function of these filters are shown in Figures 1 through 4 of
Annex 1. In spite of the theoretical advantage of Hibler's filter, it
did not prove to be as satisfactory in this application as a simple sym-
metric moving average. Consequently, the results displayed in the figures
of Annex 1 were generated using a symmetric moving average filter having
a maximum absolute lag of 25. With a sampling period of 2 ms, this moving-
average filter has a resolution bandwidth of 10 hz (equivalently, an aver-
aging period of 0.1 sec). An averaging period of about 0.1 sec is required

---

[*]   At the -20 db level.

9

DRSAR-PEL   13 November 1979
SUBJECT: Methods for Processing Signals from Rotary Potentiometers with
          Application to the Reduction of M110A2 Loader-Rammer Test Data

to achieve the proper degree of smoothing of the displacement judged necessary for this application.

9. When successive potentiometer cycles are stacked by adding the previous cumulative full-cycle value to the pot reading, small discontinuities appear at the ends of cycles. To eliminate these and other outliers from the displacement record it was desirable to use an outlier detecting and purging algorithm. Simply relying on filtering to reduce the effect of these outliers was not practical. The outlier-detecting procedure works as follows: First, the unmodified, stacked displacement signal is fitted with a (6th degree) polynomial function of time using multiple linear regression. The standard error of the estimate from this regression is then used as a measure of discrepancy of a data point from the trend. Data points which are more than about three standard errors from the fitted function were replaced by the value of the fitted function. Finally, the moving average was calculated to attenuate the pot noise. Actually, expurgation of outliers and filtering can occur in the same DO-loop of a computer program as was done in the program in Annex 2.

10. Having obtained a suitably smooth displacement function, velocity is estimated using a first-order central-difference approximation:

$$dy_i/dt \cong (y_{i+1} - y_{i-1})/2h,$$

with time step h.
Although the values of y_i above may be moving-average displacements, the differencing operation produces high-frequency noise which may be distracting to the person who examines this unsmoothed velocity estimate. Consequently, we have found it convenient to smooth the above estimate by passing the unsmoothed velocity through a digital filter whose passband somewhat exceeds that of the moving-average filter which was applied to the displacement signal. In the present application, a non-recursive filter with a max lag of 6 was used for this purpose.

11. Another, completely different approach to estimating velocity and acceleration was used and found to produce valid results if properly restricted. This approach is referred to as analytic since the velocity and acceleration can be represented analytically as polynomial functions of time. In our algorithm the moving-average displacement is fitted with a sixth degree polynomial. (A fifth degree polynomial works almost as well.) This function is, of course, analytically differentiable yielding a fourth degree polynomial estimate of acceleration. Both velocity and acceleration estimates which are derived in this manner are displayed among the results in Annex 1. Clearly, analytic estimates may be rather gross if the domain of the fitted function is too large or if time derivatives beyond the sixth are numerically significant anywhere over the domain.

DRSAR-PEL   13 November 1979
SUBJECT: Methods for Processing Signals from Rotary Potentiometers with
           Application to the Reduction of M110A2 Loader-Rammer Test Data

12. Results

The results of this study are presented in the form of plots of output from the computer program. The same types of graphs are given for each of 24 rammer tests. The sequence of the plots is as follows:

(a) Raw potentiometer signal (a function of time);

(b) Displacement signal produced by stacking the pot signal, purging and replacing outliers and scaling;

(c) Analytic estimate of velocity using the 6th degree polynomial fit to the displacement data in (b);

(d) Analytic estimate of acceleration;

(e) Unsmoothed estimate of velocity obtained by differencing the moving average displacement;

(f) Smoothed velocity estimate; from (e);

(g) Crossplot of the smoothed velocity versus the analytic estimate of displacement.

The last estimate was the most useful in comparing the results from different rams since it is independent of time zero which generally varied between rams. The sequence of graphs proceeds from the <u>bottom</u> <u>to</u> the <u>top</u> of each page through all ram numbers without a page break.

13. A description of the experimental systems tested is provided in Table 1. Table 1 also summarizes the average (AVG) and standard deviation (SD) of the ram speed obtained in the last full cycle of rotary pot motion. The first 10 rams were conducted using the M2A2 cannon, i.e., an M110 howitzer configuration. The remaining 14 rams were conducted in the M110A2 howitzer using an M201 cannon. Because of the difference in cannons the total travel of the rammer head is 85 inches in the M110 and about 93 inches in the M110A2. Due to this difference the same rammer produces a somewhat differently shaped velocity function in the two systems. This difference is quantified in the <u>Conclusions</u>. The standard loader-rammer (L/R STD) was used for the first five rams and the modified configuration (L/R MOD) for the next five. As noted in Table 1, both L/R configurations were also tested with the M201 cannon. For each of these configurations testing was done at maximum

DRSAR-PEL   13 November 1979
SUBJECT: Methods for Processing Signals from Rotary Potentiometers with
          Application to the Reduction of M110A2 Loader-Rammer Test Data

acceptable L/R system pressure (5 rams each) and at minimum acceptable
L/R system pressure (2 rams each). Although velocity differences between
L/R configurations in the M110A2 are slight, the effect of L/R system
pressure on velocity is noticeable. A reduction in the ram speed near
end-of-travel of from 0.4 to 1.0 f/s accompanies the noted pressure reduction.

14. The data set obtained from digitizing the analog rotary pot signal for
a typical ram consists of approximately 600 points. Sets of this size per-
mit data processing of the sort described above while retaining an adequately
large value of degrees of freedom. Of course, the use of a non-recursive
filter shortens the unfiltered data set at each end by the value of the
maximum lag used in the filter. Thus, in this application 25 data points
were eliminated from each end of the displacement data to obtain the moving
average displacement.

15. The first twenty figures in Annex 1 are intended to illustrate the
effect of various errors associated with the data and with the processing
methods. These illustrations support previous claims of lessons learned
and give the reader some "feel" for the problems encountered in using data
from rotary potentiometers. Starting with Rammer Test No 1 shown in Fig
5, one can observe the kind of stacking error typically encountered in pro-
cessing the pot signal. Without identifying and purging the resulting out-
liers from the displacement signal (Fig. 5) a characteristic set of spikes
is produced in the unsmoothed velocity estimate (Fig. 7). Even after smooth-
ing the velocity, anomalous bumps (reduced spikes) are seen in the velocity-
time plot (Fig. 8) and velocity-displacement plot (Fig. 9). One can also
see the effect on velocity of potentiometer non-linearity -- the 0.1 sec
shallow waves appearing in the velocity after level off.

16. Figure 10 illustrates another approach to filtering the displacement
signal prior to differencing to obtain velocity. The Hibler filter, describ-
ed earlier, was applied to the unexpurgated displacement (Fig. 5) and differ-
enced to yield the unfiltered velocity shown in Figure 10. Because of the
sharp frequency-domain cutoff and low ripple in the stop band, one would
expect the Hibler filter to perform better than a simple moving average.
However, the smoothed velocity estimate (Fig. 11) is not subjectively better
than its moving-average counterpart (Fig. 9). Further reduction of the
cutoff frequency of the filter would improve smoothness and reduce the
effect of spurious spikes in the displacement but would lack resolution and
introduce velocity bias. A better strategy for data reduction is to prepro-
cess the unfiltered displacement to detect and purge outliers. This proce-
dure does not sacrifice resolution bandwidth as does narrow-passband filter-
ing. See Figure 19 for a better estimate using data from ram test number 1.

DRSAR-PEL   13 November 1979
SUBJECT: Methods for Processing Signals from Rotary Potentiometers with
           Application to the Reduction of M110A2 Loader-Rammer Test Data

Figure 12 also illustrates the effect of smoothing with Hibler's filter --
in this case on the data from ram number 2. Here also, one may conclude
that the velocity estimated from differencing the filtered displacement
is not better than simply using a moving average on the expurgated data.
See Figure 29 for comparison.

17.   A surprising thing happened to the data for several rams: An A to
D transcription and/or tape copying error caused intervals of data to be
omitted in the final (digital) record. Figure 13 illustrates this incident
in the pot signal for ram test number 5 and Figure 14 indicates the result-
ing error in the expurgated displacement. Evidently the outlier-detecting
algorithm cannot cope with this kind of error. The consequence of this
error is serious as can be seen in Figures 15 and 16. In this case some
manual editing of the data was necessary before reprocessing (Figs. 43 and
44).

18.   One additional type of error is noteworthy -- inclusion of too many
pre-ram and post-ram data points in the displacement record. If a long
post-ram plateau occurs, as in Figure 23, the analytic velocity estimate
(Fig. 24) will be quite poor. The sixth-degree-polynomial fit becomes
inadequate if the domain is not properly bounded. By contrast, a displace-
ment record having a truncated plateau (Fig. 25) yields an excellent velo-
city estimate (Fig. 26) and a reasonable acceleration function (Fig. 27).
No attempt was made to rectify the analytic estimate of acceleration out-
side of its applicable domain.

19.   One is able to observe specific differences in the ram velocity func-
tions between different experimental systems (treatments) even when the
data contain the imperfections described here. One reason for this discrim-
ination is the consistent manner with which stacking error and filtering
bias enter the velocity estimated from run to run. These velocity differ-
ences in the JPG data are discussed under Conclusions.

20. Conclusions

    Conclusions are summarized here under two categories: general metho-
dological observations and specific inferences about the M110/M110A2 L/R
tests at JPG. Relative to methods for analyzing rotary potentiometer
signals:

    (1) It is best to stack digitized rotary potentiometer signals which
have an abrupt drop from max to min values. Therefore, a broad-band analog
signal is a desirable starting point since this affords the most abrupt drop.

DRSAR-PEL
SUBJECT: Methods for Processing Signals from Rotary Potentiometers with
          Application to the Reduction of M110A2 Loader-Rammer Test Data

13 November 1979

(2) Some stacking error appears to be unavoidable. Therefore, it is
essential to process the stacked displacement signal with an outlier-detect-
ing and purging algorithm. As a minimum, such an algorithm should obtain
departures from a global average, as was done here by polynomial regression.

(3) Occasional analog-to-digital encoding errors and digital data
omissions occur. Therefore, it is important to display the digitized
potentiometer signal graphically to assist in detecting this type of
error. In this case manual editing of the data is necessary.

(4) Elimination of stacking and encoding errors solely by high-
discrimination digital filters (such as Hibler's) seems to be impractical,
since a sufficiently narrow filter frequency passband (or long period) to
reduce the effect of the errors in the output signal would incur an objec-
tionable degree of bias.

(5) Although somewhat cosmetic, applying a digital filter to the
velocity signal to smooth it is recommended. To avoid additional bias
the passband of this filter should be larger than that applied to the
displacement signal used to develop the velocity estimate.

(6) If a gross-average velocity estimate is desired, one can obtain
a good analytic approximation from a high-degree polynomial in time fitted
to the displacement data over a restricted domain of this function. Do
not expect this analytic velocity estimate to hold outside of this limited
domain.

(7) Because of the generally arbitrary nature of time zero and be-
cause of temporal shifts due to filtering, it is recommended that compari-
sons of two distinct runs be made in phase space, i.e., via a crossplot
of velocity vs displacement.

(8) In making phase-space plots it is desirable to use a highly
smoothed estimate of displacement, e.g., by using regression, so as not
to incur anomalous multi-point function incidents.

21. With respect to the results of the M110/M110A2 L/R tests at JPG:

(1) The form of the velocity versus displacement plots are nearly
identical for repeated rams with a specific experimental system -- cannon
type, L/R type, and L/R system pressure.

(2) Differences in these plots appear between experimental systems in
two respects: the max velocity level achieved and the displacement at
which a given level is achieved.

DRSAR-PEL   13 November 1979
SUBJECT: Methods for Processing Signals from Rotary Potentiometers with
          Application to the Reduction of M110A2 Loader-Rammer Test Data

(3) During the first ten ramming tests using the M2A2 cannon at max
L/R pressure, rams 1 through 5 apply to the L/R STD configuration and rams
6 through 10 to the L/R MOD. The former generally achieve a slightly higher
peak velocity than the latter. Another distinction in these tests is in
the shape of the velocity function. The velocity of L/R STD exhibits a
somewhat more convex (hump-backed) shape than that of the L/R MOD.

(4) The shape of the velocity function which characterizes rams 1
through 5 also differs from that of rams 11 through 15. The latter set
has a decidedly sway-back shape with a shallow dip in the velocity at
midram. Additionally, a somewhat shorter rise to peak velocity is noted
in the latter set. The difference in experimental system in these sets is
simply a difference in cannon type; the M2A2 cannon was used in rams 1
through 5 whereas the M201 cannon was used in rams 11 through 15. Apparent-
ly, the standard rammer tends to increase its speed slightly at the longer
travel experienced in the M201 cannon -- 93 inches versus 85 inches in the
M2A2 cannon.

(5) A reduction in the L/R system pressure from max to min acceptable
under otherwise identical conditions causes a reduction in peak ramming
speed. This reduction is anticipated because the level-off speed is con-
trolled by a restricted flow of oil under a pressure differential which is
nearly constant throughout a ram cycle. In the L/R STD configuration this
speed reduction amounted to only about 0.4 f/s based upon the average over
the last complete pot cycle and about 1 f/s based upon the difference in
maxima (rams 11 through 15 vs 16 and 17) whereas in the L/R MOD configura-
tion this reduction was about 1 f/s (rams 18 through 22 vs 23 and 24).
For both configurations the shape of the velocity curve in phase space was
not altered by the reduction in L/R system pressure.

2 Incl   GEORGE SCHLENKER
1. Annex 1   Operations Research Analyst
2. Annex 2

                                      LANNY WELLS
                                      Operations Research Analyst

A N N E X 1

RESULTS FROM M110/M110A2 LOADER-RAMMER TESTS AT JEFFERSON PROVING GROUND, AUGUST 1979

Incl 1

TABLE 1. AVERAGE FINAL[1] RAMMING SPEED
FOR THE M110A2 LOADER-RAMMER
OBTAINED IN THE JPG TESTS, 11 AUG 79

ROUND NUMBER	SPEED (F/S)	COMMENTS
1	9.98	M2A2 Cannon
2	9.90	L/R STD[2]
3	9.80	System Pressure Max[3]
4	9.76	
5	9.85	
AVG/SD	9.858/0.086	
6	9.55	M2A2 Cannon
7	9.44	L/R MOD[2]
8	9.44	System Pressure Max[3]
9	9.41	
10	9.45	
AVG/SD	9.458/0.054	
11	9.70	M201 Cannon
12	9.59	L/R STD[2]
13	9.58	System Pressure Max[3]
14	9.66	
15	9.44	
AVG/SD	9.594/0.099	
16	9.50	System Pressure Min[3]
17	9.28	
AVG/SD	9.39/0.156	
18	9.68	M201 Cannon
19	9.89	L/R MOD[2]
20	9.80	System Pressure Max[3]
21	9.79	
22	9.67	
AVG/SD	9.766/0.092	
23	8.65	System Pressure Min[3]
24	8.84	
AVG/SD	8.745/0.134	

Notes:
(1) The "final" ramming speed was calculated as the average over the last complete rotary pot cycle.
(2) Two loader-rammer configurations were tested -- the current standard (L/R STD) and a proposed modification (L/R MOD).
(3) The pressure in the oil or nitrogen of the loader-rammer system was adjusted prior to each ram using the gage provided with the system.

FIGURE 1. MODULUS OF THE TRANSFER FUNCTION OF A
SYMMETRIC MOVING AVERAGE DIGITAL FILTER
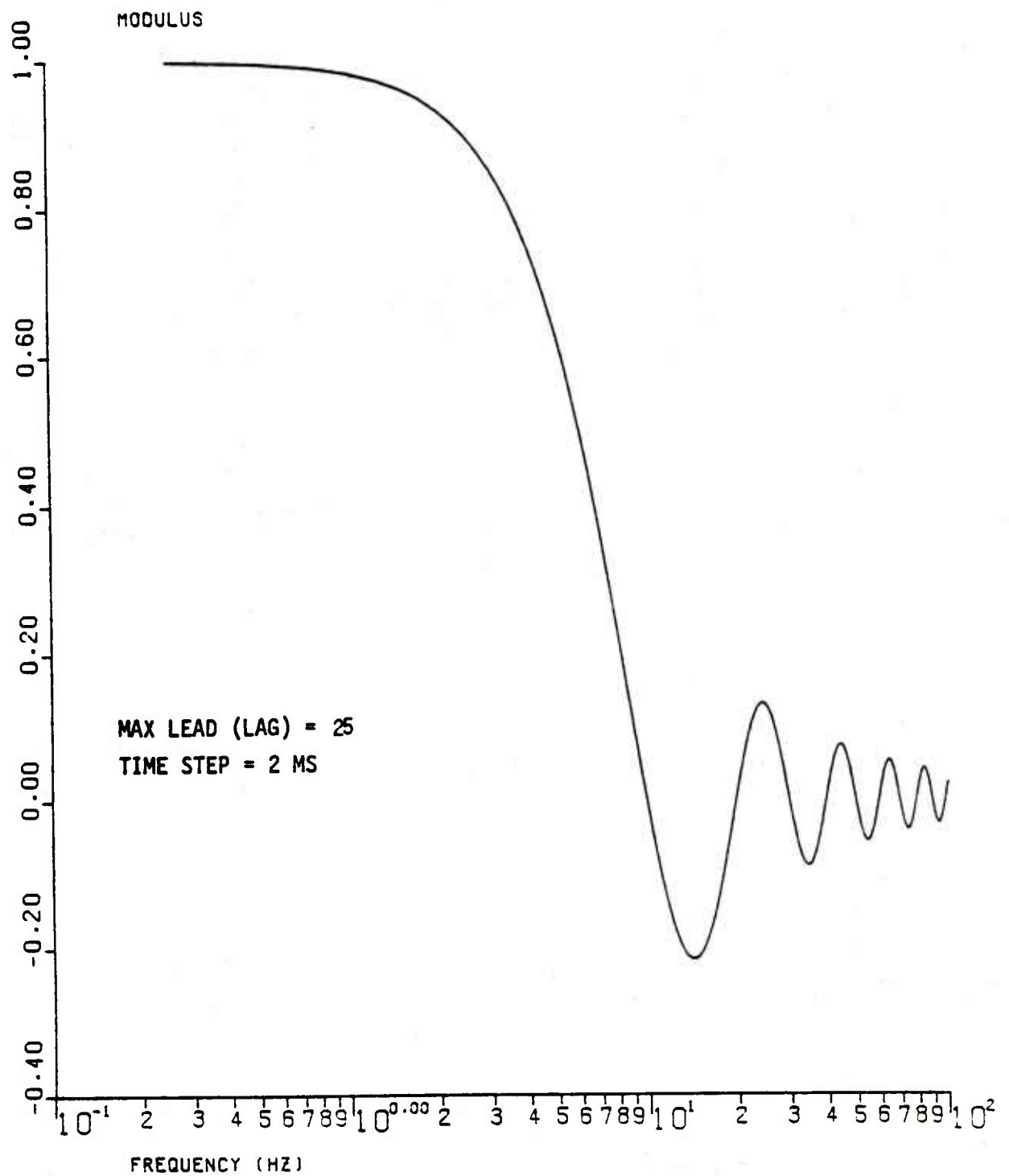
FIGURE 2.   SQUARED MODULUS OF THE TRANSFER
             FUNCTION OF A SYMMETRIC MOVING
             AVERAGE DIGITAL FILTER

21

FIGURE 3.   MODULUS OF THE TRANSFER FUNCTION
OF A SYMMETRIC NONRECURSIVE DIGITAL
FILTER USING HIBLER'S METHOD

MODULUS

PARAMETERS:
MAX LEAD (LAG) = 50
PASS BAND = 5 HZ
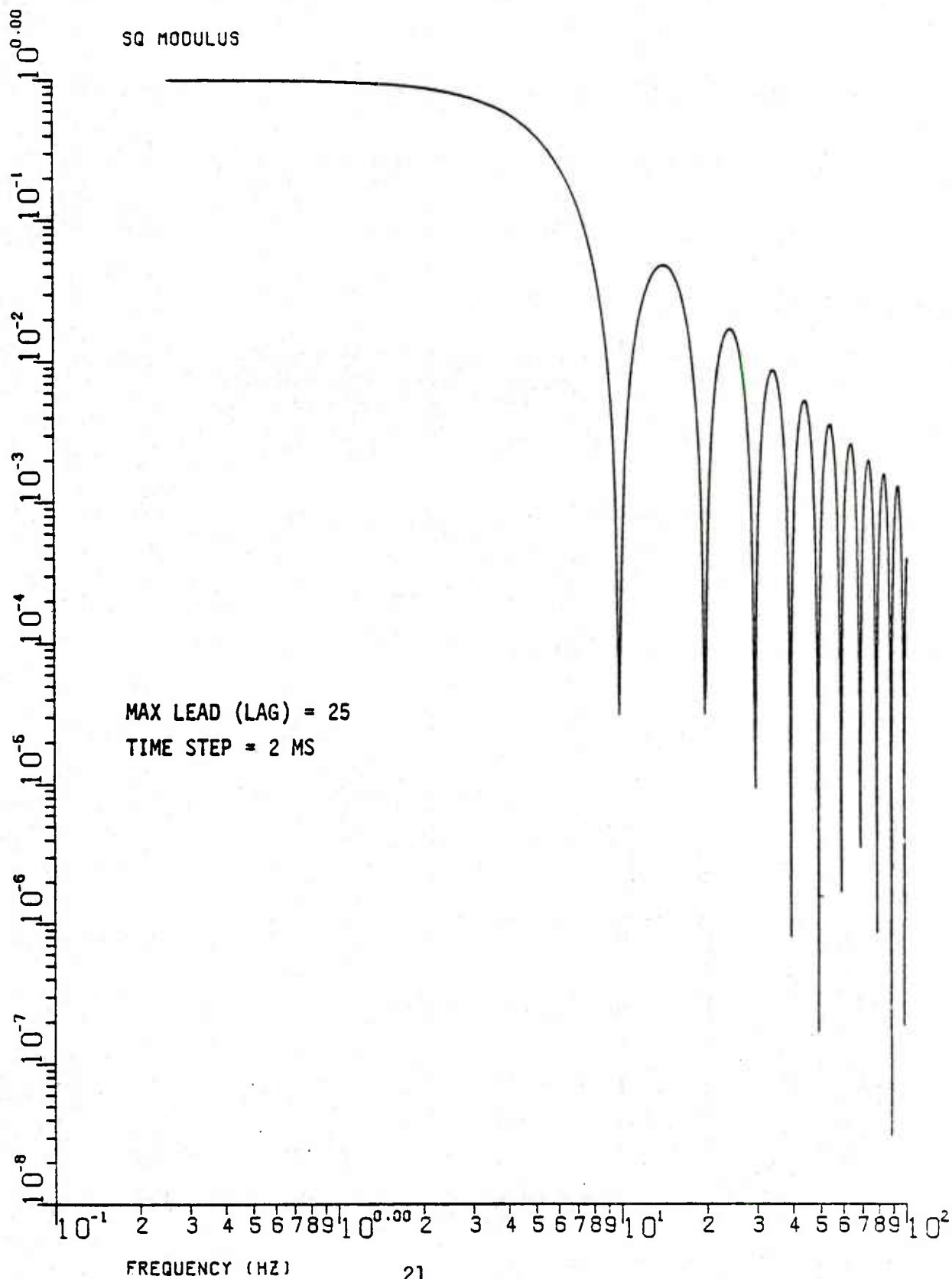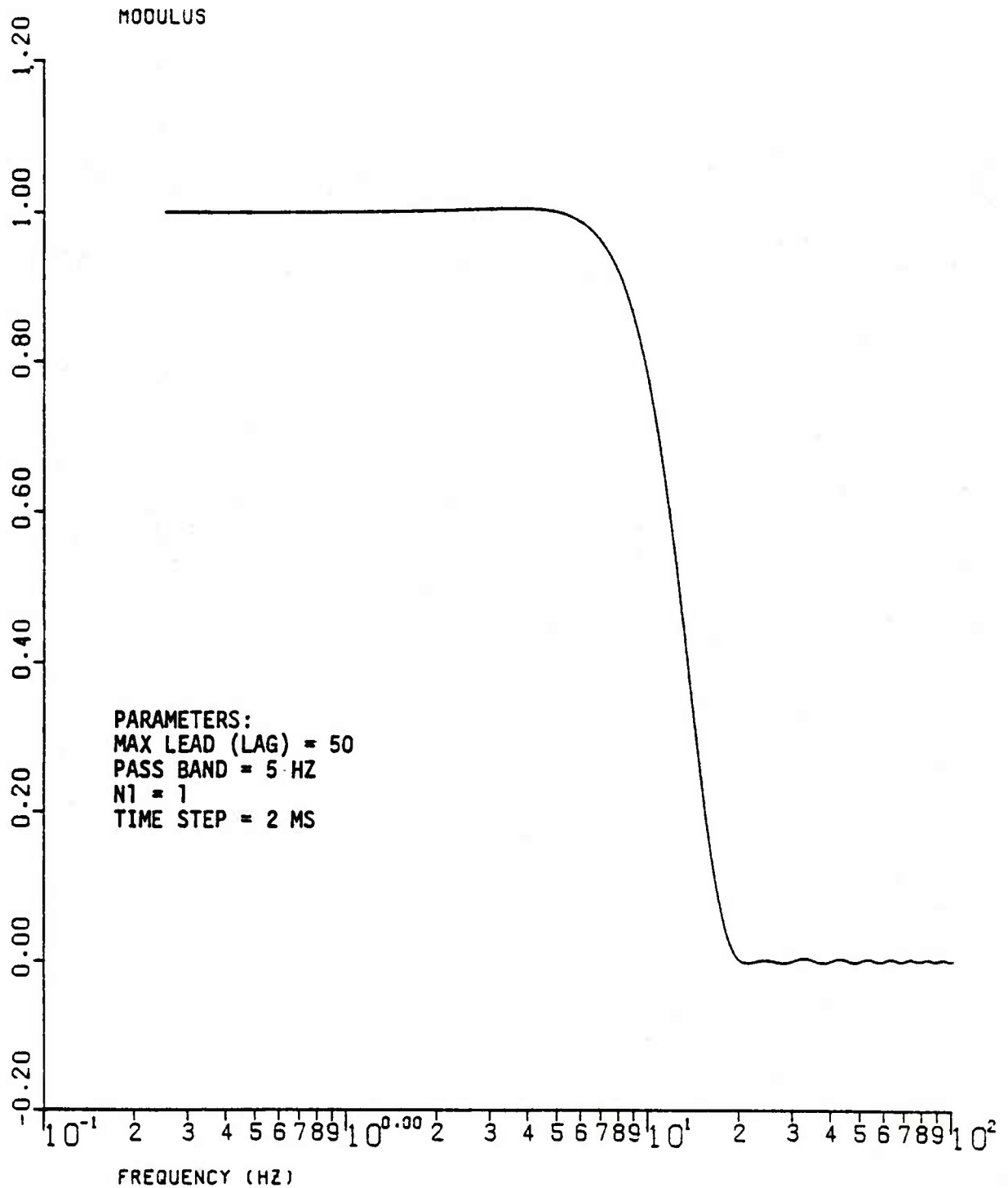N1 = 1
TIME STEP = 2 MS

FREQUENCY (HZ)

FIGURE 4.   SQUARED MODULUS OF THE TRANSFER
SQ MODULUS   FUNCTION OF A SYMMETRIC NONRECURSIVE
DIGITAL FILTER USING HIBLER'S METHOD

PARAMETERS:
MAX LEAD (LAG) = 50
PASS BAND = 5 HZ
N1 = 1
TIME STEP = 2 MS

FREQUENCY (HZ)   23

RAMMER TEST 01 AT J.P.G.   FIGURE 5.

Illustration of one type of
stacking error obtained for the
rotary potentiometer signal given
below. The outlier identification
and replacement technique was not
performed here.

TIME (SEC)

RAMMER TEST 01 AT J.P.G.   FIGURE 6.

Analog rotary potentiometer signal is digitized at a 500 hz rate.
Digital signal is displayed here.

TIME (SEC)

24
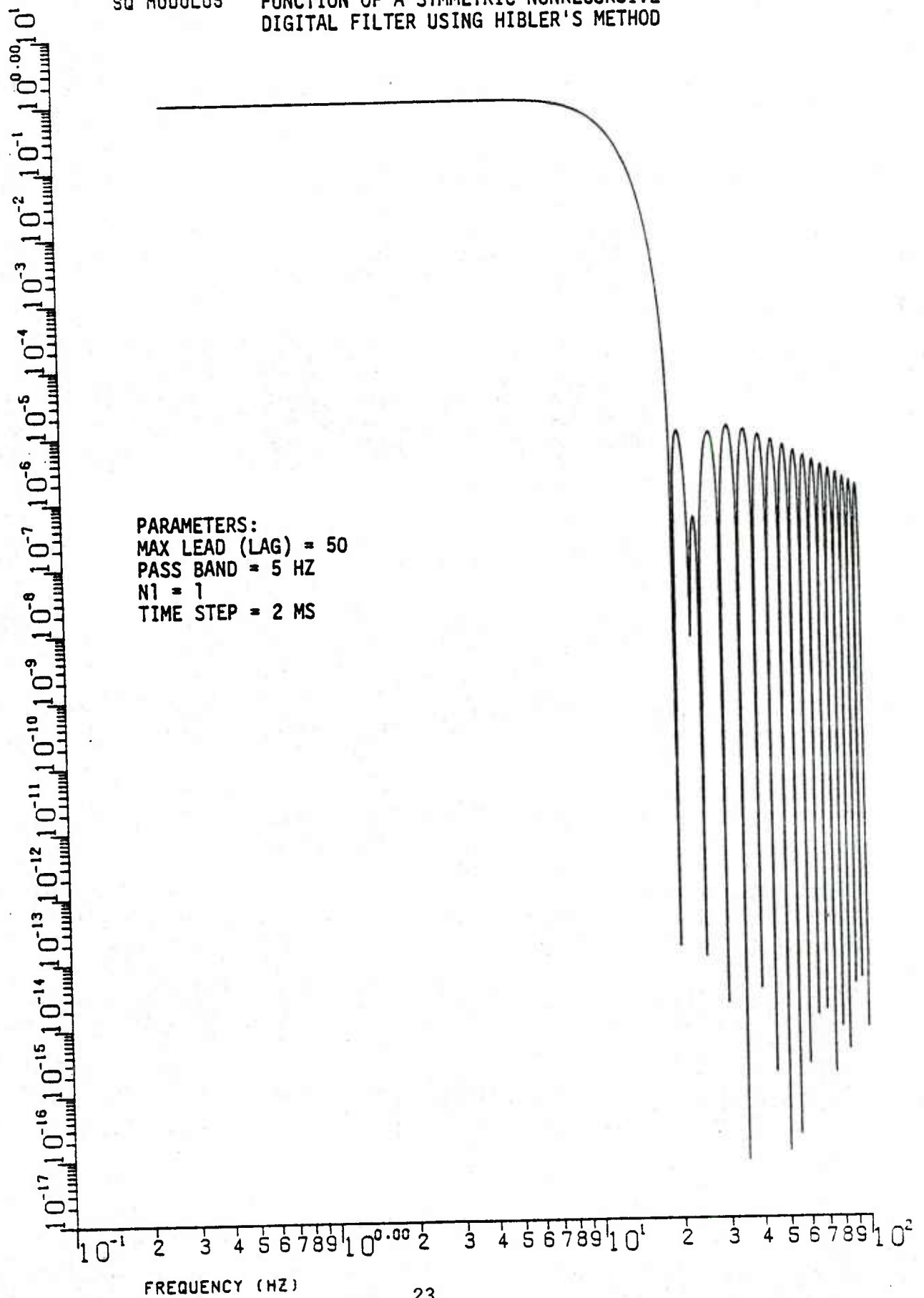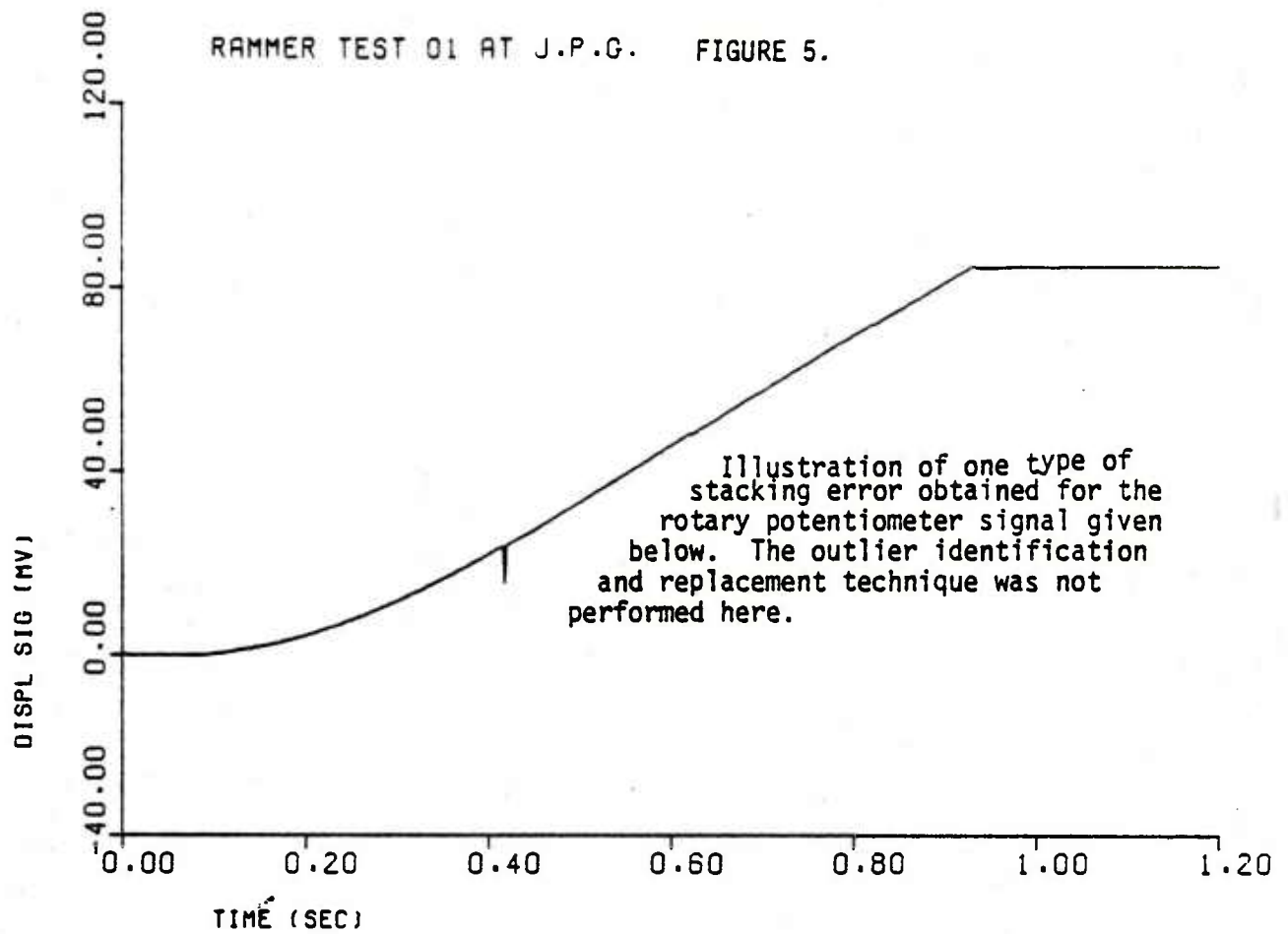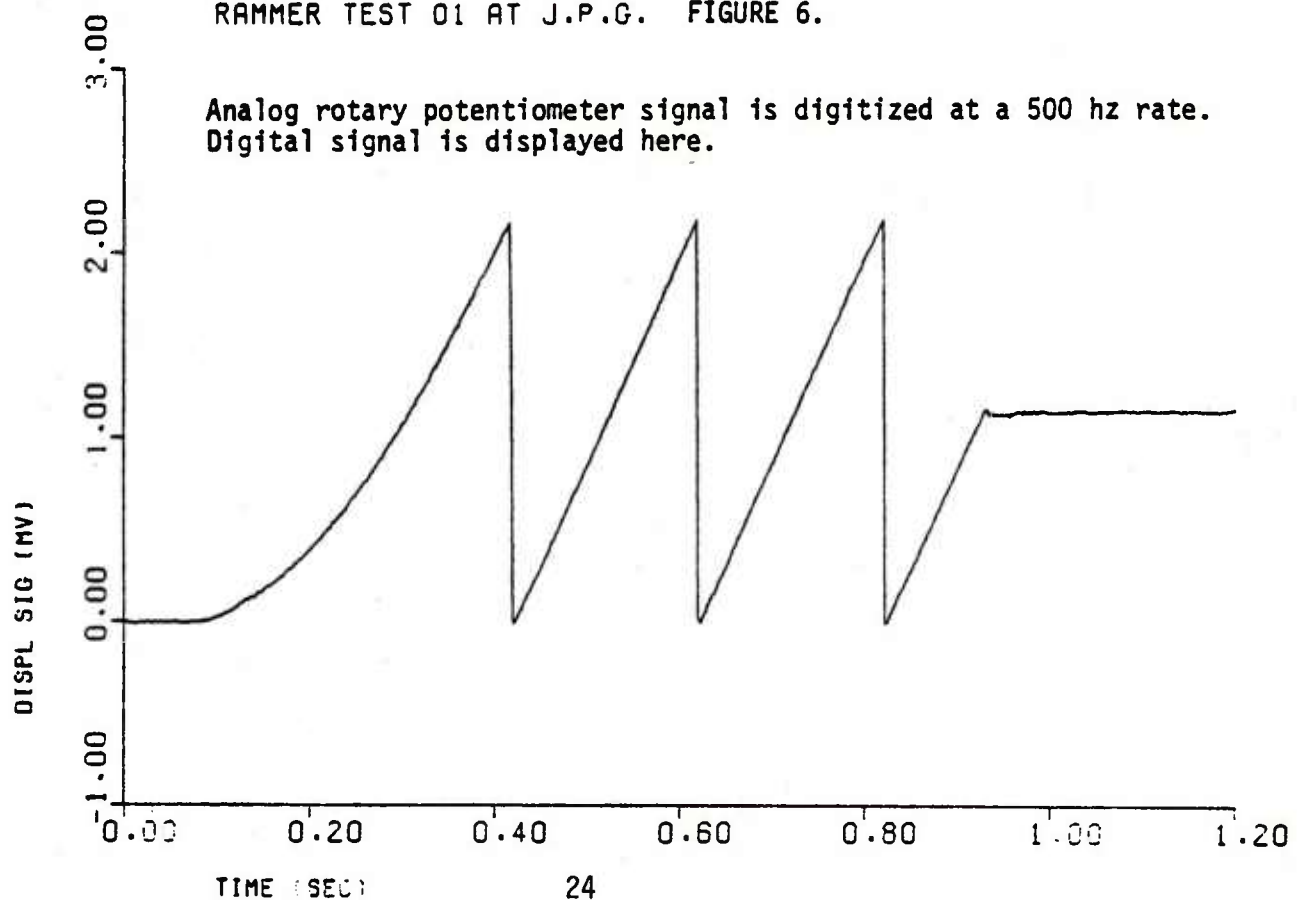
RAM EP TEST 01 AT J.P.G.   FIGURE 7.

Velocity estimate obtained from the
moving-average displacement record
having the stacking error. Anomolous
spikes appear at the ends of the moving
average window.

VEL. (F/S)

TIME (SEC)

RAMMER TEST 01 AT J.P.G.

VOID.   PLEASE DISREGARD.

ACC (F/S/S)

TIME (SEC)

25

RAMMER TEST 01 AT J.P.G.   FIGURE 9.

Smoothed velocity vs displacement
plot showing the effect of the ori-
ginal stacking error.

VEL (F/S)

DISPL (IN)

RAMMER TEST 01 AT J.P.G.   FIGURE 8.

Smoothed velocity vs time
plot showing the residual
effect of the original
stacking error.

VEL (F/S)

TIME (SEC)

26

RAMMER TEST 01 AT J.P.G. FIGURE 11.

Velocity estimate is
the smoothed version
of that given below.

TIME (SEC)

RAMMER TEST 01 AT J.P.G. FIGURE 10.

Unsmoothed velocity estimate
is obtained from a signal
generated by using Hibler's
filter (with 5 hz passband)
on the stacked potentiometer
data.

TIME (SEC)

27

RAMMER TEST 02 AT J.P.G. FIGURE 12.

Unsmoothed velocity estimate
is obtained from a signal
generated by using Hibler's
filter (with 5 hz passband)
on the stacked potentiometer
data.

VEL. (F/S)

TIME (SEC)

RAMMER TEST 02 AT J.P.G.

VOID. PLEASE IGNORE.

ACC (F/S/S)

TIME (SEC)

28

RAMMER TEST 05 AT J.P.G.   FIGURE 14.

Illustration of the
performance of the algorithms
for stacking and detecting and
eliminating outliers. Note the
effect of missing data at 0.55 sec.

DISPL SIG (MV)

120.00   80.00   40.00   0.00   -40.00

0.00   0.20   0.40   0.60   0.80   1.00   1.20

TIME (SEC)

RAMMER TEST 05 AT J.P.G.   FIGURE 13.

Missing rotary potentiometer data at 0.55 sec caused by
A to D plus transcription error.

DISPL SIG (MV)

3.00   2.00   1.00   0.00   -1.00

0.00   0.20   0.40   0.60   0.80   1.00   1.20

TIME (SEC)

29

RAMMER TEST 05 AT J.P.G.   FIGURE 16.

Illustration of the
effect of missing data
on the smoothed velocity
estimate.

VEL (F/S)

TIME (SEC)

RAMMER TEST 05 AT J.P.G.   FIGURE 15.

Illustration of the
effect of missing data
on the velocity estimated
from a moving average
displacement signal.

VEL (F/S)

TIME (SEC)

30

RAMMER TEST 01 AT J.P.G.   FIGURE 18.

Illustration of the
stacked rotary potentio-
meter signal (displacement)
after automatic identification
and deletion of outliers.

RAMMER TEST 01 AT J.P.G.   FIGURE 17.
Note that the decay to zero level occurs with finite slope.

31

RAMMER TEST 01 AT J.P.G.   FIGURE 20.

Smoothed version of the
velocity-time curve given
below.   Smoothing is done
with a symmetric non-recursive
filter having 25 hz cutoff.

VEL. (F/S)

TIME (SEC)

RAMMER TEST 01 AT J.P.G.   FIGURE 19.

Velocity estimate obtained
from first-central-difference
approximation applied to moving
average displacement signal.

VEL. (F/S)

TIME (SEC)   32
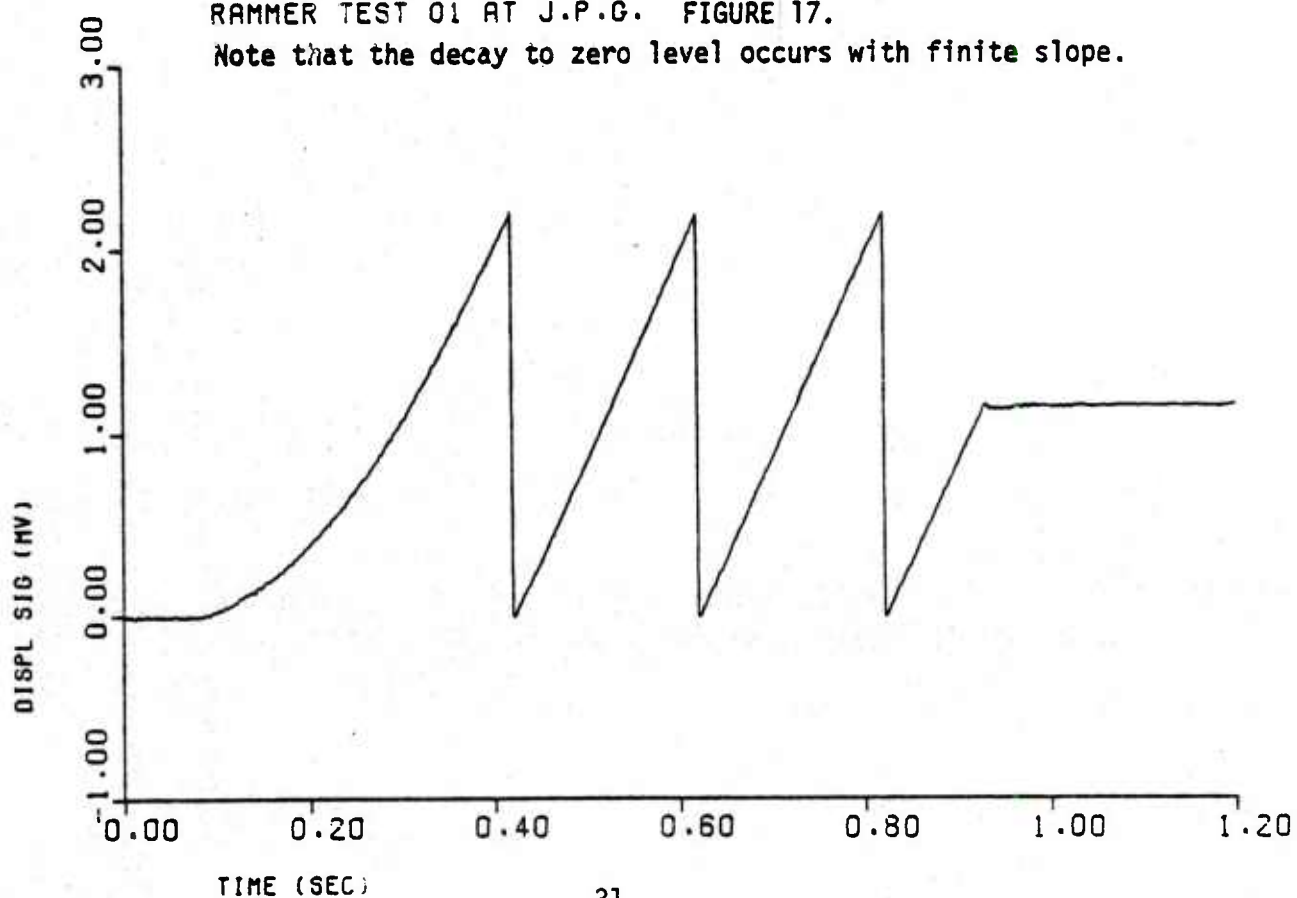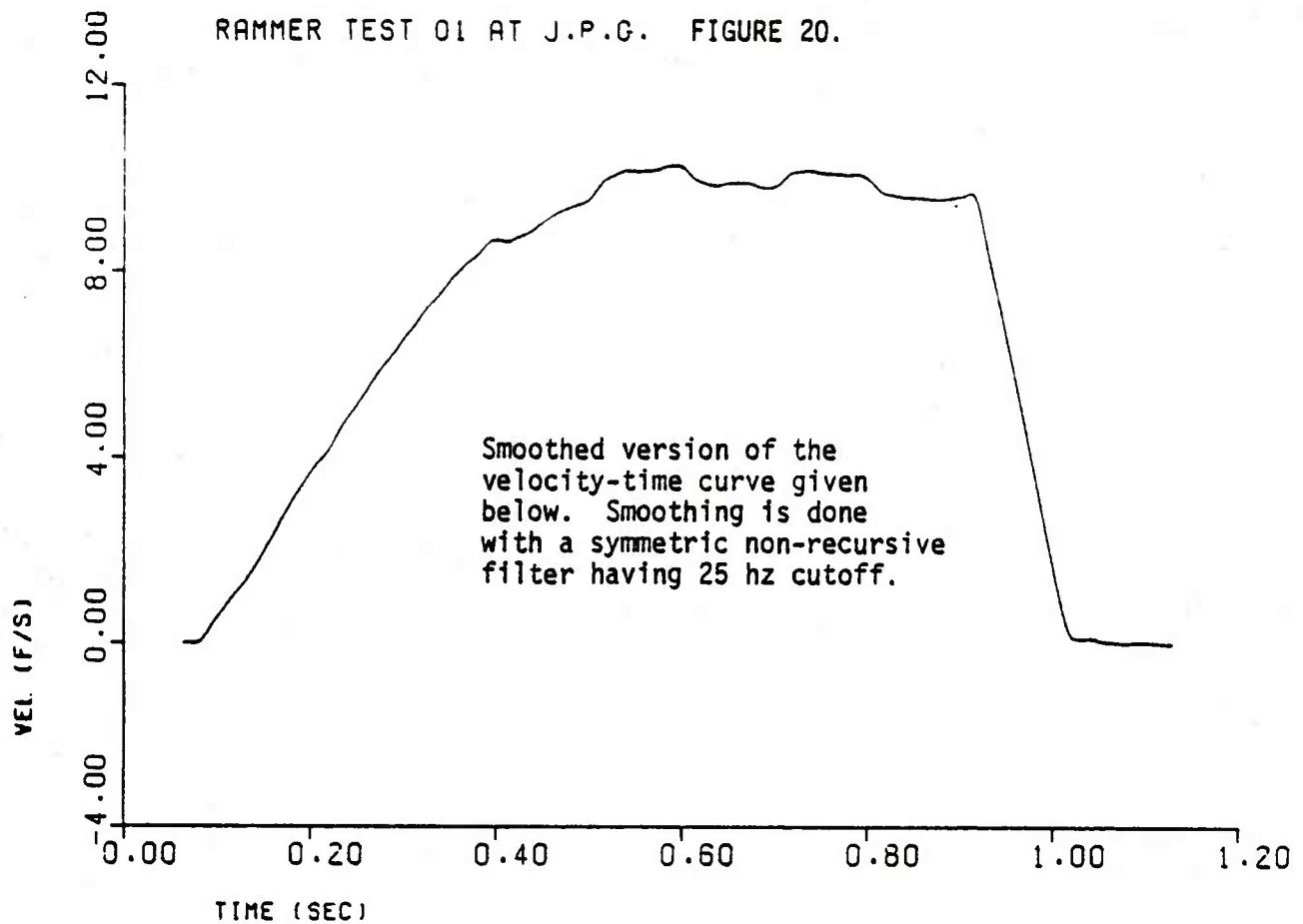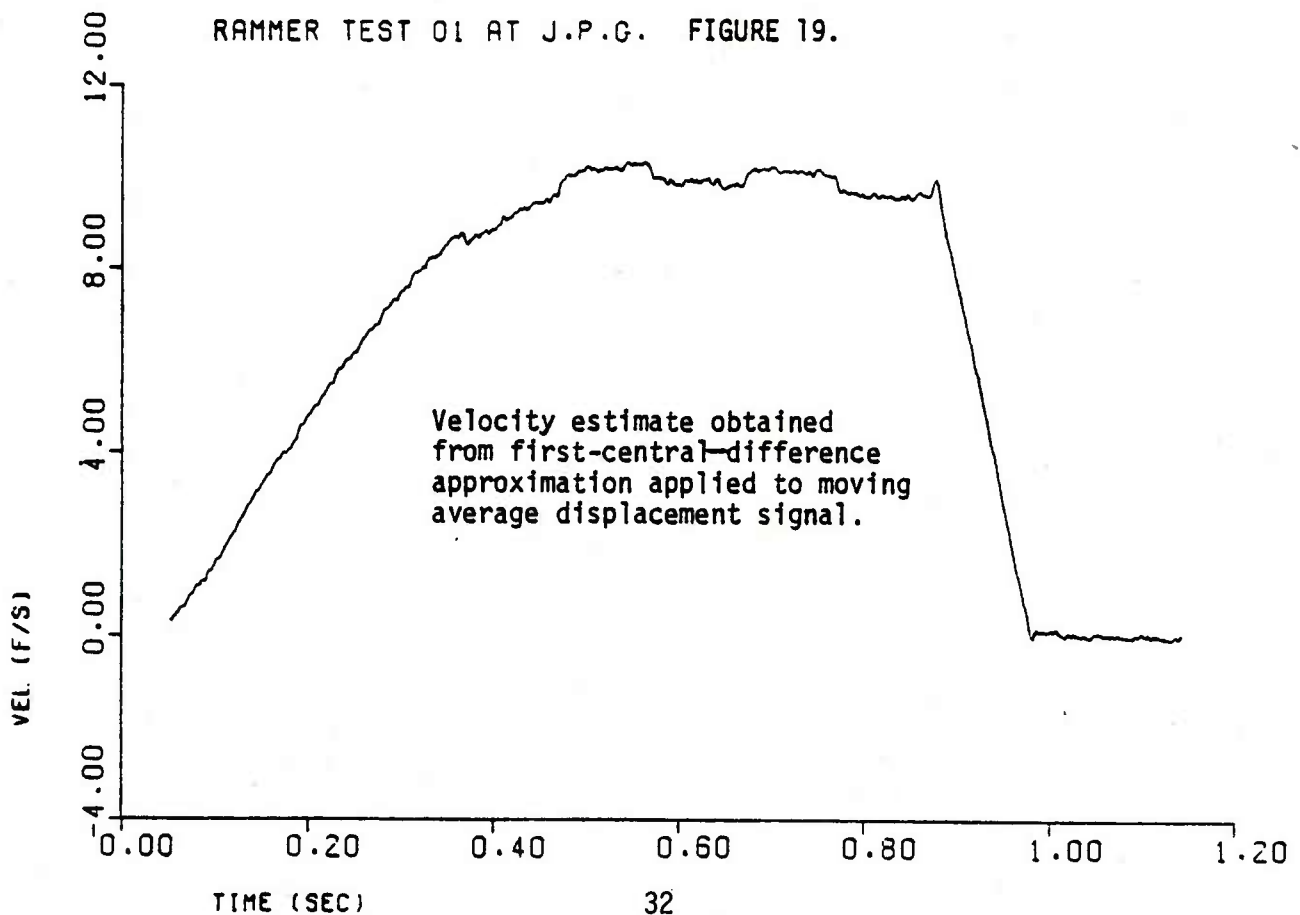
RAMMER TEST 02 AT J.P.G. FIGURE 22.

Note similarity of this rotary pot signal with that of rammer test 01.

TIME (SEC)

RAMMER TEST 01 AT J.P.G. FIGURE 21.

Crossplot of velocity versus displacement. Displacement estimate used here is obtained from a sixth degree polynomial (in time) fit to the stacked and outlier-purged potentiometer data.

DISPL (IN)

33

RAMMER TEST 02 AT J.P.G.   FIGURE 24.

Illustration of a poor
velocity estimate obtained
from a polynomial fit to the
displacement data when its domain
includes a terminal plateau, as shown
below.

RAMMER TEST 02 AT J.P.G.   FIGURE 23.

34

RAMMER TEST 02 AT J.P.G.   FIGURE 26.

Analytic estimate of the velocity obtained from a 6th degree
polynomial function in time fitted to the displacement data
shown below.

RAMMER TEST 02 AT J.P.G.   FIGURE 25.

Displacement signal
with an abbreviated terminal
plateau.   Compare with previous
displacement signal given for test
02.

35

RAMMER TEST 02 AT J.P.G. FIGURE 28.

Velocity estimate obtained
from a first-central-difference
approximation applied to the
moving average displacement
signal.

RAMMER TEST 02 AT J.P.G. FIGURE 27.

Analytic estimate of the acceleration obtained from a 6th degree
polynomial function in time fitted to the displacement signal.

36

RAMMER TEST 02 AT J.P.G.   FIGURE 30.

Crossplot of velocity versus displacement. Velocity is the smoothed first-central-difference approximation shown below as a function of time.

RAMMER TEST 02 AT J.P.G.   FIGURE 29.

37

RAMMER TEST 03 AT J.P.G.   FIGURE 32.

RAMMER TEST 03 AT J.P.G.   FIGURE 31.

38

RAMMER TEST 03 AT J.P.G. FIGURE 34.

VEL. (F/S)

TIME (SEC)

RAMMER TEST 03 AT J.P.G. FIGURE 33.

VEL (F/S)

TIME (SEC)

39

RAMMER TEST 04 AT J.P.G.   FIGURE 36.
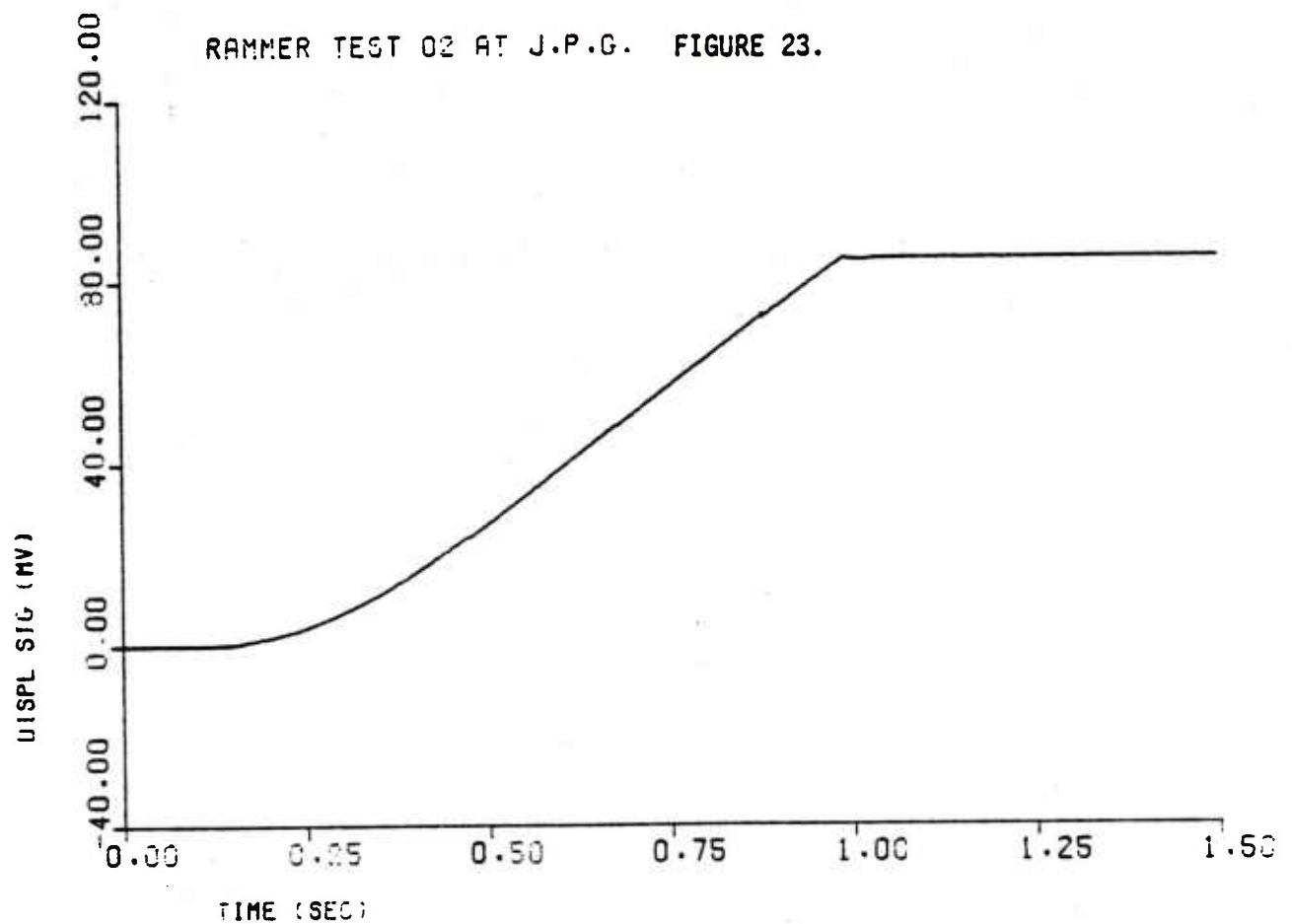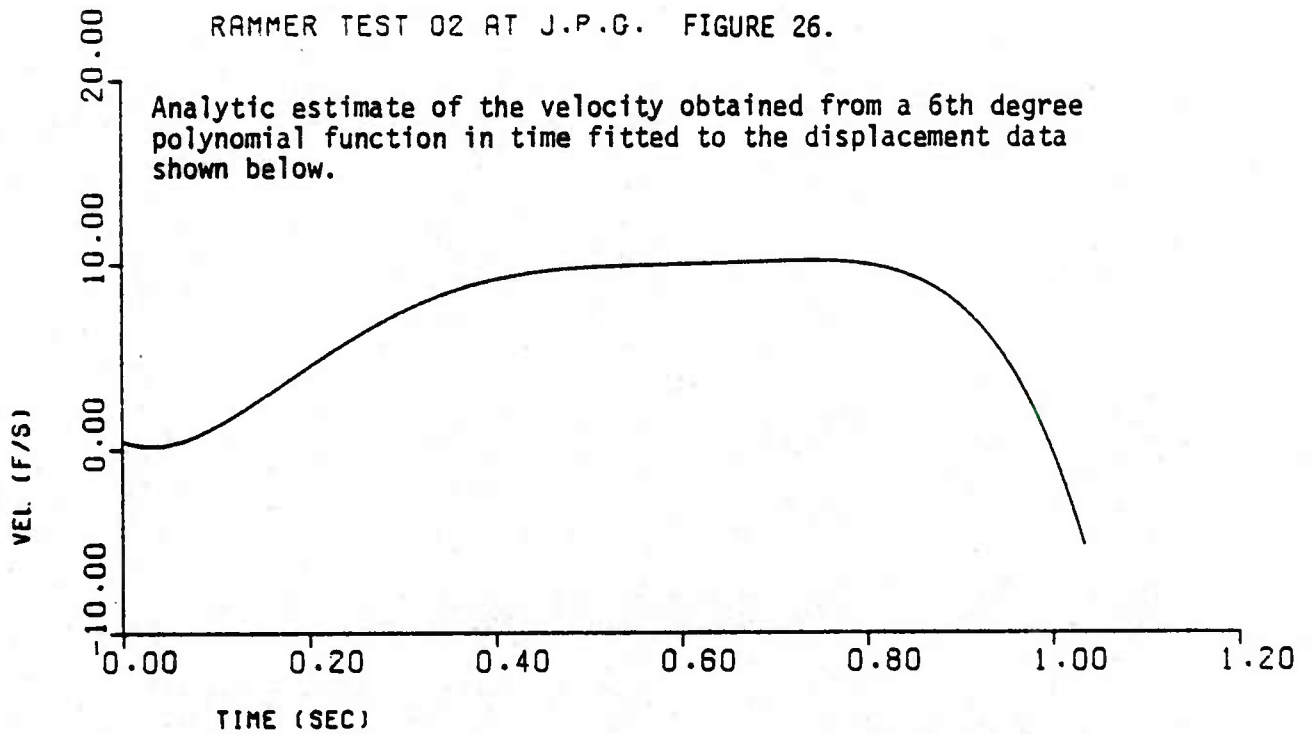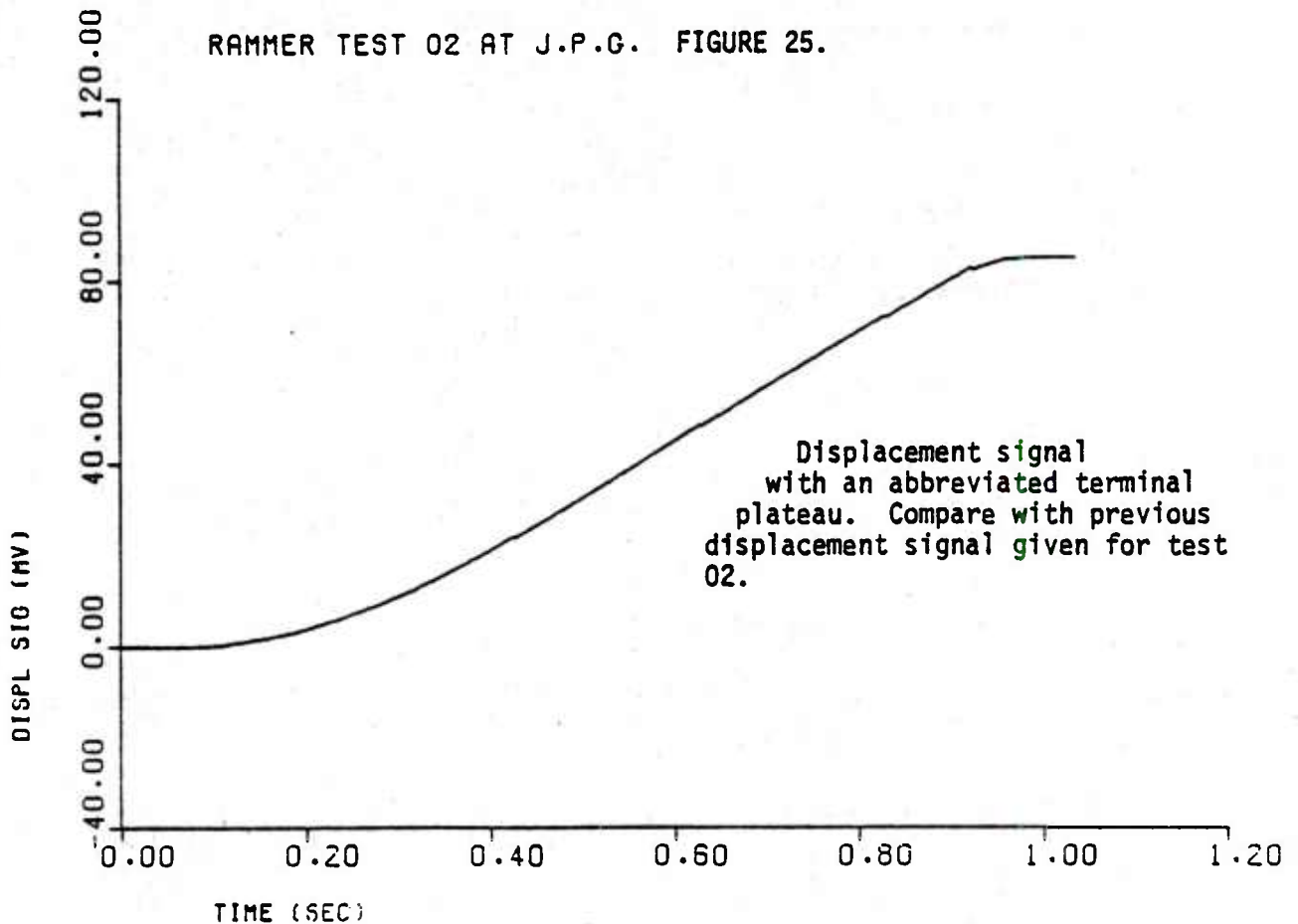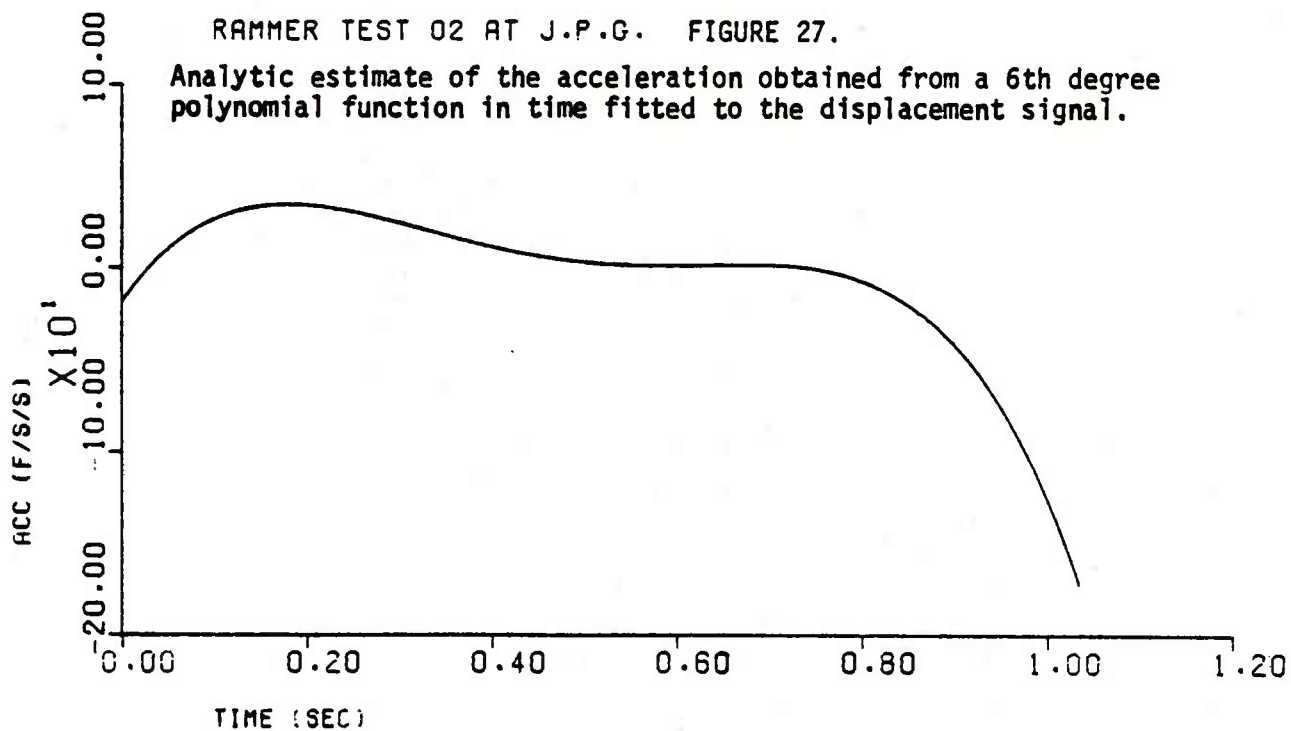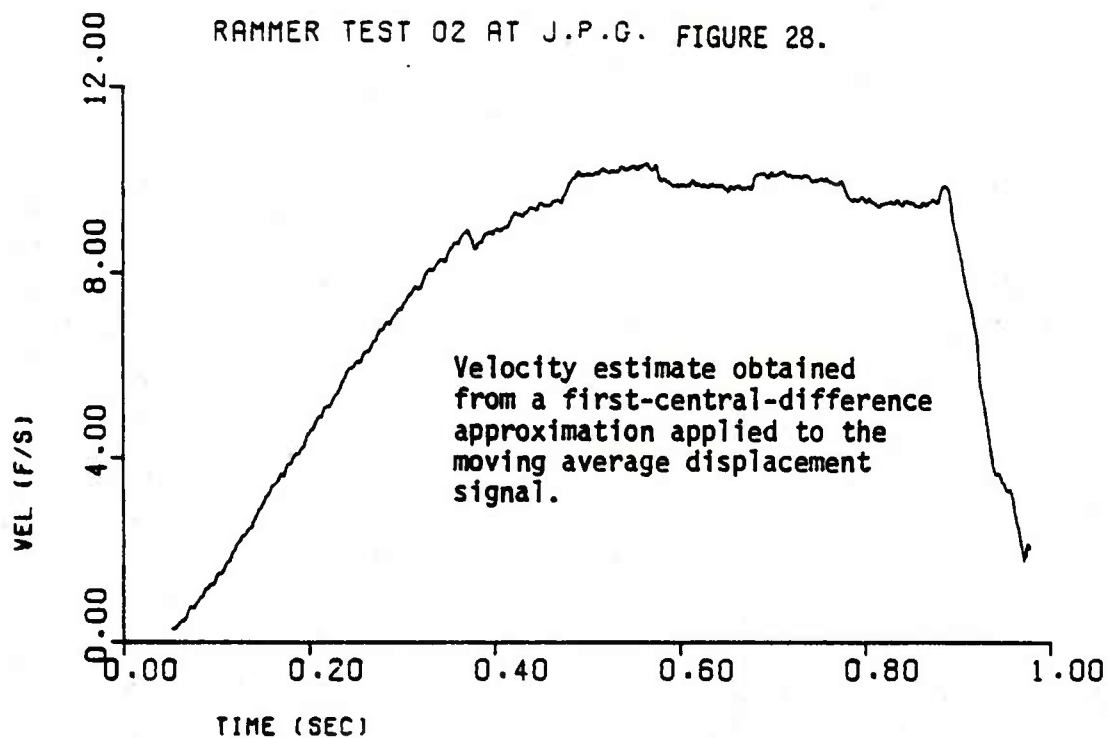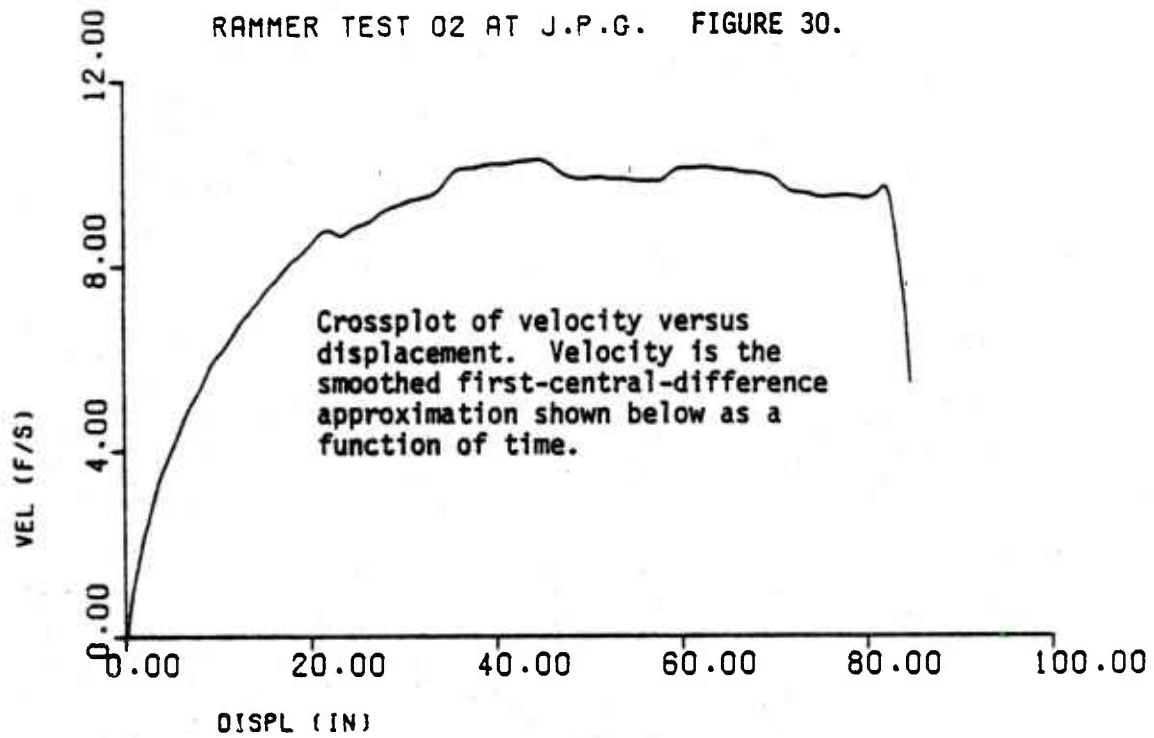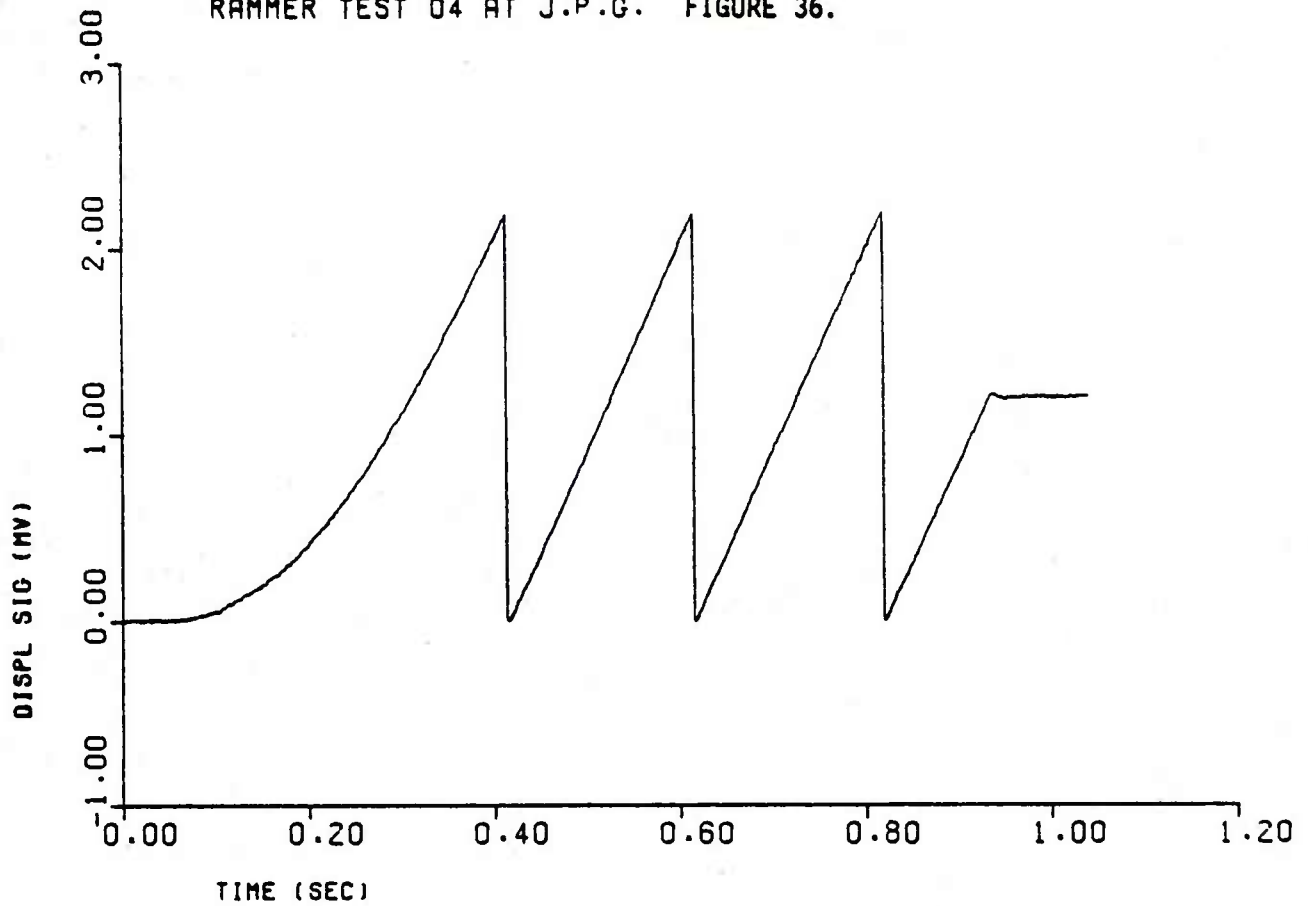

RAMMER TEST 03 AT J.P.G.   FIGURE 35.
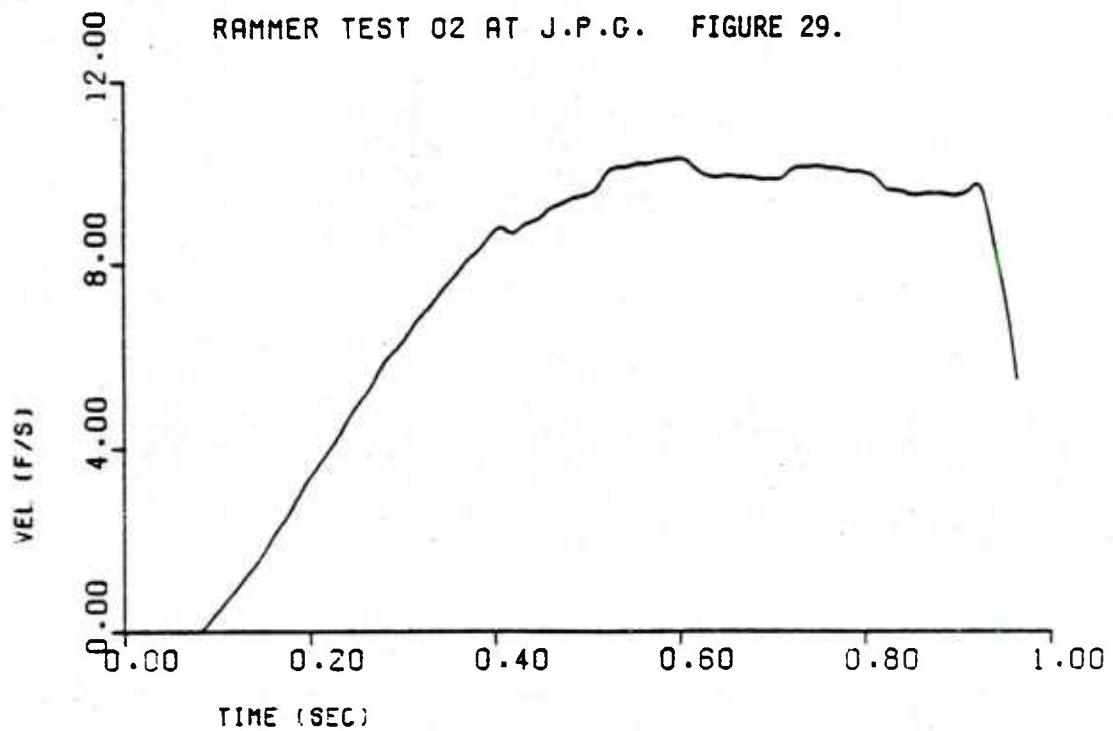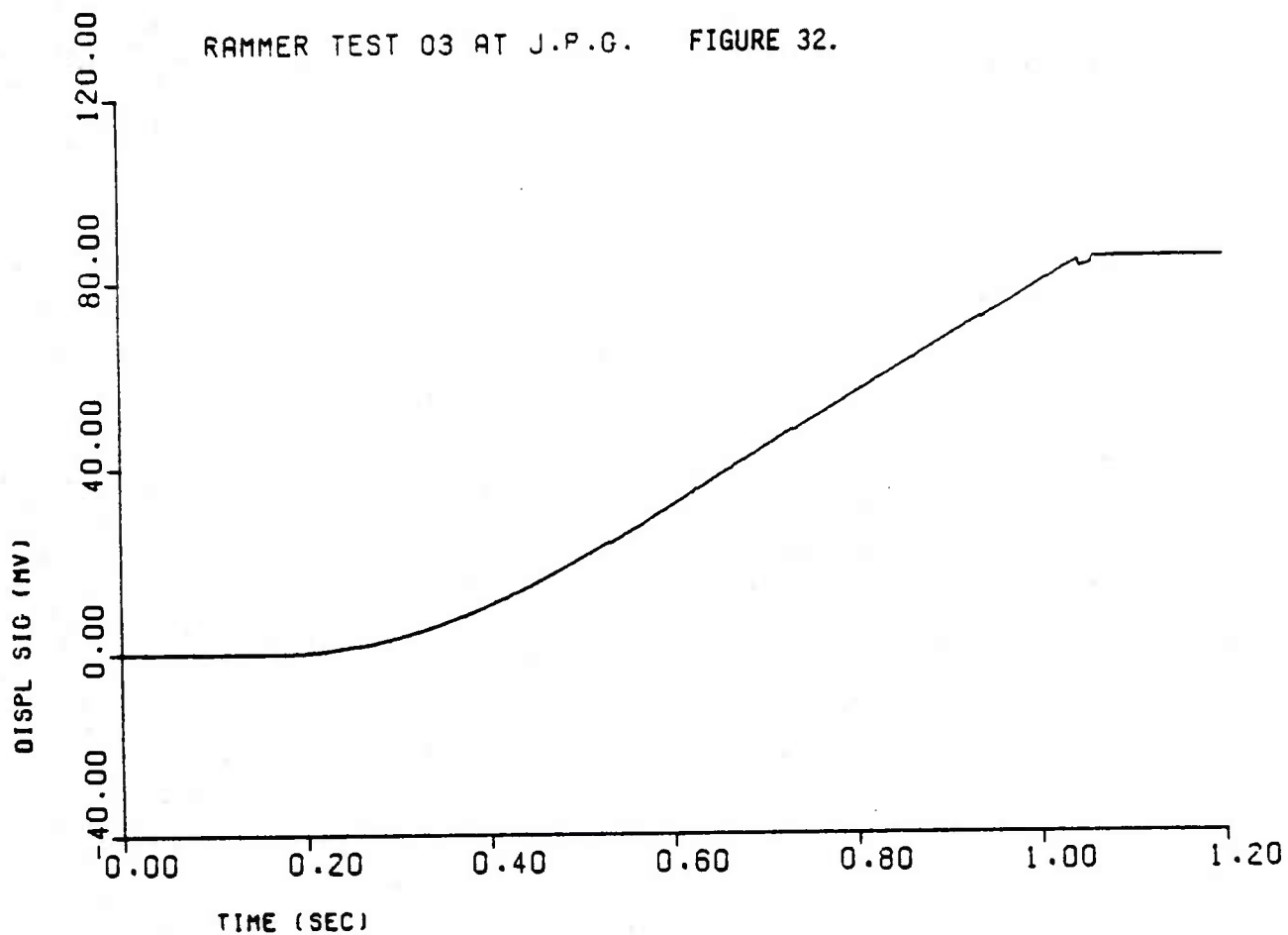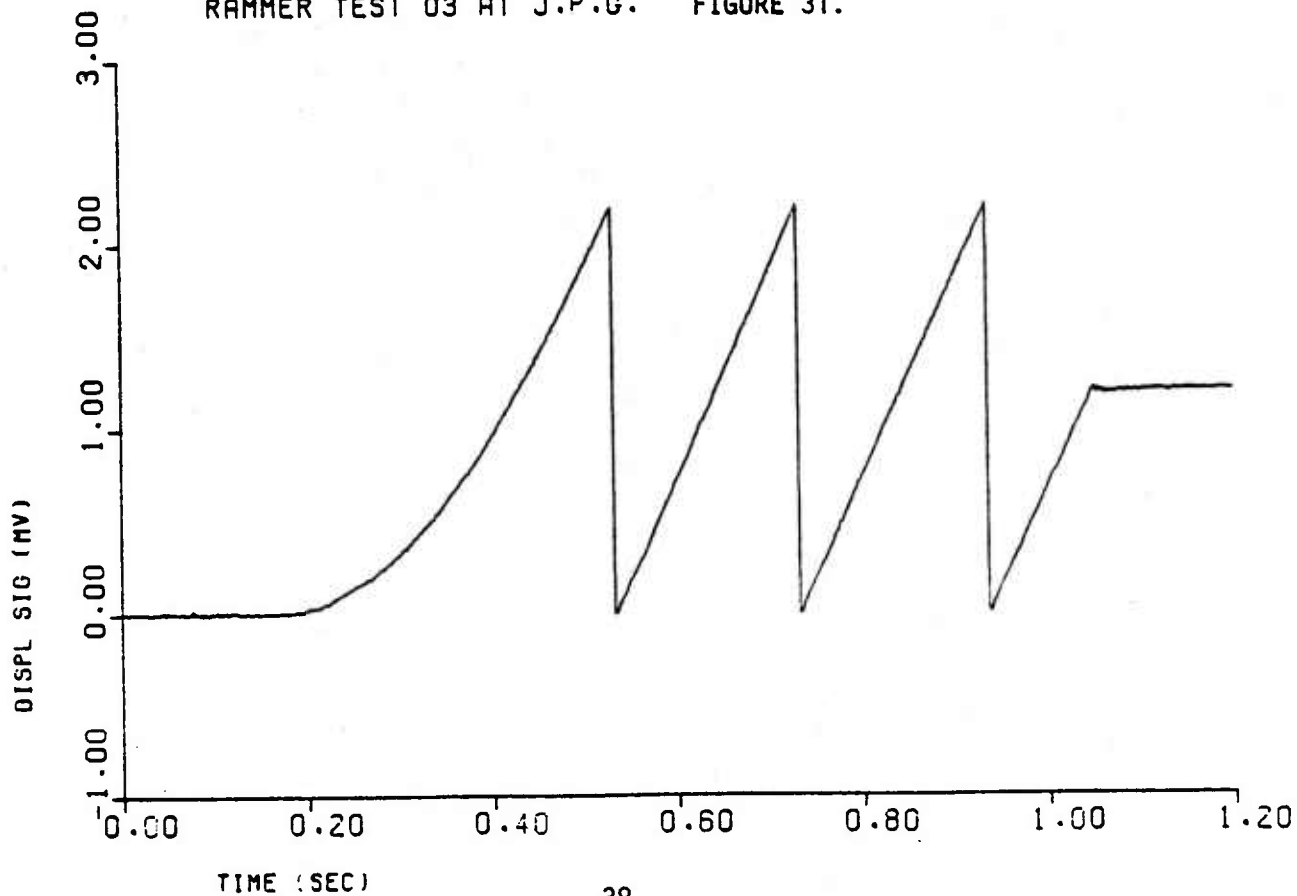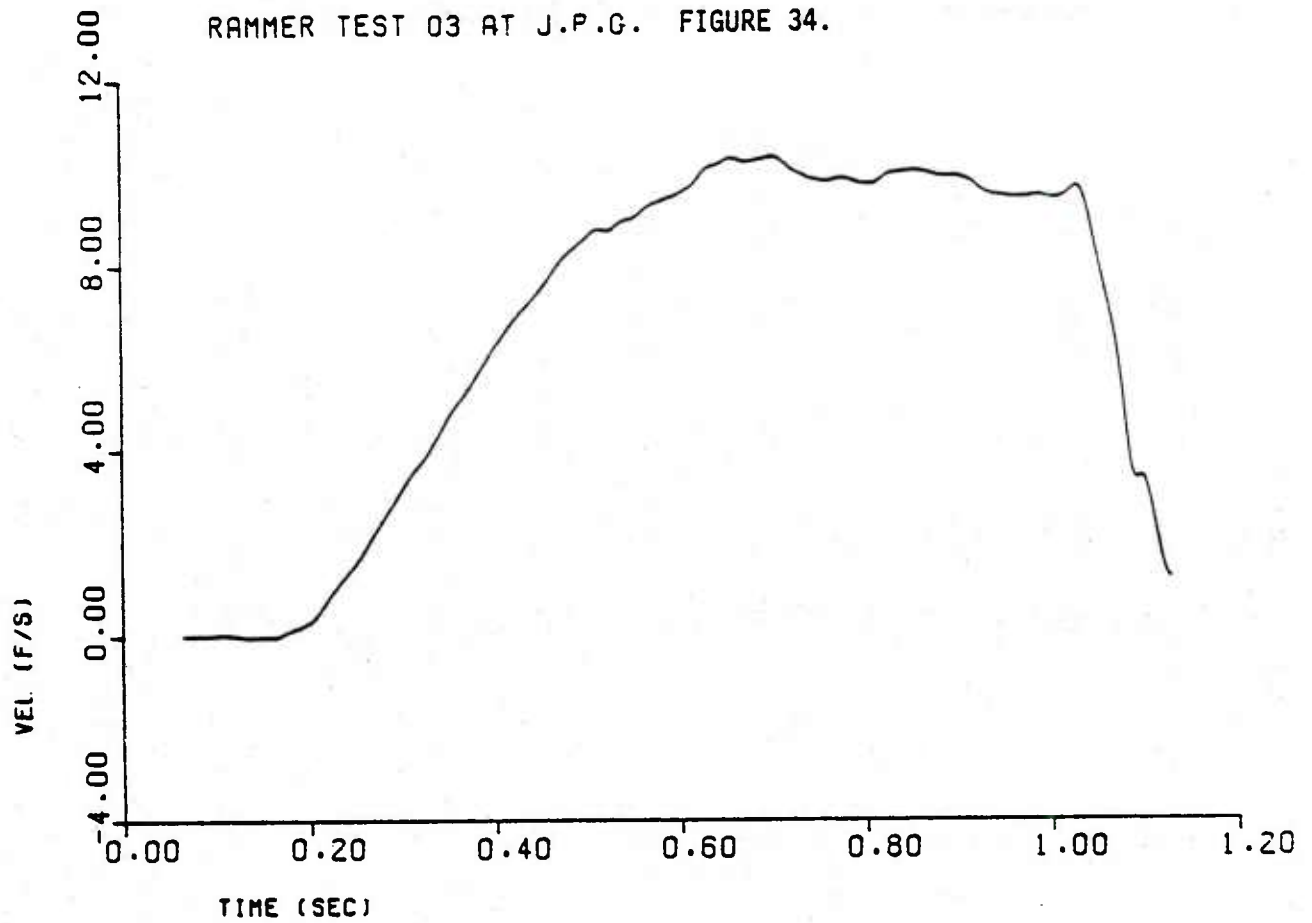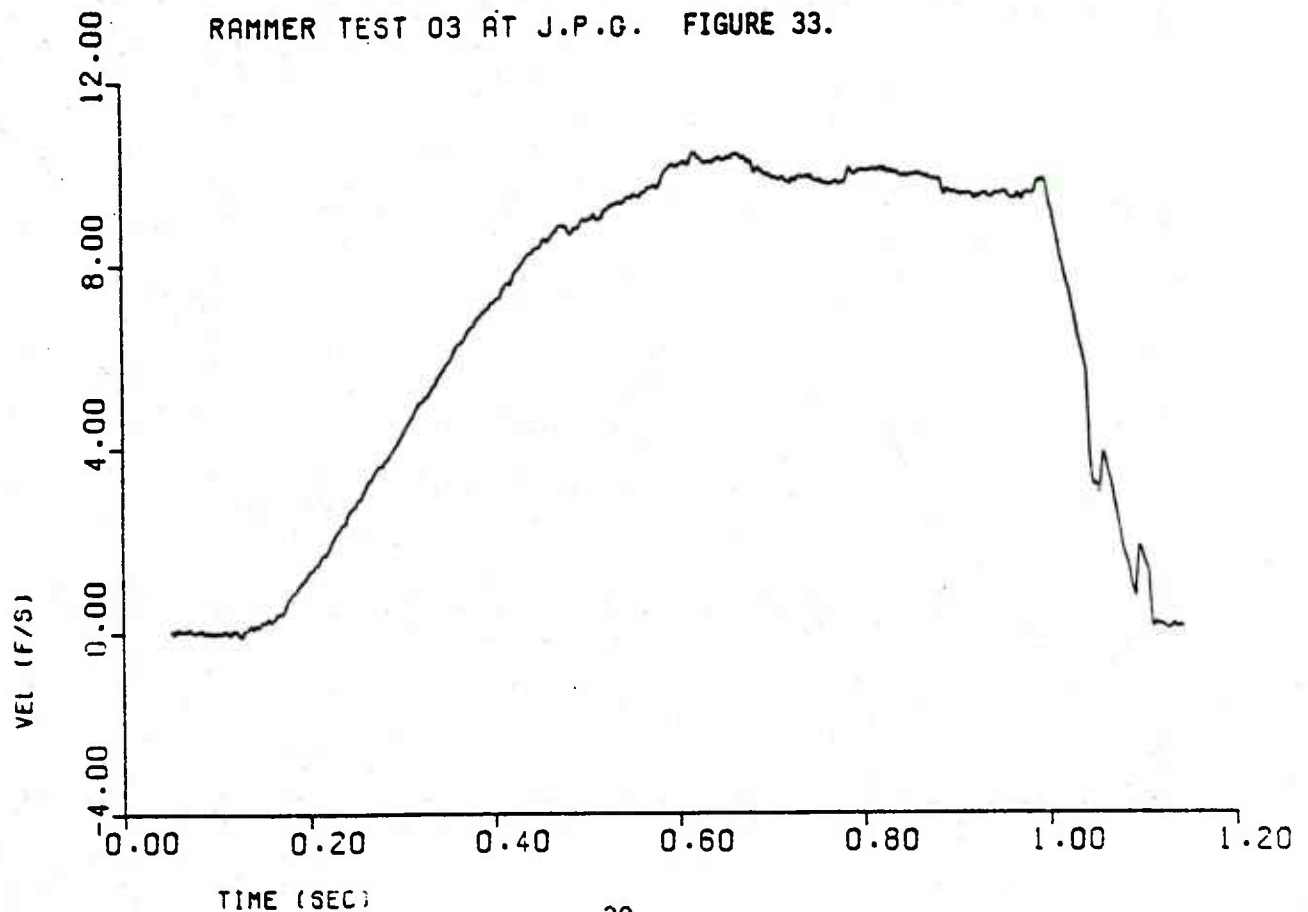

40
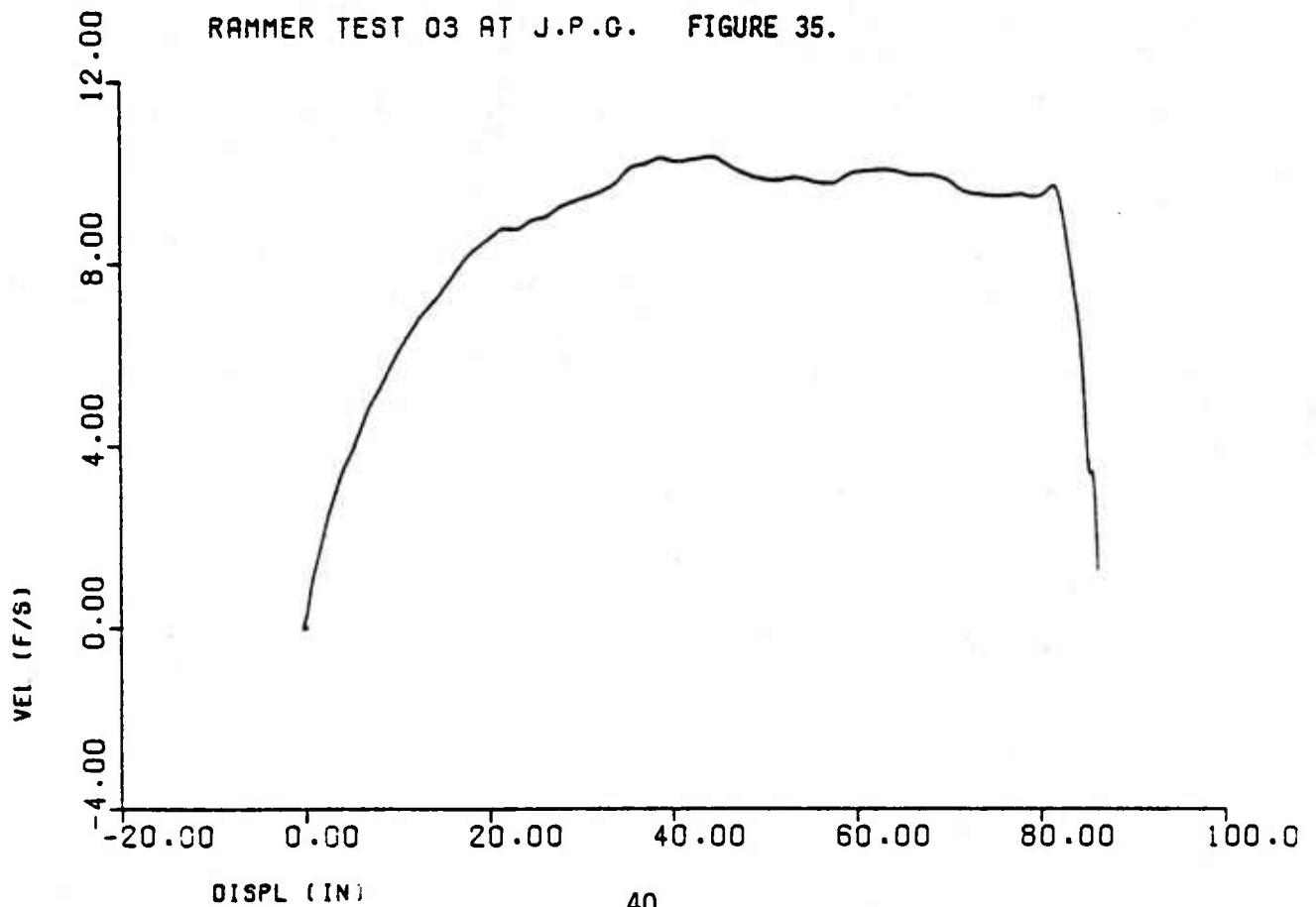
RAMMER TEST 04 AT J.P.G. FIGURE 38.
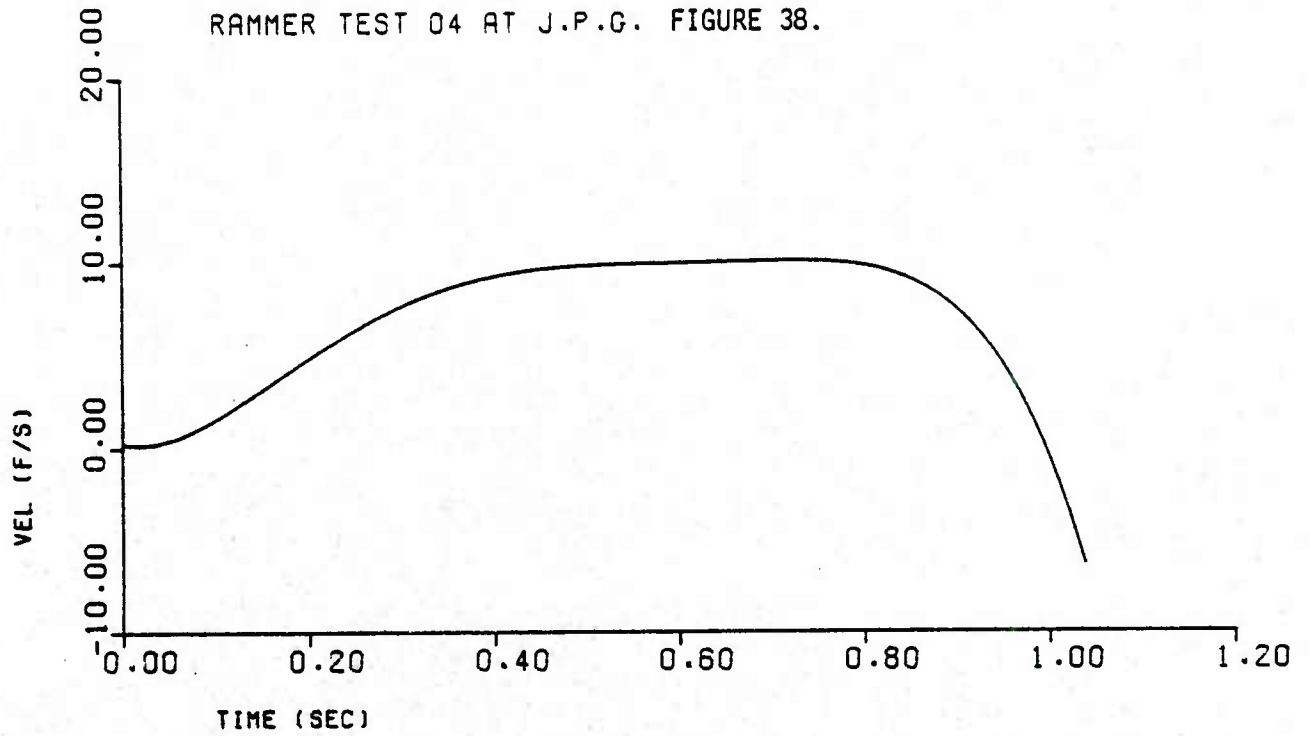
RAMMER TEST 04 AT J.P.G. FIGURE 37.

41
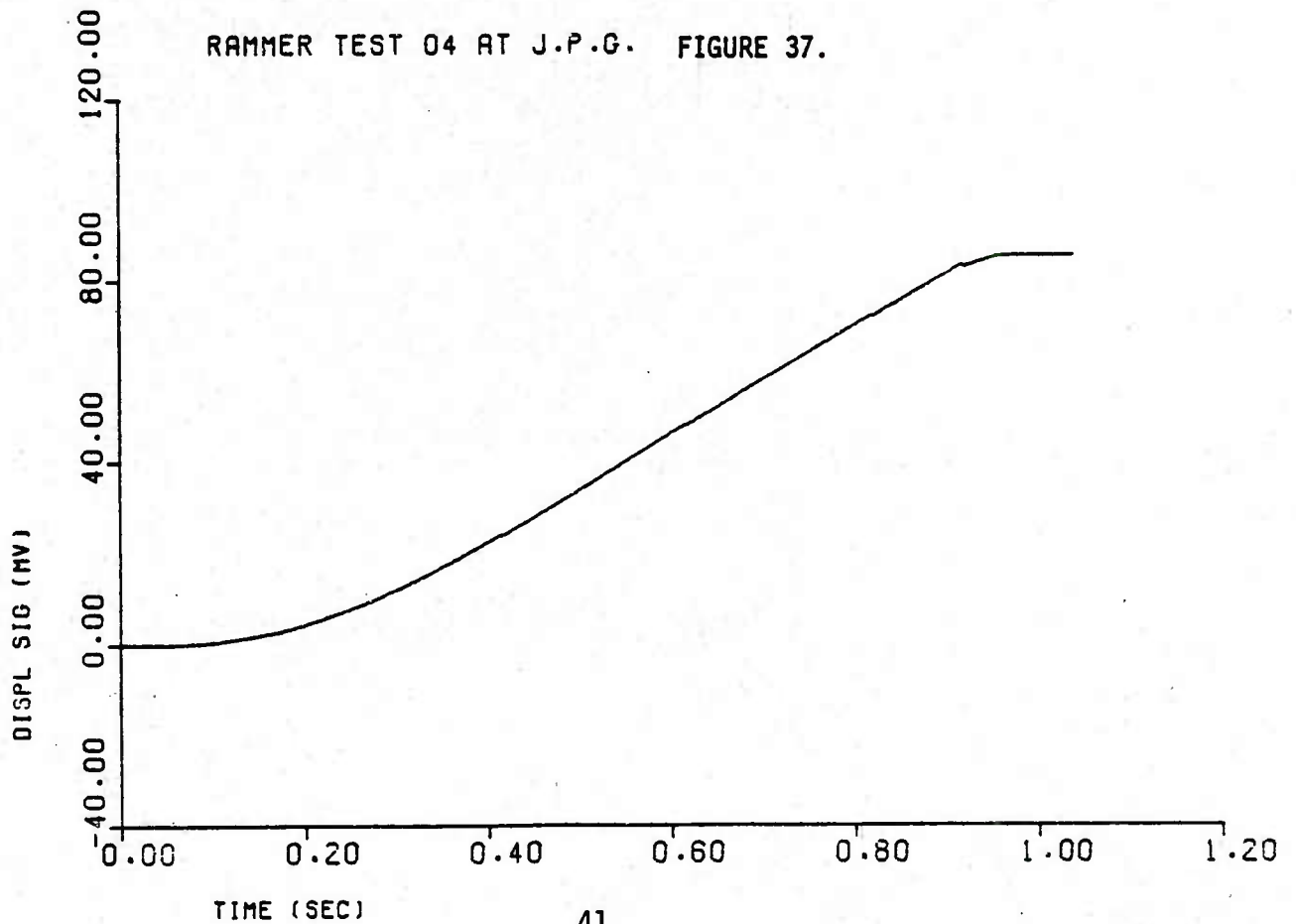
A N N E X 2

COMPUTER PROGRAM SOURCE
LISTING FOR EST.VEL.ACC
A PROGRAM FOR PROCESSING
DISPLACEMENT SIGNALS FROM
ROTARY POTENTIOMETERS TO
ESTIMATE VELOCITY
AND ACCELERATION

```
C
C        PROGRAM FOR PROCESSING DISPLACEMENT SIGNALS FROM ROTARY
C        POTENTIOMETERS TO ESTIMATE VELOCITY AND ACCELERATION
C
C        THIS PROGRAM CONTAINS EXTERNAL REFERENCES TO PRIME 400 COMPUTER
C        SYSTEM ROUTINES AND CALCOMP 925/936 SOFTWARE.  ON THE ARRCOM S&E
C        SYSTEM THE FOLLOWING LIBRARIES MUST BE LOADED:
C           1. CWVLIB
C           2. VAPPLB
C           3. VPLOTLB
C           4. VSPOO$
C
         REAL*8 DATA(1200,7),X(7),FJ,FJJM1,VEL,ACC,S,RSQ,DISPL,VELT,DELT,
        $RESTO,XT,YESTO,A(66)
         DIMENSION Y(1200),YBAR(1200),S2(1200),INFO(12),N(2),TM(1200),
        $VMA(1200),VMAS(1200),COF2(13),YEST(1200),RPOT(1200)
         INTEGER TN(16),TITLE(40),COMOFL(16),BUF(60)
         LOGICAL NSCALE
C
         COMMON/CPLCOM/ AXL,AYL
C
C        THE DATA(I,J) ARRAY IS USED TO STORE THE I'TH VALUE OF TIME TO THE
C        J'TH POWER FOR EXPONENTS UP TO AND INCLUDING NDEG.  THE VECTOR
C        WITH J=NDEG+1 CONTAINS THE VALUES OF THE SCALED AND STACKED DEPEN-
C        DENT VARIABLE, DISPLACEMENT (IN).  THE UNSCALED ROTARY POTENTIO-
C        METER DATA ARE STORED IN RPOT,
C
$INSERT SYSCOM>A$KEYS
$INSERT SYSCOM>KEYS.F
$INSERT SYSCOM>ERRD.F
C
         DATA DATA/8400*0.0/,INFO/1,2,:100000,3*'   ',6*0/,VMA/1200*0.0/,
        $YEST/1200*0.0/
         DATA COF2/1.1286702E-02,3.0793781E-02,5.7062223E-02,8.6293384E-02,
        1         1.1312581E-01,1.3202178E-01,1.3883263E-01,1.3202178E-01,
        2         1.1312581E-01,8.6293384E-02,5.7062223E-02,3.0793781E-02,
        3         1.1286702E-02/
C
C        CALL OPEN$L('INPUT  FILE TREENAME?...> ',26,A$READ,TN,32,1)
C
C        PROCESS DATA DIRECTLY FROM TAPE
C
```

```
C         CALL TNOUA('TAPE UNIT*?...> ',16)
C         REAO(1,*) NU
          NU=4
C         CALL C$M13(1,0,NU,0)              /*  OPEN TAPE TO REAO
          CALL OPEN$A(A$REAO,'PEXLOW>A>TAPE-OUMP',18,NU)
C
          OO 104 NFILE=1,24
C         CALL C$M13(6,0,NU,0)              /*  SKIP TO NEXT FILE
          CALL C$AOO7(NU)
C         IF(NFILE.LT.6) GO TO 104          /*  SKIP FIRST 4 FILES
C
C         OPEN SCRATCH FILE TO SAVE TERMINAL OALOGUE
C
          CALL OPNSFL(3,COMOFL)
          CALL CLOS$A(3)
          CALL COMO$$(:000020,COMOFL,32,0,COOE)
C
          IF(COOE.GT.0) GO TO 103
C         CALL OPEN$L('OUTPUT FILE TREENAME?...> ',26,A$WRIT,TN,32,2)
          ENCOOE(32,12,TN) NFILE
       12 FORMAT('RAMMER-TEST*',B'***')
          CALL OPEN$A(A$WRIT,TN,32,2)
          CALL TRNC$A(2)                    /*  TRUNCATE OUTPUT FILE
C
C         READ TITLE OF OATA SET
C
C         REAO(5,2) TITLE
        2 FORMAT(40A2)
C         CALL I$AM13(NU,TITLE,40,0)
          CALL I$AOO7(NU,TITLE,40,0)
          WRITE(6,1) TITLE
        1 FORMAT(1H ,40A2)
C         CALL I$AM13(NU,TITLE,40,0)
          CALL I$AOO7(NU,TITLE,40,0)
          WRITE(6,1) TITLE
C         CALL C$M13(5,0,NU,0)              /*  SKIP 3RO REC
          CALL I$AOO7(NU,BUF,40,0)
C         CALL I$AM13(NU,BUF,60,0)          /*  REAO RECORO INTO BUF
          CALL I$AOO7(NU,BUF,60,0)
          OECOOE(120,11,BUF) POINTS,OELTAT
       11 FORMAT(2G16.8)
          TIMEO=0.0
```

46

```fortran
      NLZERO=0
      NDATA=POINTS-1.0
      NSET=NDATA
      YSCALE=10.9D9
      YMIN=-0.01
      IHIB=0              /*  INDICATOR VARIABLE FOR HIBLER'S FILTER
      FC=5.0              /*  CUTOFF FREQUENCY (HZ) IN FILTER
      YD=0.0
      NCH=NLEN$A(TITLE,40)
C
C     READ CONTROL PARAMS
C
C     READ(5,*) TIMED,NLZERO,NSET,NDATA,DELTAT,YSCALE,YMIN,YO
C     NSCALE=YSNO$A('SELF SCALING DESIRED?...> ',26,A$NDEF)
      NSCALE=.FALSE.
      DELT=DELTAT
      ISTART=NLZERO+1
      ISTOP=NLZERO+NDATA
C
C     READ THE OUTLIER LAG PARAM
C
C     CALL TNOUA('OUTLIER LAG PARAMETER?...> ',27)
C     READ(1,*) MLAG
      MLAG=25
C
C     READ MIN NUMBER OF STANDARD DEVIATIONS TO DECLARE AN OUTLIER
C
C     CALL TNOUA('NUMBER OF SD S FOR OUTLIER?...> ',32)
C     READ(1,*) SDNO
      SDNO=2.64
C
C     READ DEGREE OF POLYNOMIAL FIT
C
C     CALL TNOUA('DEGREE OF FITTING POLYNOMIAL?...> ',34)
C     READ(1,*) NDEG
      NDEG=6
      NDEGP1=NDEG+1
      MAVG=2*MLAG+1
      FMAVG=FLOAT(MAVG)
      LSTART=ISTART+MLAG
      LSTOP=ISTOP-MLAG
      I1=ISTART+MAVG-1
```

47

```
C      REAO(5.*) (Y(I).I=ISTART.ISTOP)
       NREC=NDATA/8+MINO(1.MOO(NDATA.8))
       DO 13 I=1.NREC
C      CALL I$AM13(NU.BUF.60.$15)
       CALL I$ADO7(NU.BUF.60.$15)
       GO TO 13
   15 CALL PRERR
       CALL EXIT
C      IF(NFILE.NE.29) GO TO 105
C      CALL GETERR(BUF.2)
C      IF(BUE(1).NE.'IE') GO TO 106
C      CALL I$AM13(NU.BUF.60.0)
C      CALL I$ADO7(NU.BUF.60.0)
   13 DECOOE(120.*.BUF) (Y(8*I+ISTART-9+J).J=1.8)
C
C      DETERMINE AN AVERAGE INITIAL VALUE
C
       SUM=0.0
       ISP19=ISTART+19
       DO 94 I=ISTART.ISP19
   94 SUM=SUM+Y(I)
       YO=SUM/20.0
       YLIM=93.0/YSCALE+YO
C
       YRANGE=24.0/YSCALE    /*  24 INCHES PER POT CYCLE
       YMAX=YMIN+YRANGE
       TOLER=0.01*YRANGE
       IF(.NOT.NSCALE) GO TO 90
C
C      SCAN DATA FOR MAX AND MIN
C
       NCYCLE=1
       YMAX=Y(ISTART)
       YMIN=Y(ISTART)
       IGO=ISTART+1
       DO 80 I=IGO.ISTOP
       IF(Y(I).GT.YMAX) YMAX=Y(I)
       IF(Y(I).LT.YMIN) YMIN=Y(I)
   80 CONTINUE
       YRANGE=YMAX-YMIN
       YSCALE=24.0/YRANGE
       TEST=YRANGE/2.0
```

```
      YIM1=Y(ISTART)
      DO 82 I=IGO,ISTOP
      IF(ABS(YIM1-Y(I)).GT.TEST) NCYCLE=NCYCLE+1
      YIM1=Y(I)
   82 CONTINUE
      DISPF=YSCALE*(Y(ISTOP)-YO+FLOAT(NCYCLE-1)*YRANGE)
      IF(DISPF.GT.83.0 .AND. DISPF.LT.94.0) GO TO 90
C
C     FIRST SELF-SCALING PROCEDURE PRODUCES FINAL DISPLACEMENT OUT-OF-
C     BOUNDS.  TRY A SECOND.
C
      WRITE(1,85) DISPF
   85 FORMAT('FIRST SELF-SCALING FAILED!  DISPF = ',1PG15.6, ' IN')
      YRANGE=(Y(ISTOP)-YO)/(92.5/24.0-FLOAT(NCYCLE-1))
      YMAX=YRANGE+YMIN
      YSCALE=24.0/YRANGE
      TOLER=0.0
C
C     STACK DISPLACEMENT CYCLES AND ASSIGN THE ROTARY POT SIGNAL TO
C     THE VECTOR RPOT(I)
C
   90 TEST=YRANGE/2.0
      YIM1=Y(ISTART)
      RPOT(ISTART)=Y(ISTART)
      YI=Y(ISTART)
      ADDN=0.0
      ISP1=ISTART+1
      Y(ISTART)=0.0
      DO 5 I=ISP1,ISTOP
      RPOT(I)=Y(I)
      IF(Y(I).GT.YMAX+TOLER) GO TO 101
      IF(YIM1-Y(I).GT.TEST .AND. YI.LT.YLIM) ADDN=ADDN+YRANGE
      YIM1=Y(I)
      Y(I)=Y(I)+ADDN-YO
    5 YI=Y(I)
      DO 3 I=ISTART,ISTOP
      TM(I)=TIMEO+FLOAT(I-ISTART)*DELTAT
      II=I-ISTART+1
      DATA(II,1)=TM(I)
      DO 3 J=2,NDEG
      DATA(II,J)=DATA(II,J-1)*DATA(II,1)
    3 CONTINUE
```

49

```
C
C      ESTIMATE NOISE VARIANCE OF THE STACKED SIGNAL VIA POLYNOMIAL
C      REGRESSION
C
       DO 7 I=ISTART,ISTOP
       II=I-ISTART+1
     7 DATA(II,NDEGP1)=Y(I)
       CALL MLR(DATA,X,1200,7,NDATA,NDEGP1,1,.TRUE.,S,RSQ)
       VARERR=S
       SD2=SQRT(VARERR)
       SUM=0.0
       SSQ=0.0
       DO 10 I=ISTART,I1
       SUM=SUM+Y(I)
    10 SSQ=SSQ+Y(I)**2
       YBAR(LSTART)=SUM/FMAVG
       S2(LSTART)=SSQ/FMAVG-YBAR(LSTART)**2
C
C      WRITE HEADINGS
C
C      WRITE(6,14)
    14 FORMAT(1H1,'RESULTS OF TEST FOR OUTLIERS -- ORIGINAL VALUES -- REP
      $LACEMENTS',/1H0,2X,'INDEX',T12,'PDT VALUE (MV)',T29,'MOVING AVG',
      +T46,'STD DEV',T58,'REPL VAL (MV)',T76,'MOVING AVG',T89,
      *'REPL STD DEV')
C
C      RECURSIVELY CALCULATE MOVING AVERAGES AND MOVING VARIANCES AND
C      PURGE DATA OF OUTLIERS.  IF THE HIBLER-FILTER OPTION IS SELECTED,
C      THE MOVING AVERAGE IS REPLACED BY A LOW-PASS FILTERED OUTPUT.
C
       IF(IHIB.EQ.1) GO TO 107
       NOUT=0
       SERR=0.0
       DO 20 L=LSTART,LSTOP
       LPRINT=L-ISTART+1
       IOUT=0
       II=L-ISTART+1
       YESTO=X(1)
       DO 9 J=2,NDEGP1
     9 YESTO=YESTO+X(J)*DATA(II,J-1)
       YEST(L)=YESTO*YSCALE
       SERR=SERR+(YESTO-Y(L))**2
```

```
      SO1=SQRT(SERR/FLOAT(L-LSTART+1))
      IF(ABS(Y(L)-YBAR(L)).LE.SONO*SD2) GO TO 25
      IOUT=1
      NOUT=NOUT+1
C
C     Y(L) IS AN OUTLIER.  REPLACE WITH Y(L-1) ANO CORRECT MOVING MEAN
C
      HOLO1=Y(L)
      Y(L)=YESTO
      HOLO2=YBAR(L)
      YBAR(L)=YBAR(L)+(Y(L)-HOLO1)/FMAVG
C     WRITE(6,16) LPRINT,HOLO1,HOLO2,SD1,Y(L),YBAR(L),SO2
   16 FORMAT(1H ,I5,5X,1P6G15.6)
   25 YBAR(L+1)=YBAR(L)+(Y(L+1+MLAG)-Y(L-MLAG))/FMAVG
      IF(IOUT) 26,26,20
   26 CONTINUE
C     WRITE(6,18) LPRINT,Y(L),YBAR(L),SO1
   18 FORMAT(1H ,I5,5X,1P3G15.6)
   20 CONTINUE
      WRITE(6,23) NOUT
   23 FORMAT(1H0,'NUMBER OF OUTLIERS FOUNO ANO REPLACED IS ',I6)
   24 CONTINUE
C     WRITE(6,19)
   19 FORMAT(1H1,T6,'TIME (S)',T19,'M A VEL (F/S)')
      LGO=LSTART+1
      LSM1=LSTOP-1
      OO 21 L=LGO,LSM1
      VMA(L)=YSCALE/24.0/OELTAT*(YBAR(L+1)-YBAR(L-1))
C     WRITE(6,22) TM(L),VMA(L)
   22 FORMAT(1H ,1P2G15.6)
   21 CONTINUE
C
C     COPY OUTLIER-PURGEO OATA INTO OATA(I,NOEGP1)
C
      DO 30 I=ISTART,ISTOP
      Y(I)=Y(I)*YSCALE
   30 OATA(I-ISTART+1,NOEGP1)=Y(I)/12.0
      CALL MLR(OATA,X,1200,7,NOATA,NOEGP1,1,.TRUE.,S,RSQ)
C
C     WRITE HEADINOS FOR OISPLACEMENT, VELOCITY AND ACCELERATION
C
      WRITE(6,38)
```

51

```
   38 FORMAT(1H1.T6.'TIME (S)'.T19.'I OF V (IN)'.T35.'VELOCITY (F/S)'.
     $T50.'ACCEL (F/S/S)'.T67.'SIGNAL (IN)'.T82.'RESIOUAL (FT)')
      OISPL=0.00 00
      VELT=0.00 00
      OO 42 I=ISTART.ISTOP
      II=I-ISTART+1
      XT=X(1)+X(2)*OATA(II.1)
      VEL=X(2)
      ACC=2.00 00*X(3)
      OO 40 J=2.NOEG
      XT=XT+X(J+1)*OATA(II.J)
      FJ=FLOAT(J)
      FJJM1=FLOAT(J*(J-1))
      VEL=VEL+FJ*X(J+1)*OATA(II.J-1)
      IF(J.GE.3) ACC=ACC+FJJM1*X(J+1)*OATA(II.J-2)
   40 CONTINUE
      RESIO=XT-DATA(II.NOEGP1)
      OISPL=DISPL+6.00 00*OELT*(VELT+VEL)
      VELT=VEL
      XTP=12.0*XT
      WRITE(6.43) DATA(II.1).OISPL.VEL.ACC.XTP.RESIO
   43 FORMAT(1H .1P6G15.6)
C
C     ASSIGN VELOCITY TO YBAR AND ACCELERATION TO S2 FOR PLOTTING
C
      YBAR(I)=VEL
      S2(I)=ACC
   42 CONTINUE
C
C     PLOT ORIGINAL POT OATA
C
      N(1)=1
      N(2)=NOATA
      WRITE(6.41)
   41 FORMAT(1H1.T20.'ORIGINAL ROTARY POTENTIOMETER SIGNAL (MV)')
      CALL PPLOT(TM(ISTART).RPOT(ISTART).N.7.0.4.0.0.'0')
      WRITE(6.46)
      CALL CPLOT(TM(ISTART).RPOT(ISTART).N.7.0.4.0.0.0.0.1)
      XPAGE=0.5
      YPAGE=-0.5
      CALL SYMBOL(XPAGE.YPAGE.0.084.'TIME (SEC)'.0.0.10)
      XPAGE=-0.5
```

```
          YPAGE=0.5
          CALL SYMBOL(XPAGE,YPAGE,0.084,'OISPL SIO (MV)',90.0,14)
          XPAGE=0.5
          YPAGE=AYL+0.25
          CALL SYMBOL(XPAGE,YPAGE,0.098,TITLE,0.0,NCH)
C
C     PLOT UNFILTERED ORTA
C
          WRITE(6,44)
       44 FORMAT(1H1,T20,'UNFILTD DISPLACEMENT SIGNAL (MV)')
       46 FORMAT(1H ,T20,'TIME (SEC)')
          CALL PPLOT(TM(ISTART),Y(ISTART),N,7.0,4.0,0.0,'O')
          WRITE(6,46)
          CALL CPLOT(TM(ISTART),Y(ISTART),N,7.0,4.0,0.0,0.0,1)
          XPAGE=0.5
          YPAGE=-0.5
          CALL SYMBOL(XPAGE,YPAGE,0.084,'TIME (SEC)',0.0,10)
          XPAGE=-0.5
          YPAGE=0.5
          CALL SYMBOL(XPAGE,YPAGE,0.084,'DISPL SIO (MV)',90.0,14)
          XPAGE=0.5
          YPAGE=AYL+0.25
          CALL SYMBOL(XPAGE,YPAGE,0.098,TITLE,0.0,NCH)
C
C     PLOT ESTIMATE OF VELOCITY
C
          WRITE(6,74)
       74 FORMAT(1H1,T20,'ESTIMATE OF VELOCITY (F/S)')
          N(2)=NOATA
          CALL PPLOT(TM(ISTART),YBAR(ISTART),N,7.0,4.0,0.0,'V')
          WRITE(6,46)
          CALL CPLOT(TM(ISTART),YBAR(ISTART),N,7.0,4.0,0.0,0.0,1)
          XPAGE=0.5
          YPAGE=-0.5
          CALL SYMBOL(XPAGE,YPAGE,0.084,'TIME (SEC)',0.0,10)
          XPAGE=-0.5
          YPAGE=0.5
          CALL SYMBOL(XPAGE,YPAGE,0.084,'VEL (F/S)',90.0,9)
          XPAGE=0.5
          YPAGE=AYL+0.25
          CALL SYMBOL(XPAGE,YPAGE,0.098,TITLE,0.0,NCH)
C
```

53

```
C     PLOT ESTIMATE OF ACCELERATION
C
      WRITE(6,76)
   76 FORMAT(1H-,T20,'ESTIMATE OF ACCELERATION (F/S/S)')
      CALL PPLOT(TM(ISTART),S2(ISTART),N,7.0,4.0,0.0,'A')
      WRITE(6,46)
      CALL CPLOT(TM(ISTART),S2(ISTART),N,7.0,4.0,0.0,0.0,1)
      XPAGE=0.5
      YPAGE=-0.5
      CALL SYMBOL(XPAGE,YPAGE,0.084,'TIME (SEC)',0.0,10)
      XPAGE=-0.5
      YPAGE=0.5
      CALL SYMBOL(XPAGE,YPAGE,0.084,'ACC (F/S/S)',90.0,11)
      XPAGE=0.5
      YPAGE=AYL+0.25
      CALL SYMBOL(XPAGE,YPAGE,0.098,TITLE,0.0,NCH)
C
C     PLOT THE MOVING AVERAGE VELOCITY
C
      N(2)=NDATA-2*(MLAG+2)
      WRITE(6,78)
   78 FORMAT(1H1,T20,'EST. OF M. A. VELOCITY (F/S)')
      CALL PPLOT(TM(LGO),VMA(LGO),N,7.0,4.0,0.0,'V')
      WRITE(6,46)
      CALL CPLOT(TM(LGO),VMA(LGO),N,7.0,4.0,0.0,0.0,0.0,1)
      XPAGE=0.5
      YPAGE=-0.5
      CALL SYMBOL(XPAGE,YPAGE,0.084,'TIME (SEC)',0.0,10)
      XPAGE=-0.5
      YPAGE=0.5
      CALL SYMBOL(XPAGE,YPAGE,0.084,'VEL (F/S)',90.0,9)
      XPAGE=0.5
      YPAGE=AYL+0.25
      CALL SYMBOL(XPAGE,YPAGE,0.098,TITLE,0.0,NCH)
C
C     SMOOTH THE MOVING AVERAGE VELOCITY
C
      M=6
      COP=40.0*DELTAT
      KMAX=2*M+1
      II1=LGO+M
      II2=LSM1-M
```

```
C        WRITE(6,29) COP
    29 FORMAT(1H1,T10,'SMOOTHED MOVING-AVERAGE VELOCITY',/1H0,T10,
       $'CUT-OFF PERIOD (S) = ',1PG15.6,/1H0,/1H0,T6,'TIME (S)',T20,
       +'FILT VEL (F/S)',T36,'DISPL (IN)')
         DO 31 II=II1,II2
         SUM=0.0
         DO 33 K=1,KMAX
    33 SUM=SUM+COF2(K)*VMA(II+K-MLAG-1)
         VMAS(II)=SUM
C        WRITE(6,32) TM(II),VMAS(II),Y(II)
    31 CONTINUE
    32 FORMAT(1H ,1P3G15.6)
C
C        PLOT THE FILTERED MOVING-AVERAGE VELOCITY
C
         N(2)=N(2)-KMAX
         WRITE(6,79)
    79 FORMAT(1H1,T20,'EST. OF FILTERED M. A. VELOCITY (F/S)')
         CALL PPLOT(TM(II1),VMAS(II1),N,7.0,4.0,0,'V')
         WRITE(6,46)
         CALL CPLOT(TM(II1),VMAS(II1),N,7.0,4.0,0,0,0,1)
         XPAGE=0.5
         YPAGE=-0.5
         CALL SYMBOL(XPAGE,YPAGE,0.084,'TIME (SEC)',0.0,10)
         XPAGE=-0.5
         YPAGE=0.5
         CALL SYMBOL(XPAGE,YPAGE,0.084,'VEL (F/S)',90.0,9)
         XPAGE=0.5
         YPAGE=AYL+0.25
         CALL SYMBOL(XPAGE,YPAGE,0.098,TITLE,0.0,NCH)
C
C        PLOT VELOCITY VERSUS DISPLACEMENT
C
         WRITE(6,83)
    83 FORMAT(1H1,T20,'CROSSPLOT OF FILT VEL (F/S) VS DISPL (IN)')
         CALL PPLOT(YEST(II1),VMAS(II1),N,7.0,4.0,0,'V')
         WRITE(6,48)
    48 FORMAT(1H ,T20,'DISPL (IN)')
         CALL CPLOT(YEST(II1),VMAS(II1),N,7.0,4.0,0,0,0,1)
         XPAGE=0.5
         YPAGE=-0.5
         CALL SYMBOL(XPAGE,YPAGE,0.084,'DISPL (IN)',0.0,10)
```

```
      XPAGE=-0.5
      YPAGE=0.5
      CALL SYMBOL(XPAGE,YPAGE,0.084,'VEL (F/S)',90.0,9)
      XPAGE=0.5
      YPAGE=AYL+0.25
      CALL SYMBOL(XPAGE,YPAGE,0.098,TITLE,0.0,NCH)
C
C     CLOSE COMO FILE AND COPY TO OUTPUT
C
      CALL O$AD07(2,'--- TERMINAL DIALOGUE --',12,0)
      CALL COMO$$(:000060,COMOFL,32,0,CODE)
      IF(CODE.GT.0) GO TO 103
      CALL OPEN$A(A$READ,COMDEL,32,3)
   91 CALL I$AD07(3,BUF,40,$92)
      WRITE(6,93) BUF
   93 FORMAT(1H ,40A2)
      GO TO 91
   92 CALL CLOS$A(3)
      CALL DELE$A(COMOFL,32)
C
C     CLOSE INPUT AND OUTPUT FILES
C
      CALL CLOS$A(1)
      CALL CLOS$A(2)
C
C     SPOOL OUTPUT
C
      CALL SPOOL$(1,TN,32,INFO,DATA,7168,ICODE)
      IF(ICODE.GT.0) GO TO 60
      CALL TNOU(' ',1)
      CALL TNOUA('YOUR SPOOL FILE IS ',19)
      CALL TNOU(INFO(8),6)
  104 CONTINUE
C 106 CALL C$M13(-4,0,NU,0)
  106 CALL CLOS$A(4)
      CALL PLOT(8.0,0.0,999)
      CALL EXIT
  105 CALL TNOU('UNEXPECTED EOF!',16)
      GO TO 106
  107 CONTINUE
C
C     FILTER THE STACKED INPUT SIGNAL AND PLACE IN YBAR(I)
```

56

```
C
      CALL HFILTR(FC.DELTAT.MLAG.NDATA.ISTART.Y.YBAR)
      GO TO 24
C
C     PRINT ERROR MESSAGE
C
   60 CALL ERRPR$(K$NRTN.ICODE.0.0.'SPOOL$'.6)
      CALL EXIT
  101 WRITE(1.102) YMAX.YMIN.YSCALE.I.Y(I)
  102 FORMAT('INCONSISTENT INPUT DATA'.//'YMAX = '.1PG15.6./'YMIN = '.
     $1PG15.6./'YSCALE = '.1PG15.6./'Y('.I3.') = '.1PG15.6)
      CALL TNOUA('ERI '.4)
      CALL EXIT
  103 CALL ERRPR$(K$NRTN.CODE.0.0.'COMO$$'.6)
      END
      SUBROUTINE C$AD07(NU)
    1 CALL I$AD07(NU.IBUF.1.0)
      IF(AND(IBUF.:177400)-:000400) 1.2.1
    2 RETURN
      END
      SUBROUTINE HFILTR(FC.DELTAT.MLAG.NDATA.ISTART.Y.Z)
C
C     HIBLER'S NON-RECURSIVE. GENERAL-PURPOSE. LOW-PASS FILTER
C
      EXTERNAL H
      DIMENSION C(101).Y(1).Z(1)
C
      DATA PI/3.1415926536/
C
C     INPUTS:
C        FC     - CUTOFF FREQUENCY (HZ)
C        DELTAT - TIME STEP (SEC)
C        MLAG   - MAX NUMBER OF LAGS USED IN THE SYMMETRIC FILTER
C        NDATA  - NUMBER OF DATA POINTS IN THE (Y) INPUT
C        ISTART - POSITION OF FIRST DATA POINT IN INPUT ARRAY
C        Y      - INPUT ARRAY
C     OUTPUTS:
C        Z      - OUTPUT ARRAY
C
C                 NOTE: LENGTH OF OUTPUT VECTOR HAS BEEN SHORTENED BY
C                 MLAG POINTS AT THE START AND BY MLAG POINTS AT THE END
C
```

```
      EMLAG=FLOAT(MLAG)
      NCOEFS=2*MLAG+1
      LSTART=ISTART+MLAG
      LSTOP=ISTART+NDATA-1-MLAG
      IF(LSTOP.LE.LSTART) GO TO 104

      N1=2.0*FMLAG*FC*DELTAT+0.001
      IF(N1.LT.1) GO TO 106
C
C     CALCULATE FILTER COEFS
C

      DO 10 I=1,NCOEFS
      N=IABS(I-MLAG-1)
      EN=FLOAT(N)
      JMAX=MLAG-1
      SUM=0.0

      DO 20 J=1,JMAX
      FJ=FLOAT(J)
      SUM=SUM+H(J,N1)*COS(PI*EN*FJ/FMLAG)
   20 CONTINUE

      C(I)=(SUM+H(0,N1)/2.0+H(MLAG,N1)/2.0*COS(PI*FN))/FMLAG
   10 CONTINUE
C
      C(1)=C(1)/2.0
      C(NCOEFS)=C(NCOEFS)/2.0


C
C     PERFORM THE FILTERING (CONVOLUTION) OPERATION
C
      DO 25 L=LSTART,LSTOP
      SUM=0.0
      DO 26 J=1,NCOEFS
      K=L-MLAG+J-1
   26 SUM=SUM+C(J)*Y(K)
   25 Z(L)=SUM
      RETURN

  104 WRITE(1,105)
  105 FORMAT('ERROR IN INPUT TO SUBROUTINE HFILTR.  LENGTH OF FILTERED S
```

58

```
      $ERIES IS NOT POSITIVE1')
       CALL EXIT
  106 WRITE(1,107)
  107 FORMAT('ERROR IN INPUT TO SUBROUTINE HFILTR.   N1 IS LESS THAN UNIT
     $YI')
       CALL EXIT
       END
       FUNCTION H(I,N1)
       IF(I.GT.N1) GO TO 1
       H=1.0
       RETURN

    1 IF(I.EQ.N1+1) H=0.77
       IF(I.EQ.N1+2) H=0.23
       IF(I.GT.N1+2) H=0.00
       RETURN
       END
```

SENSITIVITY OF INTERIOR BALLISTICS

IN THE M110A2

TO

PROPELLING CHARGE TEMPERATURE

George Schlenker

DRSAR-PEL   5 December 1979

MEMORANDUM FOR RECORD

SUBJECT: Sensitivity of Interior Ballistics in the M110A2 to Propelling
          Charge Temperature

1. Reference:

    a. FONECON between Brian Walters (DRSAR-HA) and George Schlenker
(DRSAR-PEL), 29 Nov 79, subject as above.

    b. Firing Tables No. FT 8-Q-1, HQDA, Jan 76, title: Cannon, 8-Inch
Howitzer, M201 on Howitzer, Heavy, Self-Propelled, 8-Inch, M110A1 Firing
Projectile, HE, M106.

2. Background

    The brief study reported in this memorandum was initiated in response
to the Reference a phone conversation. Although information concerning
the sensitivity of muzzle velocity of the subject system to propelling
charge temperature is readily available, as in Reference b, it did not
appear that comparable information on sensitivity of peak chamber pressure
existed for all charge zones. Pressure information was urgently needed
to satisfy the requirements of government ammunition contractors. This
MFR provides such estimates in a consistent manner for all zones of the
M1 and M2 propelling charges and for the M106 and M650 projectiles.

3. Methodology

    Ballistic calculations were made using the ARRCOM interior ballistics
simulation for the M110/M110A2 howitzer system. This computer model had
been developed during CY 79 to analyse the performance of the howitzer
with various projectiles fired from both well seated positions and from
fallback positions, i.e., with the projectile resting upon the charge.
Only well seated projectiles were simulated here. It was anticipated that
configurational differences in the M106 and M650 projectiles would produce
different ballistic sensitivity to charge temperature. Consequently, both
projectiles were examined using the M1 (green bag) propelling charge.
Additionally, the M106 projectile was examined with the M2 (white bag)

propelling charge*. Peak chamber pressure and muzzle velocity were obtained in the M201 cannon using these charges at charge temperatures of 0, 70, and 145 deg F. These results are summarized in Table 1.

4. The effect of propelling charge temperature on model parameters is treated in the following way. Heat added (or removed) from the charge by raising (or lowering) the temperature relative to ambient, 70 deg F, is considered to appropriately raise (or lower) the flame temperature by requiring conservation of energy.** Additionally, the effect of heat addition (or removal) increases (decreases) the linear burning rate of the solid propellant. This phenomenon can be treated (over a restricted range of temperature) by making the linear burning rate at 1 ksi, β, a linear function of temperature. Thus,

$$\beta(T) = \beta_0 + \frac{\partial \beta}{\partial T} (T - T_0) \ ,$$

where $\beta(T)$ is the burning rate coefficient function of temperature T, and and where β_0 is the nominal value at temperature T_0. The partial derivative, $\partial \beta / \partial T$, is considered constant over the domain of $\beta(T)$. However, it is noted that experimental evidence indicates that $\partial \beta / \partial T$ decreases with decreasing temperature. Comparison of the calculated with experimental (Reference b) decrease in muzzle velocity with change in charge temperature from 70 to 0 deg F (Table 2) shows a somewhat larger calculated decrease. By inference, $\partial \beta / \partial T$ must decrease with decreasing temperature. Unfortunately, the form of $\partial \beta / \partial T$ is not provided from propellant data available in the SPIA manual. Therefore, the accuracy of ballistic estimates suffers for charge temperatures less than about 0 deg F.

---

* Thermochemical parameters, propellant grain dimensions, and charge weights specific to certain charge lots were used in the simulations. These lots were: for the M1 charge IND 69797, and for the M2 charge BAJ 67951.

**Energy conservation requires that the isochoric adiabatic flame temperature, T_v' , existing after changing the charge temperature by ΔT be related to the ambient flame temperature T_v by the relation:

$$RT_v'/(\gamma - 1) = RT_v/(\gamma - 1) + C_{solid} \Delta T \ ,$$

where R is the gas constant and γ is the ratio of specific heats for the propellant gas. The specific heat of the solid propellant, in consistent units, is C_{solid}.

SUBJECT: Sensitivity of Interior Ballistics in the M110A2 to Propelling Charge Temperature

5. Results

The peak chamber pressures and muzzle velocities calculated for all computer runs are given in Table 1. Average values of the pressure sensitivity coefficient $\partial \beta / \partial T$ and of the velocity sensitivity coefficient $\partial V_o / \partial T$ are given here for each charge zone. It is generally a good approximation to take these coefficients as constants for zones 1G through 5G as can be seen by the linearity of p_{max} and V_o with T in Figures 1 and 2. However, at the higher zones using the M2 charge there is a noticeable departure from linearity. This phenomenon has been observed experimentally in other systems, and is not just an artifact of the simulation. Consequently, the calculated average values of $\partial p / \partial T$ and $\partial V_o / \partial T$ for zones 5W, 6W, and 7W should not be used for extrapolation.

6. There are two conspicuous aspects of the numerical results which deserve attention: (1) Ballistic sensitivity increases in absolute value with increasing zone; (2) The multi-perforated 5W charge is substantially more sensitive than the single-perforated 5G. One should also notice that the ballistic sensitivity is less with the M650 projectile than with the M106 projectile at the same zone.

7. To provide some measure of validity in the calculated sensitivities, a comparison is made between calculated and nominal values of muzzle velocity sensitivity obtained from the Firing Tables (Reference b). One possible reason for differences observed is simply due to differences between propelling charge lots. Apart from this, the assumptions regarding the linear burning rate, mentioned above, also contribute to error.

GEORGE SCHLENKER
Operations Research Analyst

TABLE 1. CALCULATED SENSITIVITIES OF CHAMBER PRESSURE AND MUZZLE VELOCITY TO PROPELLING CHARGE TEMPERATURE IN THE M201 CANNON WITH THE M106 AND M650 PROJECTILES

Proj. Type	Charge Zone	P_{max} (ksi) at Chg Temp (°F)			Avg* $\partial p/\partial T$ (psi/°F)	V_o (f/s) at Chg Temp (°F)			Avg $\partial V_o/\partial T$ (f/s/deg F)
		0	70	145		0	70	145	
M106	1G	8.6	9.0	9.4	5.37	820	827	835	0.102
	2G	10.1	10.6	11.1	7.15	905	913	922	0.114
	3G	12.2	12.8	13.5	9.26	1007	1016	1026	0.128
	4G	16.0	16.9	17.8	12.49	1154	1164	1176	0.148
	5G	23.1	24.5	26.0	19.68	1377	1389	1402	0.177
	5W	13.2	14.7	16.6	23.40	1450	1477	1505	0.377
	6W	18.9	21.2	24.1	35.74	1683	1716	1748	0.446
	7W	27.5	31.1	34.7	49.39	1945	1982	2019	0.512
M650	1G	8.3	8.6	8.9	3.92	811	818	826	0.101
	2G	9.7	10.1	10.5	5.61	896	904	912	0.108
	3G	11.6	12.2	12.8	7.72	997	1005	1014	0.123
	4G	15.1	15.8	16.6	10.48	1142	1152	1162	0.143
	5G	21.7	23.0	24.2	17.21	1361	1373	1386	0.172

* Average over the temperature range -- 0 to 145 deg F.

TABLE 2. COMPARISON OF CALCULATED AND EXPERI-
MENTAL VALUES OF VELOCITY SENSITIVITY
TO PROPELLING CHARGE TEMPERATURE
IN THE M201 CANNON WITH THE M106 PROJECTILE

Charge Zone	Temperature (deg F)	Calc. ΔV_o (f/s)	Tabulated* ΔV_o (f/s)	V_o at 70°F (f/s)
1G	0	-7.0	-7.5	833
	145	7.8	9.2	
2G	0	-8.0	-8.5	912
	145	8.6	9.8	
3G	0	-8.9	-9.5	1012
	145	9.7	11.2	
4G	0	-10.4	-10.8	1156
	145	11.1	12.0	
5G	0	-12.5	-12.5	1388
	145	13.2	14.4	
5W	0	-27.4	-23.3	1464
	145	27.3	26.4	
6W	0	-32.4	-27.2	1708
	145	32.2	30.3	
7W	0	-37.2	-30.5	1995
	145	37.0	34.1	

* Firing Tables No. FT 8-Q-1, HQDA, Jan 76, title: Cannon,
8-Inch Howitzer, M201 on Howitzer, Heavy, Self-Propelled,
8-Inch, M110A1 Firing Projectile, HE, M106.
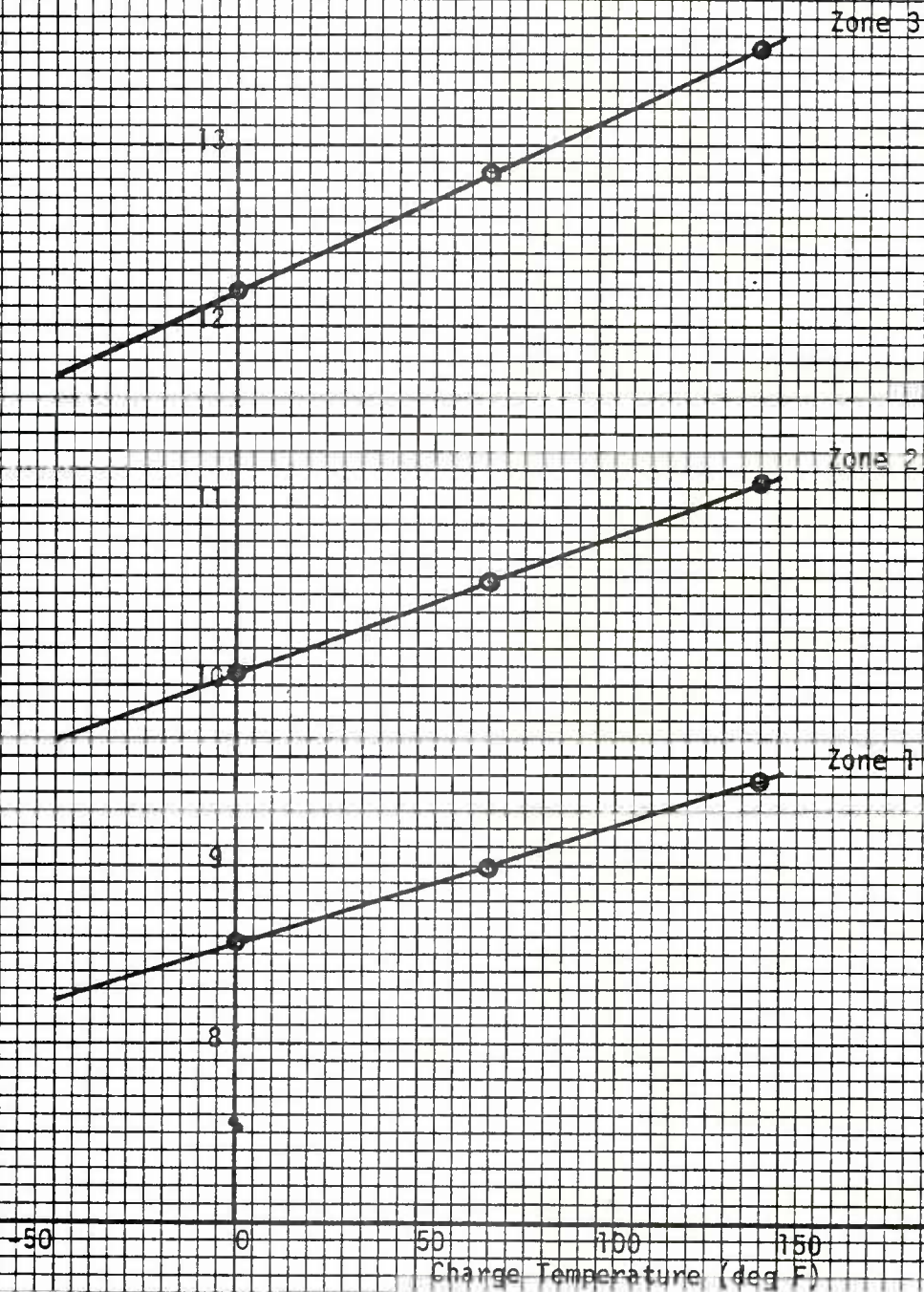
Figure 1a.   Peak Chamber Pressure Versus Propelling Charge
Temperature with the M106 Projectile in the M201 Cannon.
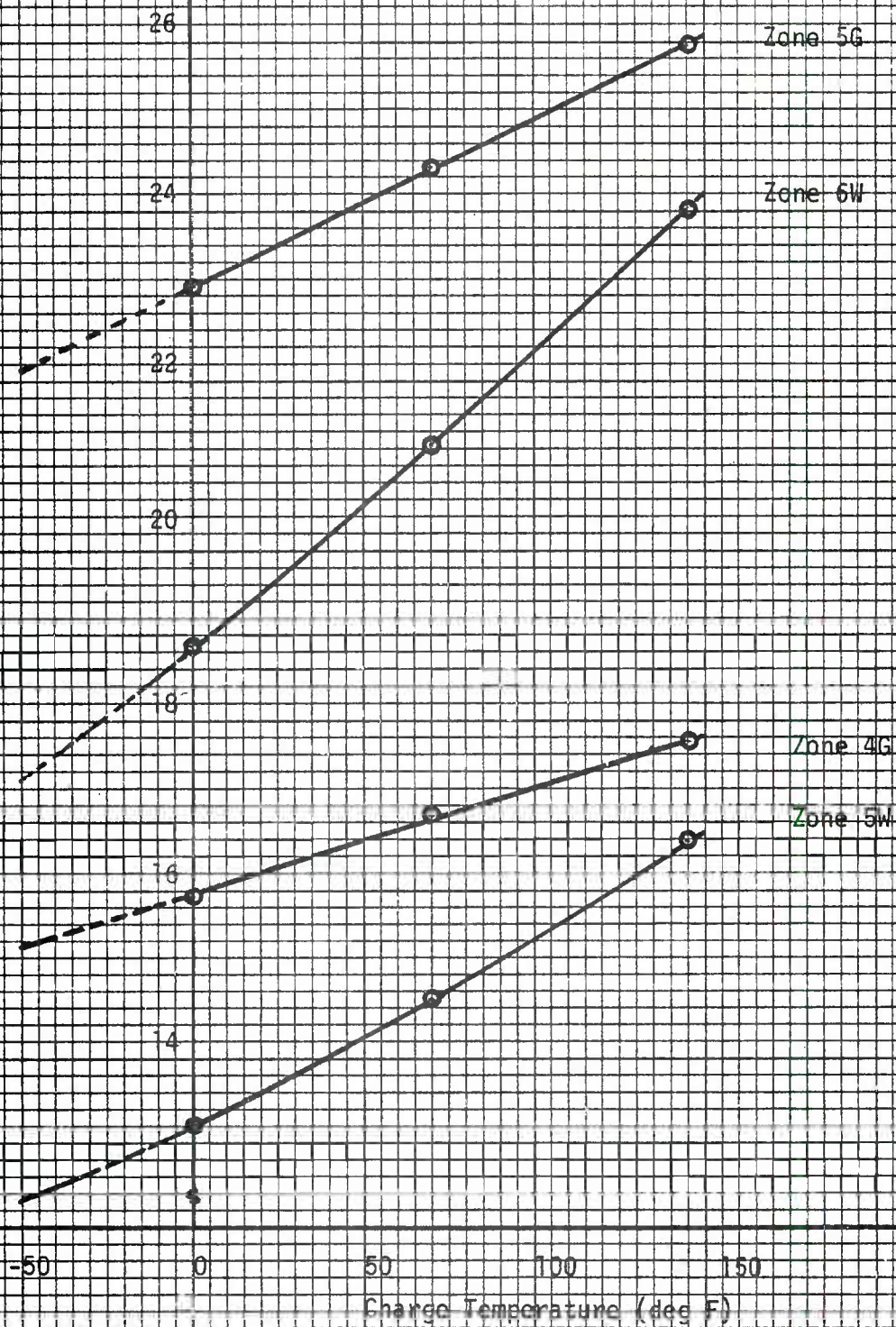
Figure 16. Peak Chamber Pressure versus Propelling Charge Temperature with the M106 Projectile in the M201 Cannon.

69

Figure 2a. Muzzle Velocity Versus Propelling Charge Temperature with the M106 Projectile in the M201 Cannon.

PM-M1—10 X 10 TO 1 INCH
10TH LINE HEAVY
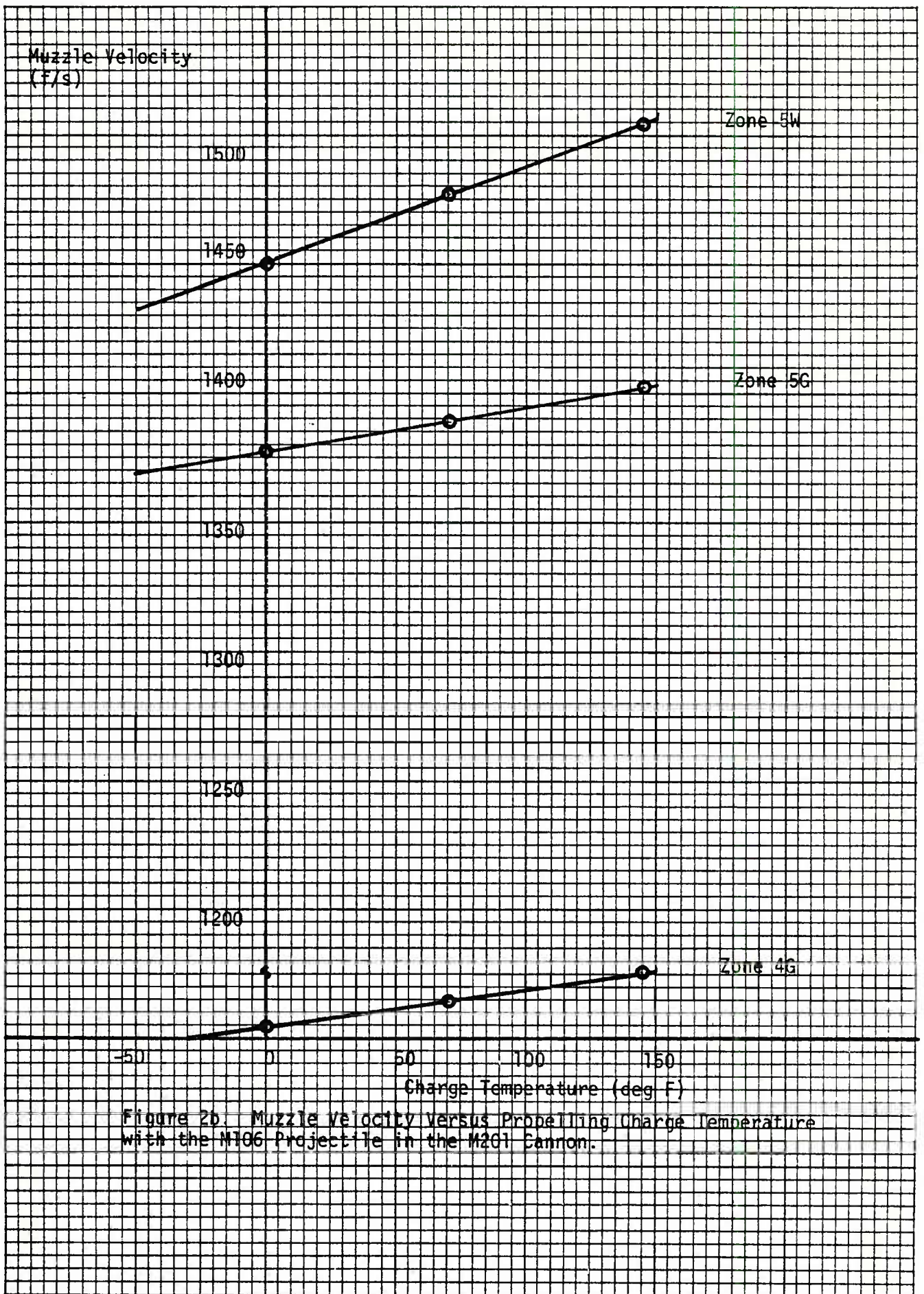
Figure 2b. Muzzle Velocity versus Propelling Charge Temperature with the M106 Projectile in the M201 Cannon.

<u>Memorandum for Record</u>

INTERIOR BALLISTICS

OF THE

M106, M650 AND M422 PROJECTILES

IN THE

M110A2 HOWITZER

WHEN FIRED FROM FALLBACK POSITIONS

George Schlenker

DRSAR-PEL   11 December 1979

MEMORANDUM FOR RECORD

SUBJECT: Interior Ballistics of the M106, M650, and M422 Projectiles in
           the M110A2 Howitzer When Fired From Fallback Positions

1. Reference:

    a. Conversations between LTC Stiehl, DRCPM-NUC-M (RIA), and George
Schlenker, DRSAR-PEL, Nov 79, subject as above.

    b. Proceedings of In-Process Review, DRCPM-M110E2, 10 Sep 79, subject:
M110 Cannon Damage Study.

    c. Projectile Damage Annex to TPR, DRSAR-PEL, 5 Oct 79, subject:
TECOM Project No. 2-MU-003-106-026.

    d. Firing Record No. P-82733, TECOM, APG, 29 Nov 78, subject: Malfunc-
tion Investigation Projectile, 8-Inch, M106 in M201 and M2A1 Howitzer Tubes
(Projectile Fallback).

    e. Report No. 1375, MTD Jefferson PG, May 77, title: Artillery Ammu-
nition Master and Reference Calibration Chart.

2. Background

    The study reported in this memorandum grew out of the Reference a conver-
sations. The request to study the interior ballistics of the M422 projectile
when fired from fallback is motivated by concern over the risk of catastrophic
damage to the projectile (and weapon) when fired in this manner. Previous
emphasis in fallback studies in the M110/M110A2 weapon system had focused
on damage to the cannon. Following an in-process review (IPR) of the Cannon
Damage Study in Sep 79 (Reference b), increased attention was given the risk
of damaging the projectile when firing from fallback. This increased empha-
sis is illustrated by a proposed test program request (TPR) (Reference c),
suggested by the M110A2 system manager, for investigating the frequency and
type of damage incurred by each of the following types of projectiles fired
from fallback: M106, M650 and M509. Although the M422 was omitted from
this TPR, the present study is a first step in assessing the risk of damage
to this projectile.

3. Present evidence for the kind of damage to the projectile expected
when firing from fallback comes from Reference d. In firing an inert
M106 projectile in hard* fallback at zone 2, smear camera coverage record-
ed a separated fuse and a cracked projectile ogive. From the foregoing,
considerable interest has been generated in describing the collision
between projectile and cannon when firing from fallback. This memorandum
describes the relative velocity of projectile and tube at first major
collision when the area on and near the front bourrelet first contacts the
rifling. Also calculated and displayed is the peak axial force arising
from this interaction. For comparative purposes results are obtained for
the three projectile types: M106, M650, and M422.

4. Methodology

    Ballistic calculations were made using the ARRCOM interior ballistics
simulation for the M110 and M110A2 howitzer systems. This computer model
had been developed during CY 79 to analyse the performance of the howitzer
with the M106 projectile fired from both well seated positions and from
fallback using the M1 and M2 propelling charges. To accommodate the needs
of this study, changes** were made to the program to facilitate the analysis
of other projectiles and other propelling charges, including the multi-
grain M80 charge.

5. Phenomena simulated in this program include: (1) the burning of black
powder in the base pad igniter with accompanying change in black powder
grain size and unburnt mass; (2) heat transfer to and ignition of the main
propelling charge; (3) heat loss to the projectile and cannon with conduction
of heat within the materials; (4) mixing of the gas components -- air, igniter
gas, and charge gas -- producing the thermochemistry of the mixture; (5) gas
mass loss past the obturator (blowby) throughout the interior ballistic
cycle; (6) burning of the propellant grain components with associated grain
dimensional change; (7) pressurization of the area behind the obturator;
(8) development of forward pressure resisting projectile motion due to blow-
by and compression of the gas in front of the projectile; (9) axial accele-
ration of the projectile; (10) acceleration of the unburnt charge; (11)

----

*   When fallback occurs abruptly from a nearly seated position at a high
    quadrant elevation, viz, 1150 mils.
** Projectile and charge data were formerly represented in DATA statements.
    With the requirement to simulate several other projectile and propelling
    charge types, the program was restructured to transmit projectile and charge
    data through COMMON statements from subroutines to the main program. Addi-
    tional program changes were required to accommodate the use of charges
    having a mixture of grains from different propellant lots (having different
    thermochemistry), as is the case for the M80 propelling charge.

SUBJECT: Interior Ballistics of the M106, M650, and M422 Projectiles in
           the M110A2 Howitzer When Fired From Fallback Positions

rearward acceleration of the recoiling parts; (12) development of axial
resisting forces on the projectile generated by interaction with the gun
tube. The pitch and transverse dynamics of the projectile are, specifi-
cally, not simulated.

6.   Due to its extraordinary nature in interior ballistics, the force of
interaction between projectile and tube during collision merits delineation
here. Empirical evidence regarding damage to the lands of the M201 cannon
indicates that the M106 projectile, typically, plastically deforms the
driving surface of the lands over a printed area, A_{cln}, which subsequently
fails mechanically. (A_{cln} is approximately 2 (in^2).) This collision area
experiences the material yield stress, σ_{yld},* during the interaction. Thus,
an empirical estimate of the peak interfacial lands loading experienced in
the M201 cannon - M106 projectile interaction is just

$$F_n = A_{cln}\ \sigma_{yld}\ .$$

The axial force associated with F_n is

$$F_{zo} = F_n\ (\sin \alpha + \mu \cos \alpha)$$

with μ the coefficient of friction and with α the helix angle of the rifling
of twist T, given by

$$\alpha = \tan^{-1}(\pi/T)\ ,$$

neglecting slip with respect to the rifling. However, this force can be
expected to be a function of the relative velocity, $\dot{z}$, of the colliding
bodies. To account for this, the model assumes that F_{zo} occurs at an
axial collision speed $\dot{z}_0$ ** (which can be estimated) and that the maximum
axial force due to an initial collision at speed $\dot{z}$ is a linear function
of $\dot{z}$. Thus,

$$F_{z\ max} = F_{zo}\ \dot{z}/\dot{z}_0\ .$$

If the projectile were being torqued to follow the rifling, an axial resist-
ing force would be generated F_{z1} :

$$F_{z1} = \frac{2\ \pi\ \rho^2}{T}\ \frac{(\sin \alpha + \mu \cos \alpha)}{(\cos \alpha - \mu \sin \alpha)}\ \frac{\ddot{z}\ M}{g}\ ,$$

---

* $\sigma_{yld} = 1.6\ 10^5$ (psi) , approximately.

** $\dot{z}_0 = 540$ (f/s) , as given in this program.

where

   ρ is the projectile radius of gyration in calibers,

   $\ddot{z}$ the relative axial acceleration, M is the projectile weight, and g
is the gravitational constant. If the projectile angular velocity exceeds
that required to follow the rifling during collision, the axial force due
to collision is assigned F_{z1} .

7. Data

     The author's previous experience with interior ballistic simulation
supports the claim that calculated ballistics will be in better agreement
with experimental firings if the specific chemical composition of a pro-
pellant lot -- as opposed to nominal composition -- is used to calculate
the thermochemical parameters of the combustion products and these para-
meters are used in the simulation. Experience also indicates that the
distribution of grain size actually measured from samples of the propellant
lot should be used for best results rather than using a fictitious single
average grain geometry. (The computer simulation actually uses nine grain
size classes obtained by treating grain dimensions as independent gaussian
random variables.) Lots of M1 and M2 propelling charges have been treated
in the manner described for previous studies.

8. For this study, data for the two propellant lots used in the 1976 lots
of M80 charges (PA-76E001A001/2) were used to calculate* the thermochemi-
cal parameters which characterize each propellant lot. Results of these
calculations are given in Table 1.

9. Data on the M80 propelling charge were,parenthetically, difficult to
obtain and contained inconsistencies. For example, the data on pages 48
through 51 of Reference e indicates that the zone 1 charge contains single-
perforated propellant with an 0.0375 (in) web, whereas information from
Radford Arsenal, the propellant producer, indicates that the correct des-
cription should have been seven-perforated propellant with a nominal
0.0360 - 0.0365 (in) web. Additionally, the web of the MP zone 2 and
zone 3 increments given in Reference e is incorrect. The value given
there is 0.055 (in) whereas the propellant lot acceptance data sheets
show an average web of 0.068 (in). Charge weight increments provided by
the PM-NUC were also incorrect. The correct values, found in Table 1,
were obtained from propellant acceptance sheets and confirmed by lot firing

---

*   Calculations use the Hirschfelder-Sherman method with chemical constants
    supplied by the Naval Ordnance Station, Indian Head.

records. Since the zones of the M80 charge consist of a mixture of pro-
pellant lots, values of the thermochemical parameters are adjusted for each
zone by taking a mass-weighted average of the lot-specific parameters.
These results are found in Table 2.

10.   During fallback, the projectile compresses the somewhat loosely bagged
propelling charge. Due to the great sensitivity of fallback interior
ballistics to initial position of the base of the projectile, it is impor-
tant to properly estimate the extent of propelling charge compression.*
The degree of compression depends upon the manner in which the projectile
falls back. If fallback is abrupt and occurs at a high quadrant elevation
(QE), compression of the charge is much greater than if the projectile
gradually slides back at a low QE. The former condition is referred to as
hard fallback and is the condition simulated here.

11.   In hard fallback on the M1 propelling charge, the stresses induced in
the bag can rupture bag seams. However, when rupture does not occur, the
resulting charge deformation appears to occur at nearly constant charge
volume, with charge diameter increasing to preserve volume. Based upon
experiments with compression in the M1 charge, axial compression of the
M80 charge at constant charge volume is expected to be limited by the
maximum diameter permitted by the chamber. The uncompressed and compress-
ed dimensions of the M80 charge assumed for this study are given in Table
3A. Table 3B displays the empirical basis for the assumption of constant
charge volume. Note that the different studies of charge compression have
yielded quite different results. This indicates that a substantial inherent
uncertainty exists regarding the initial position of the base of projectile
when fallback occurs. In the M201 cannon the presence of standoff lugs on
the breechface presents an additional complication. The one-inch deep lugs
can be expected to partially penetrate the charge during fallback compres-
sion. A penetration of 0.5 inch is assumed here.

12.   The parameters which characterize the projectile in the interior ballis-
tics program are shown in Table 4. Of particular significance for fallback
is the maximum diameter of the obturator and its axial position. The leak-
age of combustion gas is controlled by the minimum annular cross section
over the projectile between the cannon internal profile and the projectile.

---

* The difference in ballistics associated with a highly compressed as
  opposed to a moderately compressed charge is marked. In the YPG fall-
  back tests reported in Reference b, the two conditions were produced
  experimentally. With the M106 projectile and the M1/Z2 charge, hard
  fallback produced a peak pressure of 18.6 ksi, whereas a peak pressure
  of 15.0 ksi occurred with a nearly uncompressed charge at 200 mils QE.

DRSAR-PEL   11 December 1979
SUBJECT: Interior Ballistics of the M106, M650, and M422 Projectiles in
           the M110A2 Howitzer When Fired From Fallback Positions

Generally, this throat occurs at the forward lip of the obturator max dia-
meter. The projectile volume behind this position is considered in calcu-
lating the free volume for the gas. All axial dimensions pertaining to
the gun projectile interface -- ZSEAT, ZCLN -- are referenced to the refer-
ence end of the gun tube on cannon drawings.

13. Results

     An abbreviated set of ballistic output parameters, calculated for
both fallback and well seated projectiles is displayed in Tables 5 and 6.
For the fallback case a relatively limited number of applicable experi-
mental firings exists. Peak chamber pressure and muzzle velocity have
been the only comparable variables successfully measured in experimental
firings. Attempts to measure collision accelerations have been unsuccess-
ful. The simulated results which can be compared are in substantial
agreement with the pressures and velocities obtained from the Reference d
Fallback Tests for zones 2 through 5. Calculated velocities are generally
somewhat in excess of those measured (20 to 30 f/s) but peak pressures
agree within the measurement error. As expected, there is better agree-
ment with experiment for the case of well seated projectiles.

14. The ballistics for well seated projectiles are offered here primarily
for comparison with those for fallback. For the M650 and M422 projectiles
there have been no fallback firings to validate the simulated results.
However, these projectiles do not appear to introduce any new phenomena
with respect to fallback interior ballistics. Consequently, the accuracy
of results is considered comparable to that with the M106 projectile.
One should note that the collision velocity at first major collision may
not be the best measure of the severity of the interaction because this
model does not consider the effects of pitching and transverse motions.
Using axial collision velocity as the measure of severity, one can assert
that the worst case for the M106 and for the M650 occurs at zone 2. For
the M422 projectile the worst case occurs at zone 1 of the M80 propelling
charge. This fact is due primarily to the longer travel to first colli-
sion at zone 1 -- 13.5 (in) versus 8.1 (in) at zone 2 and to the approxi-
mately 1 (in) travel at start of ignition of the M80 propelling charge.

15. Graphical results for the worst-case zones are included in Annex 1.
A glossary of the ballistic variables displayed in Annex 1 is given in
Table 7. Fallback simulations for the M106, M650 and M422 projectiles are
presented first, in that order followed by the standard (well seated)
results for each of these projectiles for the same zones. In discussing
the graphical results the following points are noted. The interval from
the time at which the black powder igniter starts to burn until the main

charge is ignited is shorter for the fallback case than for the standard
for all projectiles. The projectile has not traveled very far at the
instant of ignition -- typically, about an inch. For all projectiles
there is a shorter risetime to peak pressure for fallback than for the
corresponding standard case. The pressure and acceleration curves for
standard ballistics are seen to be quite smooth after shot start. How-
ever, for the fallback case two major disturbances in the smoothness of
acceleration are evident following the occurrence of peak pressure. The
discontinuities are due, first, to the forward bourrelet striking the
rifling, which starts projectile spinup, and, second, to the rotating
band engaging the rifling. There is a significantly greater peak pres-
sure in the fallback case than in the standard case. For example, at
zone 2 with the M106 projectile, in hard fallback the peak pressure is
18.8 ksi versus 10.6 ksi in the standard case. With the M650 projectile
using the M1/Z2 charge, fallback peak pressure exceeds 17 ksi whereas
standard peak pressure is about 10 ksi. The amplification of pressure
relative to standard due to fallback is not as great with the M422 using
the M80/Z1 -- 12.0 versus 9.8 ksi. For the M106 and M422 projectiles,
the calculated muzzle velocity is significantly higher (about 50 f/s) in
fallback than in the standard case. However, for the M650 projectile the
calculated muzzle velocity is not greatly different in the two cases.
The likely cause of the lower velocity for the M650 than for the M106
projectile at the same zone in fallback is the greater mass loss -- 1.66
versus 1.15 lbm -- due to the smaller max obturator diameter of the M650.
In fact, without the large amount of blowby the muzzle velocity in fallback
would be much greater than it is.*

Summary

16. This study examines the ballistics of several projectiles - M106,
M650, and M422 fired from both fallback and well seated positions in the
M201 cannon. Motivation for this study is a growing concern for the
safety of these projectiles (and weapon) when firing from fallback. The
ballistic simulation produces estimates of the state of the projectile
at first major collision with the gun tube. The largest axial collision
velocities are produced with zone 2 of the M1 propelling charge using M106
and M650 projectiles. These collision velocities are 558 and 486 f/s, res-
pectively, the former being sufficient to cause damage to the M106. For
the M422 projectile, the worst case occurs with zone 1 of the M80 pro-
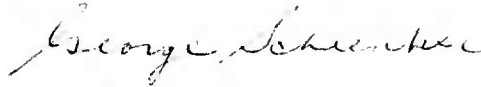pelling charge where the calculated collision velocity is 389 f/s. Graphs

---

* Experimental muzzle velocities with M106 fallback are 20 to 30 f/s
  greater than standard. Because of this relatively small incremental
  velocity and a higher drag, the change in range due to fallback may
  go unnoticed. Change in range is not a reliable indication of fallback.

DRSAR-PEL   11 December 1979
SUBJECT: Interior Ballistics of the M106, M650, and M422 Projectiles in
           the M110A2 Howitzer When Fired From Fallback Positions

of ballistic variables are presented in Annex 1 to display the differences
between fallback and standard cases for each of the projectile types.

                                   George Schlenker

1 Incl   GEORGE SCHLENKER
Annex 1   Operations Research Analyst

TABLE 1

COMPARISON OF NOMINAL THERMOCHEMISTRY OF
M6 PROPELLANT WITH THAT USED IN THE
M80 PROPELLING CHARGE

Propellant Composition

Active Ingredients	Weight Fraction		
	Nominal	RAD 69535	RAD 69693
Nitrocellulose (13.15%N)	0.8689	0.8707	0.8709
Dinitrotoluene	0.0975	0.0976	0.0988
Dibutyl phthalate	0.0336	0.0317	0.0303
Sum	1.0000	1.0000	1.0000

Additives	Nominal	RAD 69535	RAD 69693
Diphenylamine	0.0091	0.0100	0.0112
Potassium sulphate	0.0099	0.0109	0.0110
Water (liq)	0.0050	0.0080	0.0044
Ethyl alcohol (resid.)	0.0090	0.0021	0.0134
Sum	0.0330	0.0310	0.0400

Thermochemical Parameter	Nominal	RAD 69535	RAD 69693
T_v (deg K)	2549.0	2597.7	2517.8
γ	1.2544	1.2524	1.2552
n (gm mol/gm)	0.04405	0.04355	0.04426
F (ft lbf/lbm)	0.3122×10^6	0.3146×10^6	0.3099×10^6
η (in^3/lbm)	30.134	29.881	30.232
M (gm/gm mol)	22.703	22.963	22.593

TABLE 2

VARIATION OF THERMOCHEMICAL
PROPERTIES WITH ZONE IN THE
M80 PROPELLING CHARGE USING
PROPELLANT LOTS RAD69535 AND RAD69693

Parameter (dimension)	Zone 1	Zone 2	Zone 3
charge mass (1bm)	7.456	15.925	31.206
mass fract. of zone 1 propellant	1.0000	0.4682	0.2389
T_v (deg K)	2598	2555	2537
γ	1.2524	1.2539	1.2545
n (gm mol/gm)	0.04355	0.04393	0.04409
F (10^6 ft lbf 1 lbm)	0.3146	0.3121	0.3110
n (in^3/lbm)	29.881	30.068	30.148
M (gm/gm mol)	22.963	22.766	22.681
grain OD (in)	0.2065	0.3745	
grain PD (in)	0.0215	0.0346	
nom. web (in)	0.0355	0.0677	
grain length (in)	0.4800	0.8610	
std dev OD (%)/(10^{-3}in)	3.32/6.8	1.65/6.2	
std dev. len. (%)/(10^{-3}in)	1.65/7.9	1.18/10.2	
α, burn rate expon.	0.875		
β, burn rate at 1 ksi (in/s)	0.235		
$\partial\alpha/\partial T$ (deg K^{-1})*	-6.8^{-4}_{10}		
$\partial\beta/\partial T$ (in/s/deg K)*	1.0^{-3}_{10}		

* Inferred from strand burner data given in SPIA Manual.

TABLE 3A

ESTIMATE OF COMPRESSION IN THE M80 PROPELLING CHARGE

Dimensions of the M80 Propelling Charge Uncompressed Diameter 7.75 (in)
Uncompressed Total Length 24.25 (in)

Parameter	Zone 1	Zone 2	Zone 3
Incremental Length (in)	5.20	6.50	12.55
Overall Uncomp. Length (in)	5.20	11.70	24.25
Est. Overall Comp. Length (in)	4.32	9.73	20.16
Initial Position in M201 Cannon (in) (ZSTART)	7.6	13.0	23.5

TABLE 3B

ESTIMATES OF COMPRESSION IN THE
M1, 8-INCH PROPELLING CHARGE

Zone No.	Uncompr.[1] Chg. Length (in)	Initial Analytic Est. Compr. Length (in)	Compressed Length Experimental Ests.	
			[2]	[3]
1	9.25	8.25	7.50	5.25
2	11.00	10.25	8.80	6.25
3	13.25	11.50	10.75	11.50
4	17.00	14.50	13.75	15.25
5	22.00	19.50	19.00	15.00

(1)   APG Firing Record P82733, Sep 78.

(2)   Based upon compression of lot IND 69797 with a static load of 150 lb. in a 8.5 (in) cylinder. Reference: Mario Miranda, YPG, Jul 79.

(3)   Based upon the ARRADCOM Charge Damage Assessment Tests using hard fallback at 1150 mils. Reference: Carl Gardner, DRDAR-LC, Aug 79.

Using the uncompressed length[1] and associated nominal max diameter of 6.5 (in) and the experimental[2] compressed length, the following are the constant-volume charge diameters after compression:

Zone	Diam. (in)
1	7.2
2	7.3
3	7.2
4	7.2
5	7.0

The initial position of the base of the projectile resting on the propelling charge after a hard fallback from a seated position in the M201 Cannon is estimated to be 3.3 (in) plus the compressed charge length, as measured from the reference end of the gun tube. This value assumes that the standoff lugs on the breech penetrate to 0.5 (in) depth into the propelling charge.

TABLE 4

PROJECTILE PARAMETERS USED IN THE INTERIOR
BALLISTICS OF FALLBACK PROGRAM

Description of Parameter	Program Name	Projectile Type		
		M106	M650	M422
Projectile mass (lbm)	EMP	200	199	242
Radius of gyration (cal)	RGRYN	0.3842	0.3887	0.3315
Dist. from base of proj. to max diam. of obturator (in)	ZBOPRB	6.49	3.92	3.19
Volume aft of obturator (in^3)	VBOP	294.4	115.2	141.0
Max diam. of obturator (in)	DIAOBT	8.28	8.21	8.35
Width of band (in)	WDBAND	1.94	2.04	3.25
Dist. from obturator to seated position (in)	ZRBSET	0.00	2.04	2.13
Diameter of seat (in)	DIASET	8.28	8.15	8.15
Dist. from reference end of tube to base of seated proj. (in) in M201 cannon	ZSEAT	36.30	38.06	38.73
in M2A2 cannon		28.26	30.02	30.78
Dist. from reference end of tube to base of proj. at collision (in) in M201 cannon	ZCLN	28.7	25.7	21.1
in M2A2 cannon		20.7	17.7	13.2

TABLE 5

SUMMARY OF CALCULATED INTERIOR BALLISTICS
IN THE M201 CANNON FOR SEVERAL PROJECTILES
FIRED FROM HARD* FALLBACK

Simulated conditions are given below.

Proj. Type	Chg. Type	Zone	Peak Press (ksi)	Muzzle Velocity (f/s)	Collision Velocity (f/s)	Axial** Col Force (k lbf)
M106	M1	1	16.1	865	539	135
		2	18.8	959	558	140
		3	21.6	1066	552	138
		4	26.3	1218	523	131
		5	31.1	1428	275	110
M650		1	14.5	815	473	119
		2	17.2	910	486	122
		3	20.0	1019	467	117
		4	24.6	1174	411	109
		5	29.8	1395	93	113
M422	M80	1	12.0	936	389	109
		2	19.7	1392	329	110
		3	36.7	1995	0	19

* Abrupt drop from the seated position at 1150 mils QE.
** The ratio of axial to cross-axial collision force in the M201 cannon is 0.4237 under the assumption that the projectile is following the rifling.

Conditions:

Propelling charge temperature -- 70 deg F.
Cannon condition -- new.
M1 charge lot no IND 69797.
M80/Z1 propellant lot no RAD 69535.
M80/Z2/Z3 propellant lot no RAD 69693.

TABLE 6

SUMMARY OF CALCULATED INTERIOR BALLISTICS
IN THE M201 CANNON FOR SEVERAL
PROJECTILES FIRED FROM A SEATED* POSITION

Simulated conditions are given below.

Proj. Type	Charge Type	Zone	Peak Press (ksi)	Muzzle Velocity (f/s)
M106	M1	1G	9.0	827
		2G	10.6	913
		3G	12.8	1016
		4G	16.9	1164
		5G	24.5	1389
	M2	5W	14.7	1477
		6W	21.2	1716
		7W	31.1	1982
M650	M1	1G	8.6	818
		2G	10.1	904
		3G	12.2	1005
		4G	15.8	1152
		5G	23.0	1373
M422	M80	1	9.8	874
		2	14.5	1279
		3	29.3	1880

* Projectile is assumed to have been rammed 0.120 (in) beyond the
  initial contact position.

Conditions:

Propelling charge temperature -- 70° F.
Cannon condition -- new.
M1 charge lot no IND 69797.
M2 charge lot no BAJ 67951.
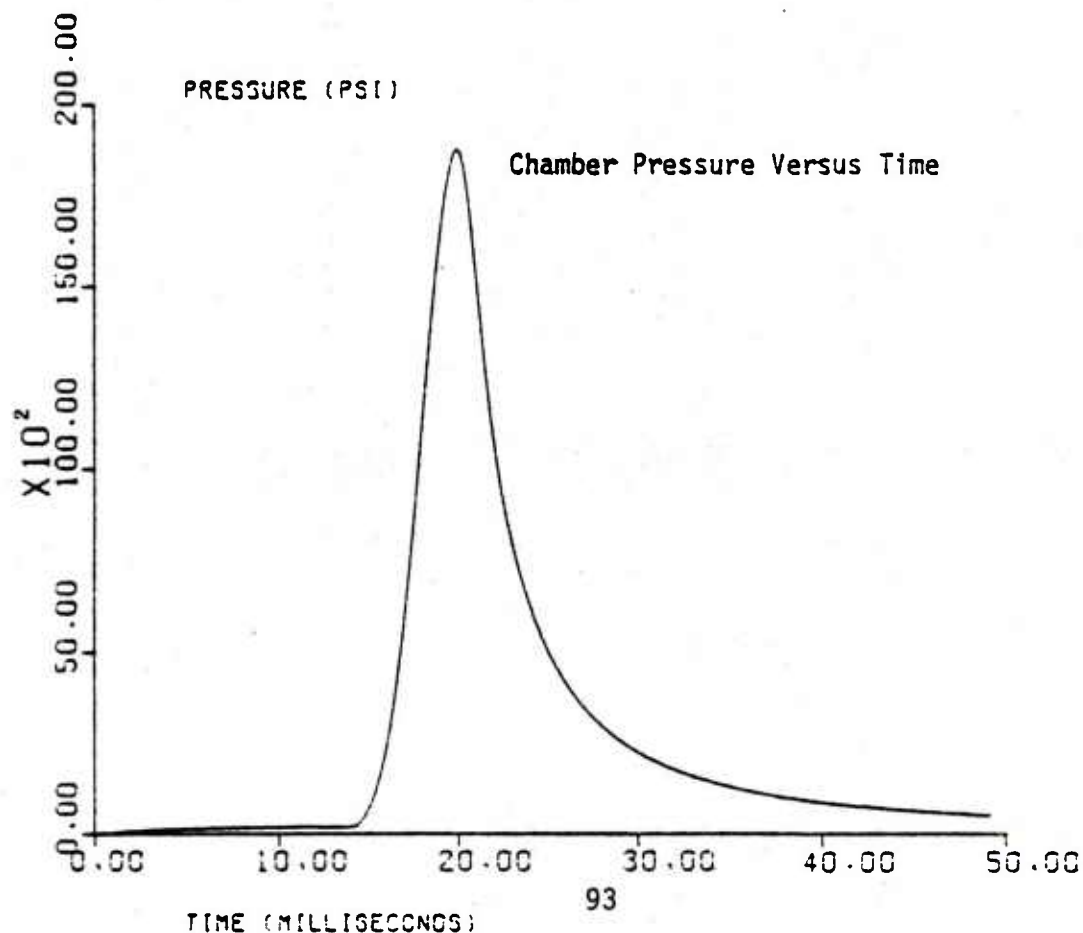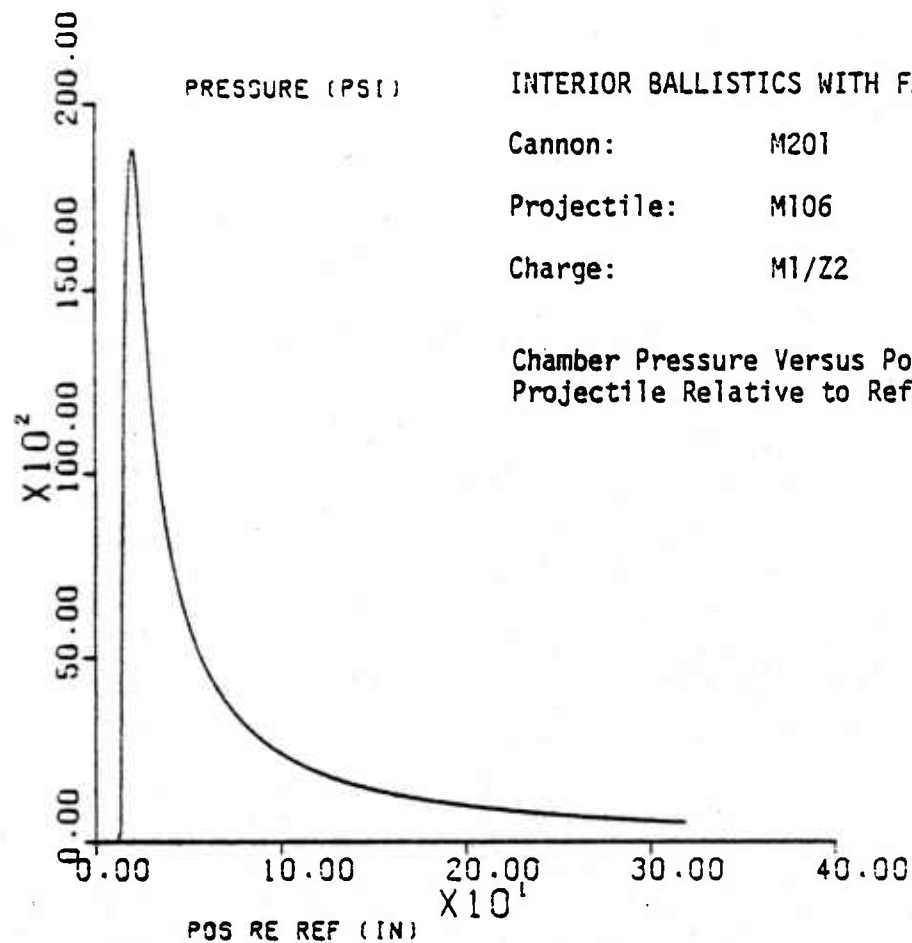M80/Z1 propellant lot RAD 69535.
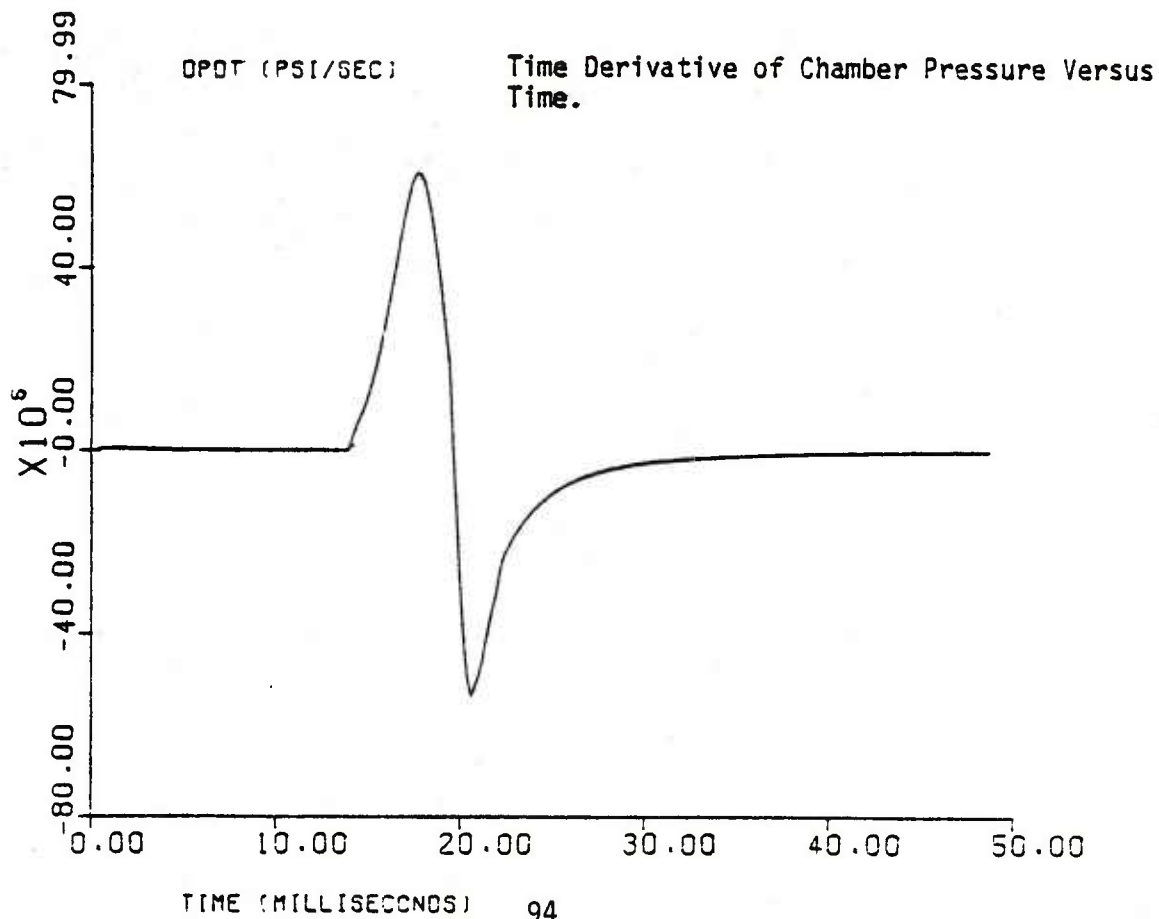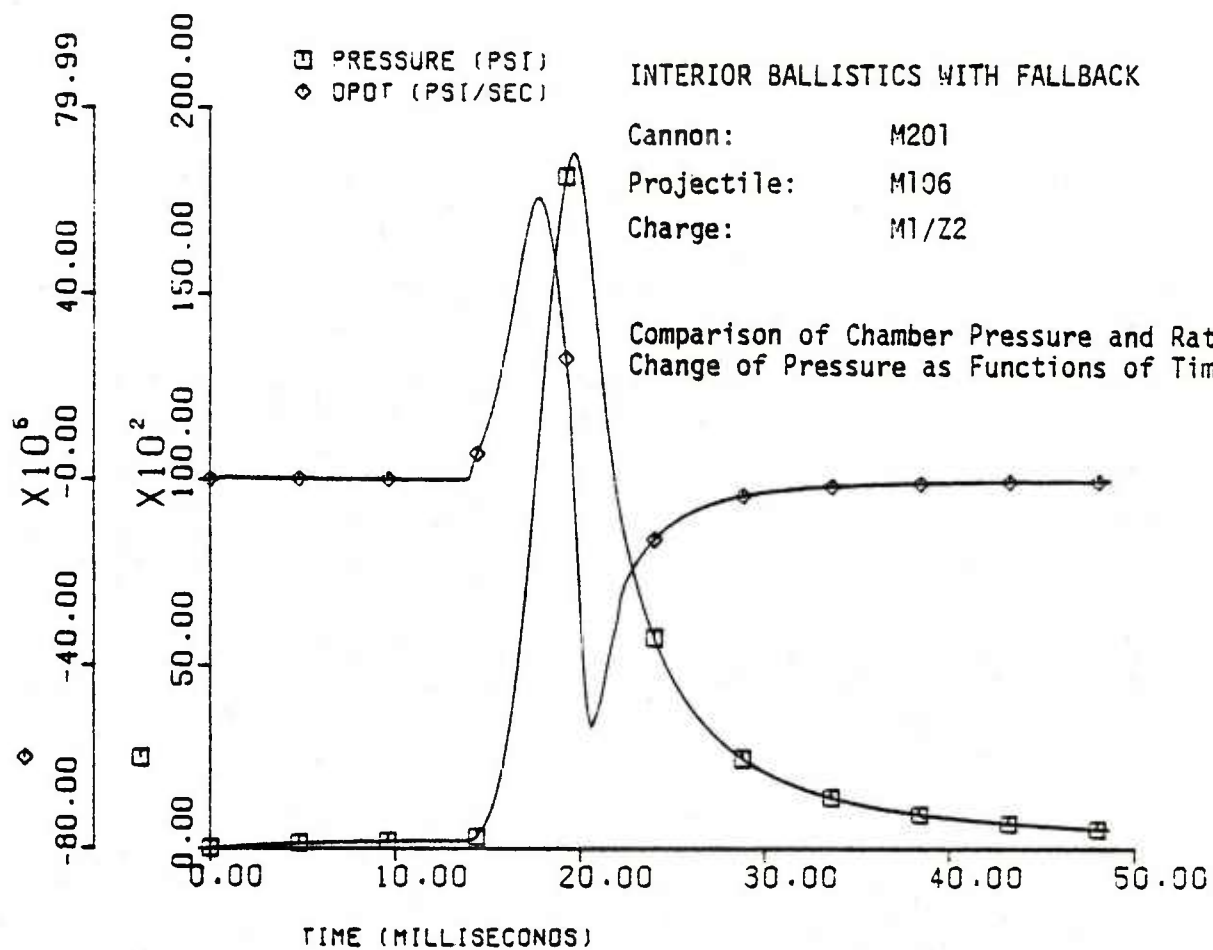M80/Z2/Z3 propellant lot RAD 69693.

TABLE 7

ABBREVIATIONS USED IN PLOTS OF
BALLISTIC SIMULATION OUTPUT

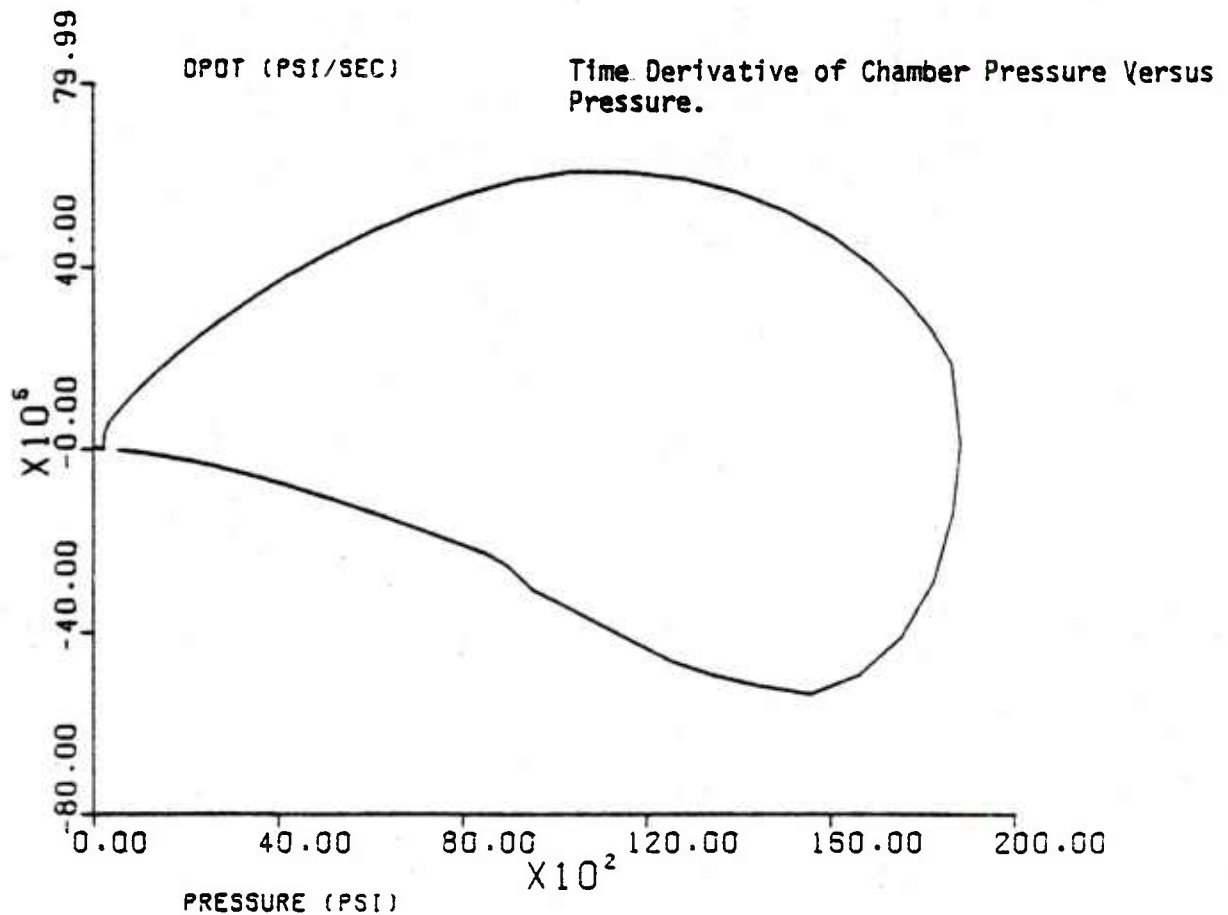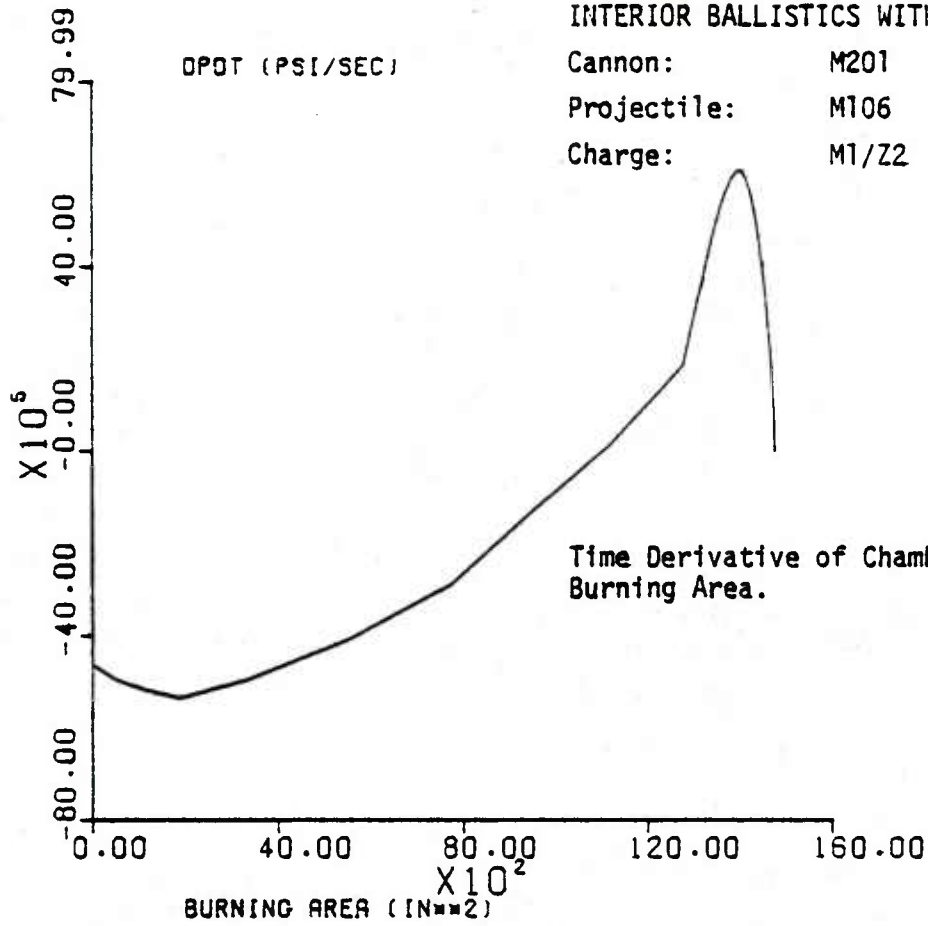| Label Used on Graphs	Detailed Description
PRESSURE	Space-mean or chamber pressure (psia)
DPDT	Pressure time derivative (psi/s)
ACCELERATION	Projectile axial acceleration (g)
GRAIN ID (ENDS)	Propellant gain inside diam. at ends of single perf. grain (in)
GRAIN OD	Propellant grain outside diam. for both SP and MP grain (in)
GRAIN ID (CNTR)	Propellant grain inside diam. at the center of single perf. grain (in)
CHG VOLUME	Volume of unburnt propellant in propelling charge (in^3)
BURNING AREA	Area of burning surface of propellant (in^2)
MASS LOSS	Mass of gas lost by escape past obturator (lbm)
MASS OF GAS	Mass of gas remaining behind projectile (lbm)
VELOCITY	Projectile velocity (f/s)
INTERNAL ENERGY	Internal energy of remaining gas (ft-lbf)
DISPLACEMENT	Displacement of projectile relative to initial position (in)
POS RE REF	Position of the base of the projectile relative to the reference end of the tube (in)
WALL TEMPERATURE	Temperature at surface of chamber wall (deg K)
TEMPERATURE	Space-mean temperature of gas (deg K)
HEAT LOSS	Thermal loss to cannon and projectile (ft lbf)
SPIN	Projectile rotational frequency (hz)

ANNEX 1
GRAPHICAL RESULTS OF
INTERIOR BALLISTICS FOR
M106, M650, AND M422 PROJECTILES
FIRED FROM FALLBACK AND
WELL SEATED POSITIONS IN
THE M201 CANNON

PRESSURE (PSI)
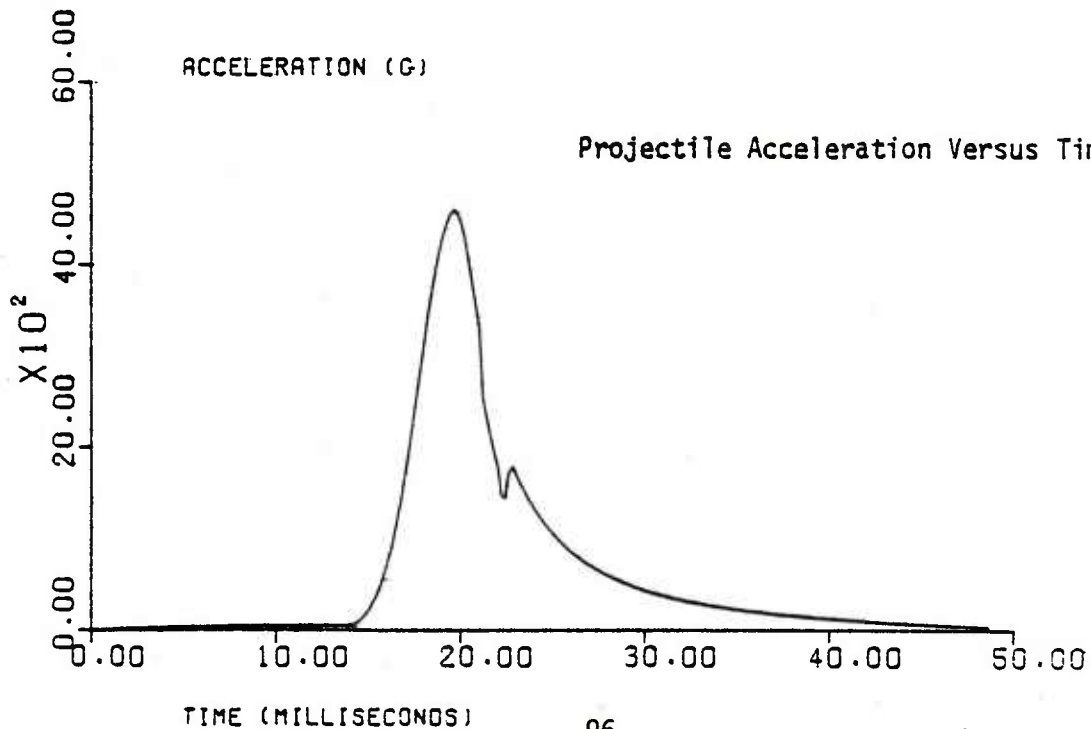
INTERIOR BALLISTICS WITH FALLBACK

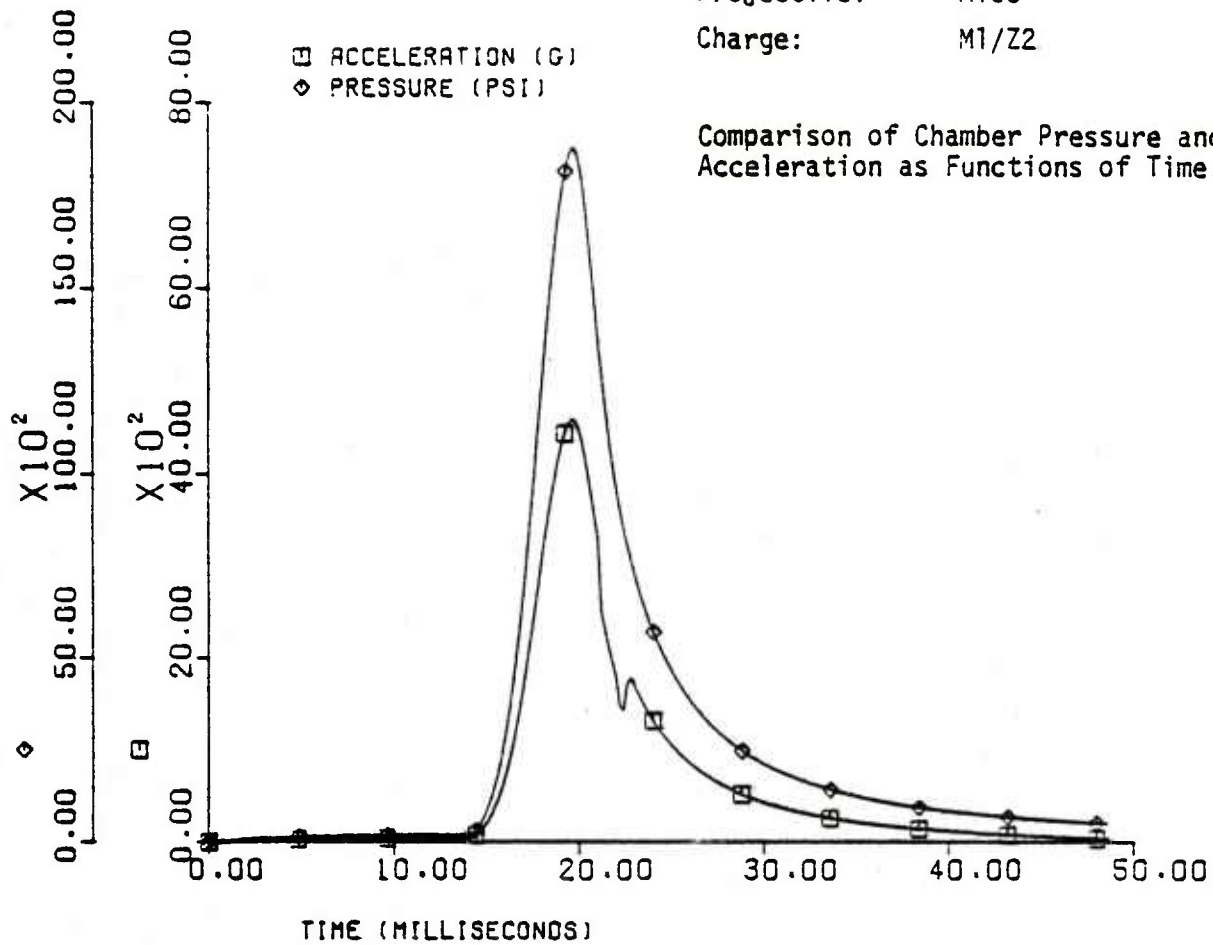Cannon: M201

Projectile: M106

Charge: M1/Z2

Chamber Pressure Versus Position of Base of
Projectile Relative to Reference End of Tube.

$X10^2$

POS RE REF (IN)

$X10^1$

PRESSURE (PSI)

Chamber Pressure Versus Time

$X10^2$

TIME (MILLISECONDS)

PRESSURE (PSI)
DPDT (PSI/SEC)
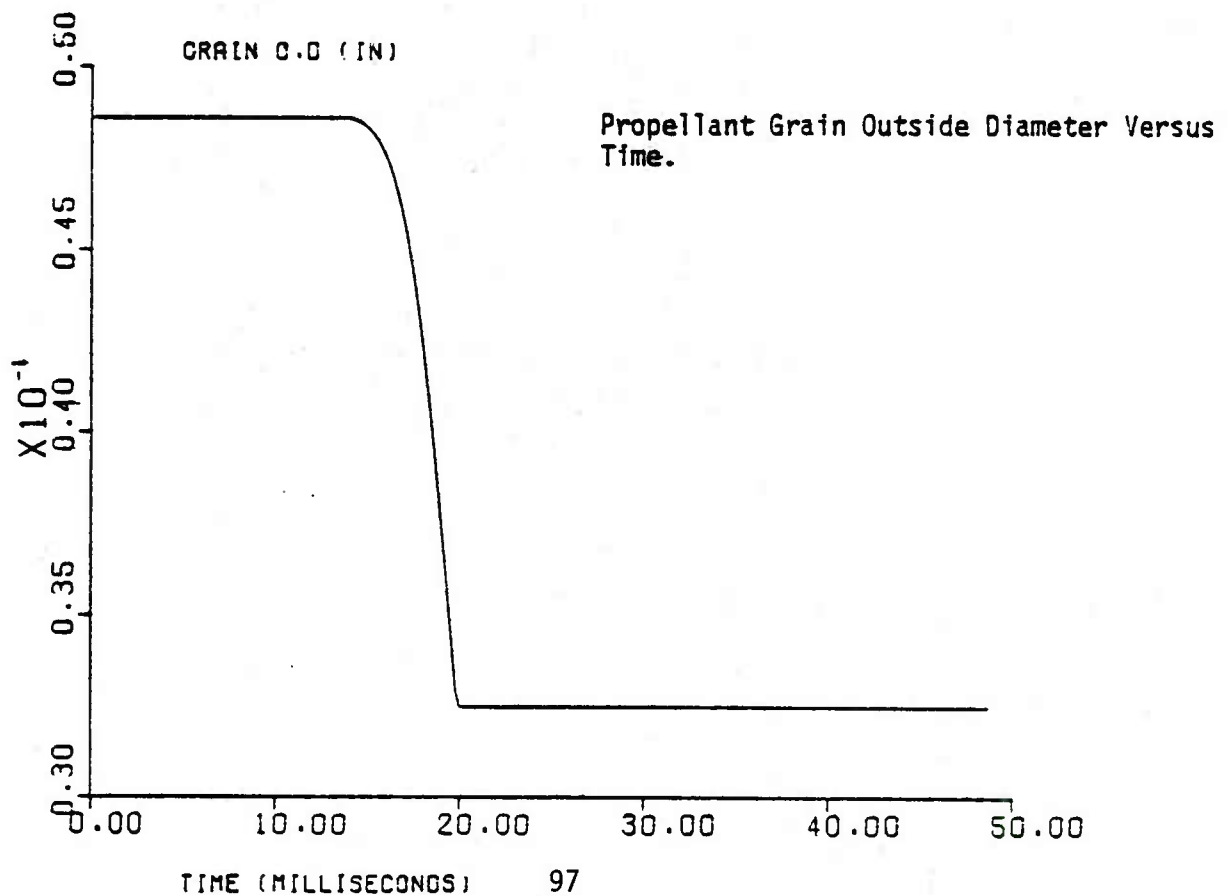
INTERIOR BALLISTICS WITH FALLBACK

Cannon: M201
Projectile: M106
Charge: M1/Z2

Comparison of Chamber Pressure and Rate of Change of Pressure as Functions of Time.

TIME (MILLISECONDS)

DPDT (PSI/SEC)

Time Derivative of Chamber Pressure Versus Time.

TIME (MILLISECONDS)   94

INTERIOR BALLISTICS WITH FALLBACK

Cannon: M201
Projectile: M106
Charge: M1/Z2

Time Derivative of Chamber Pressure Versus Burning Area.

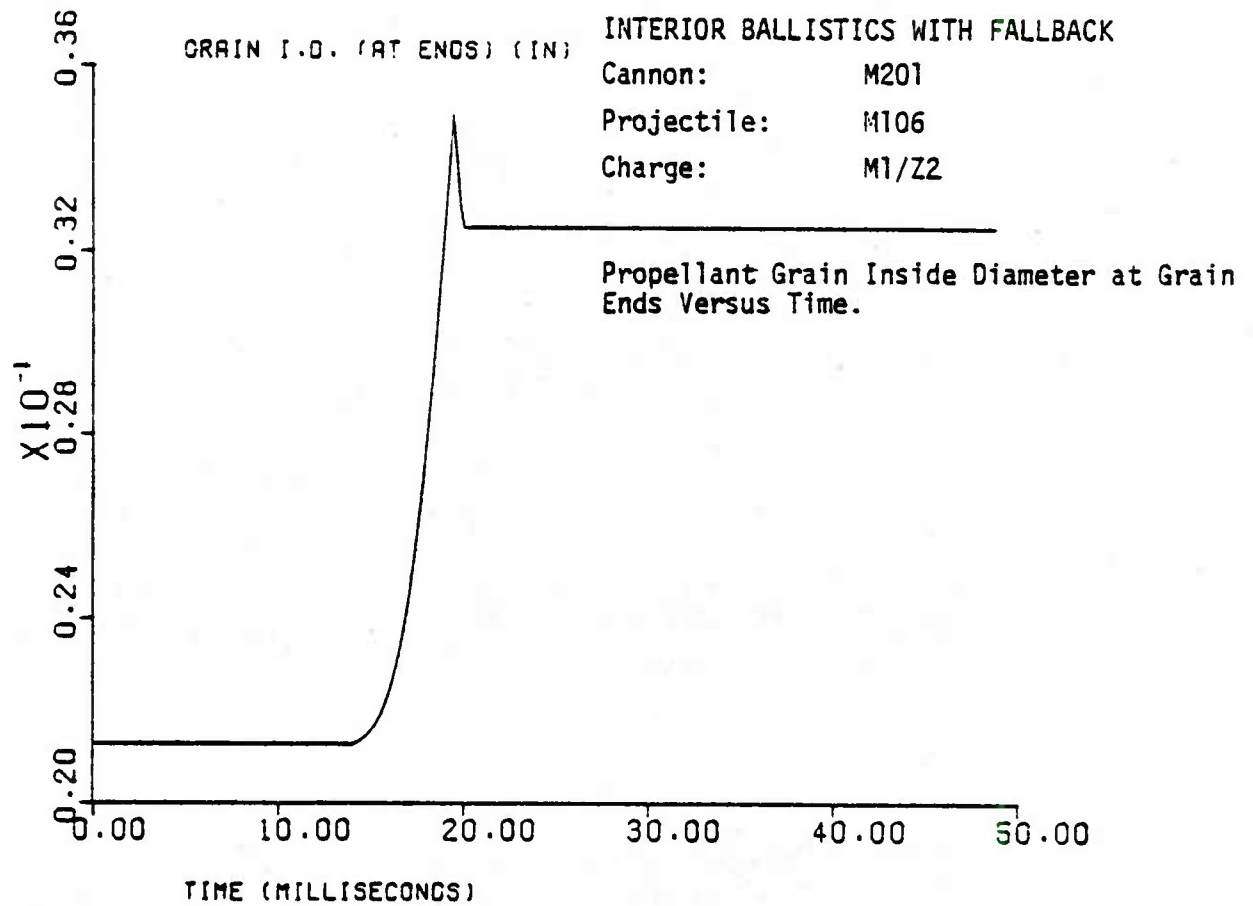Time Derivative of Chamber Pressure Versus Pressure.

95

INTERIOR BALLISTICS WITH FALLBACK

Cannon: M201

Projectile: M106

Charge: M1/Z2

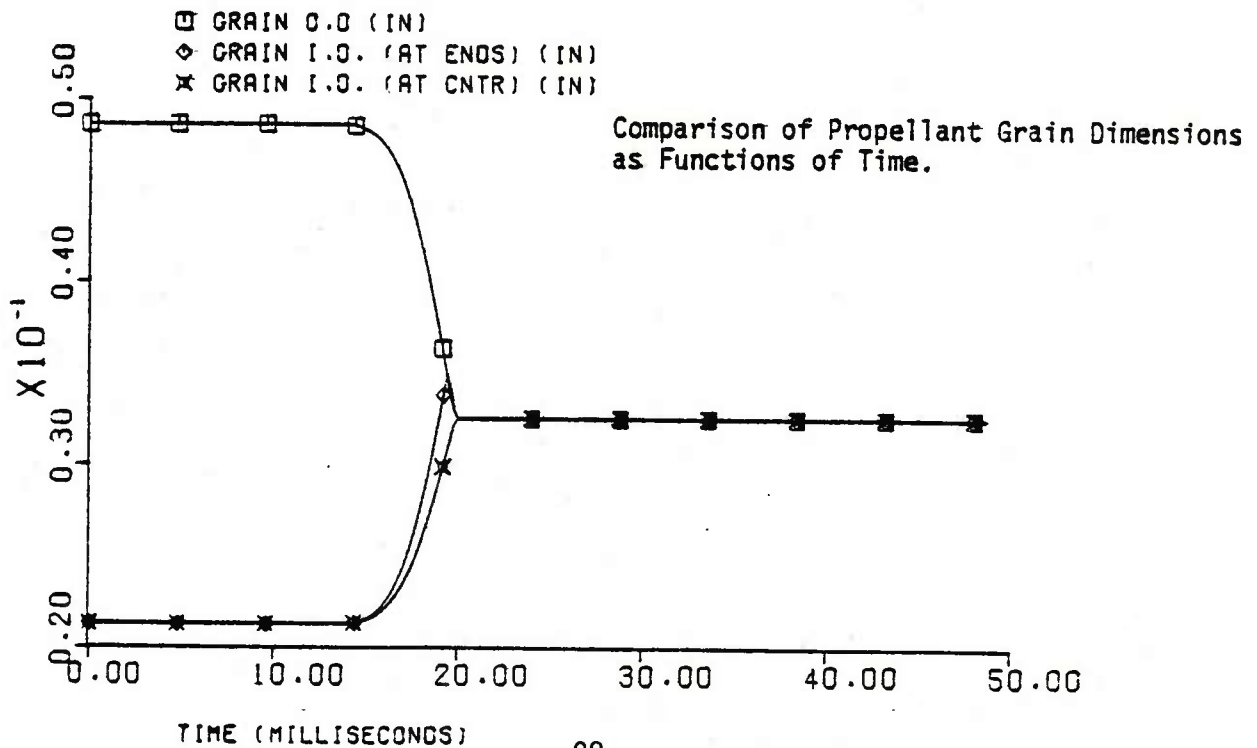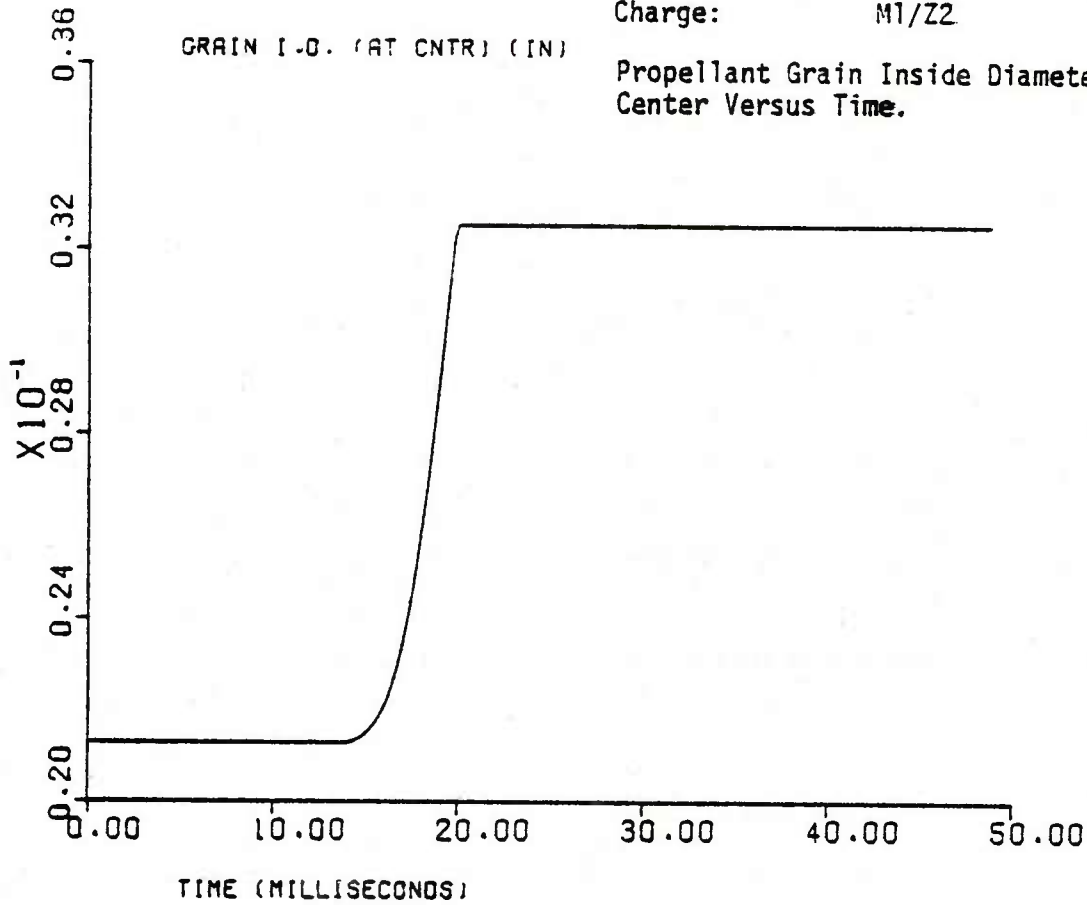Comparison of Chamber Pressure and Projectile Acceleration as Functions of Time.

☐ ACCELERATION (G)
◇ PRESSURE (PSI)

TIME (MILLISECONDS)

ACCELERATION (G)

Projectile Acceleration Versus Time.

TIME (MILLISECONDS)

96

GRAIN I.D. (AT ENDS) (IN)

INTERIOR BALLISTICS WITH FALLBACK

Cannon:	M201
Projectile:	M106
Charge:	M1/Z2

Propellant Grain Inside Diameter at Grain Ends Versus Time.

TIME (MILLISECONDS)

GRAIN O.D (IN)

Propellant Grain Outside Diameter Versus Time.

TIME (MILLISECONDS)   97

INTERIOR BALLISTICS WITH FALLBACK
Cannon: M201
Projectile: M106
Charge: M1/Z2

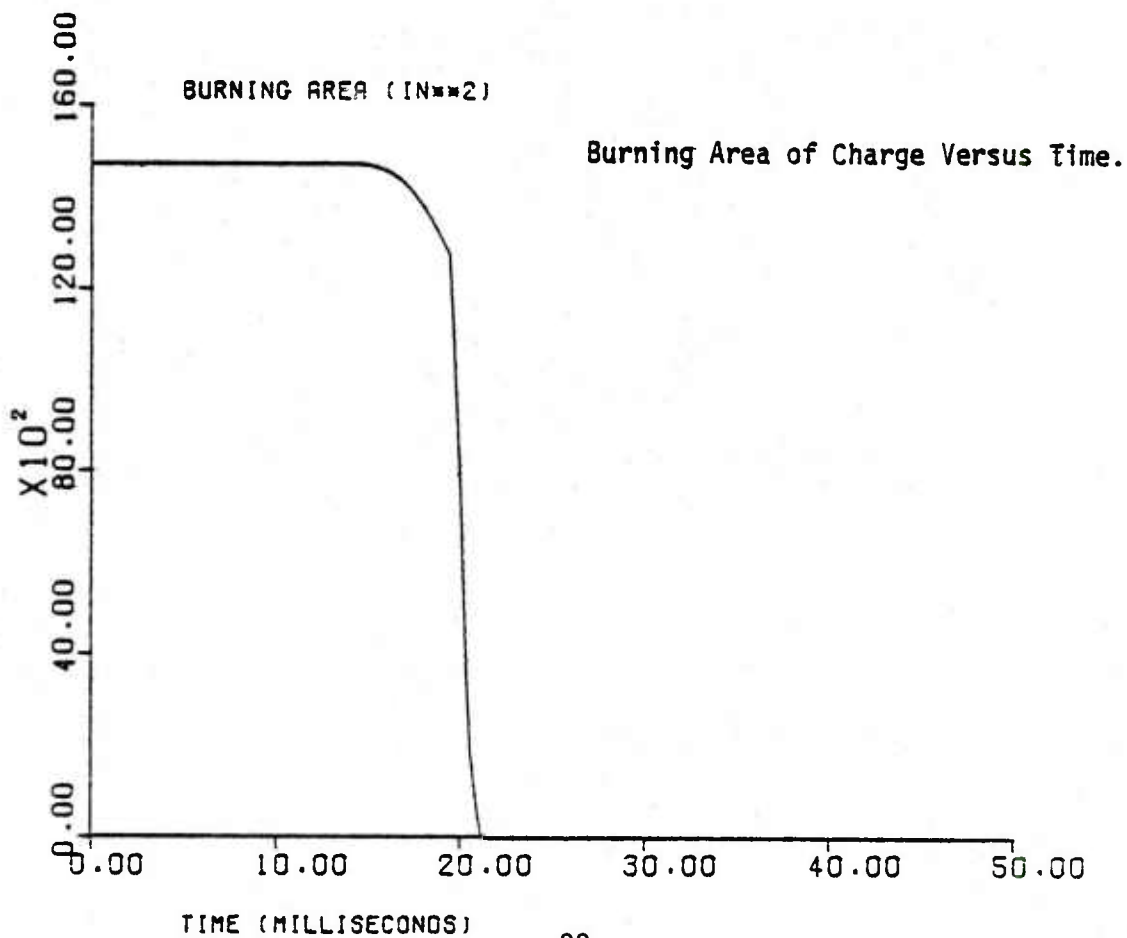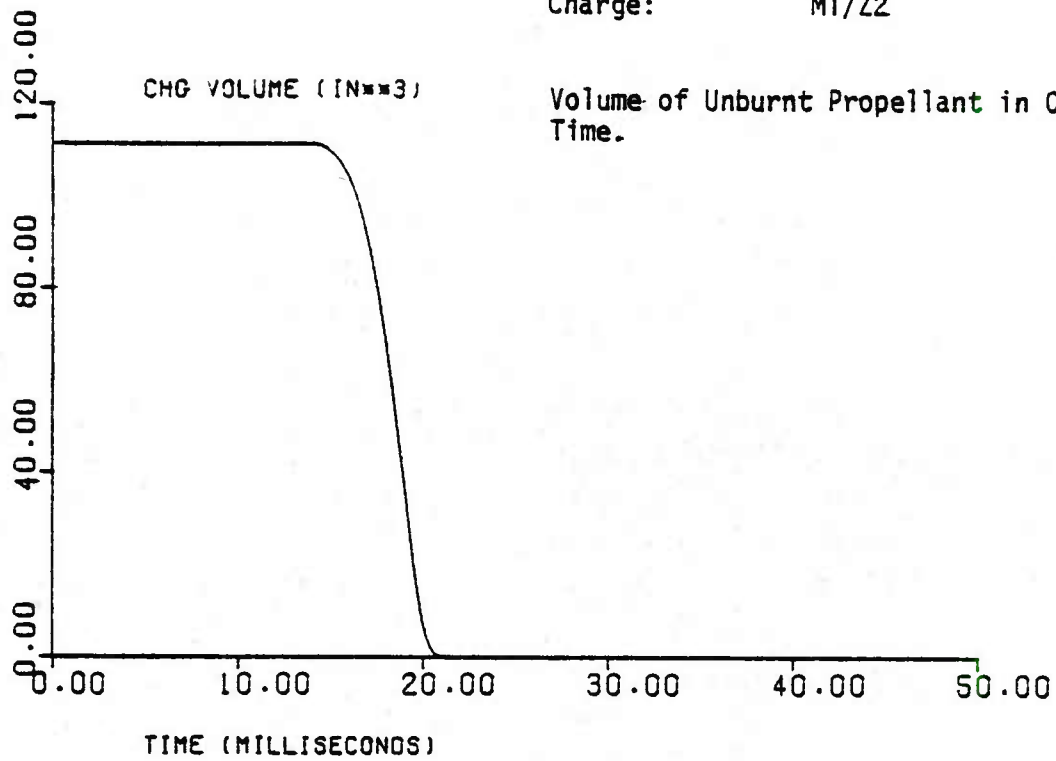Propellant Grain Inside Diameter at Grain Center Versus Time.

Comparison of Propellant Grain Dimensions as Functions of Time.

98

INTERIOR BALLISTICS WITH FALLBACK
Cannon: M201
Projectile: M106
Charge: M1/Z2

Volume of Unburnt Propellant in Charge Versus Time.

CHG VOLUME (IN**3)

TIME (MILLISECONDS)

Burning Area of Charge Versus Time.

BURNING AREA (IN**2)

$\times 10^2$
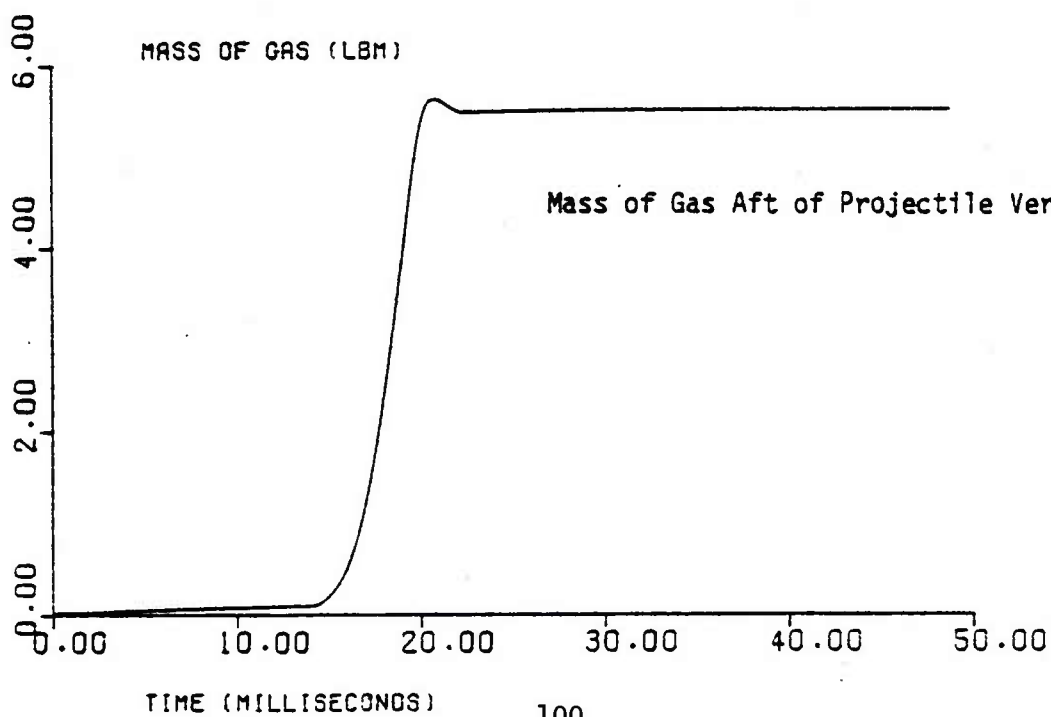
TIME (MILLISECONDS)

99
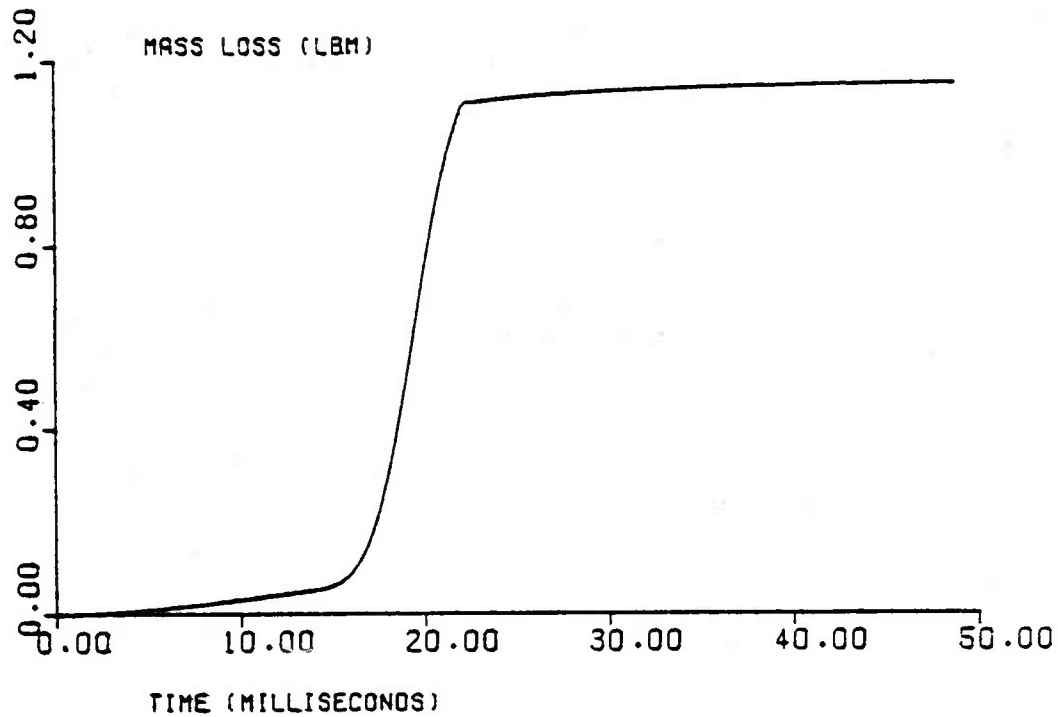
INTERIOR BALLISTICS WITH FALLBACK
Cannon: M201
Projectile: M106
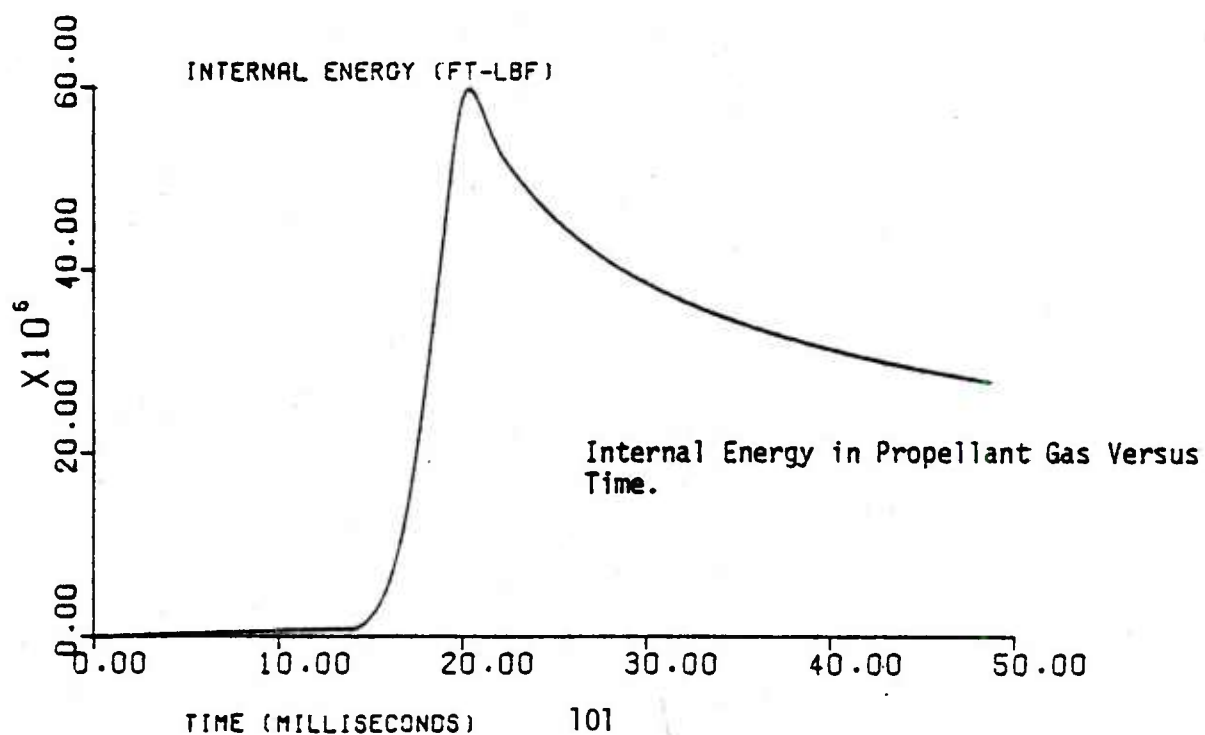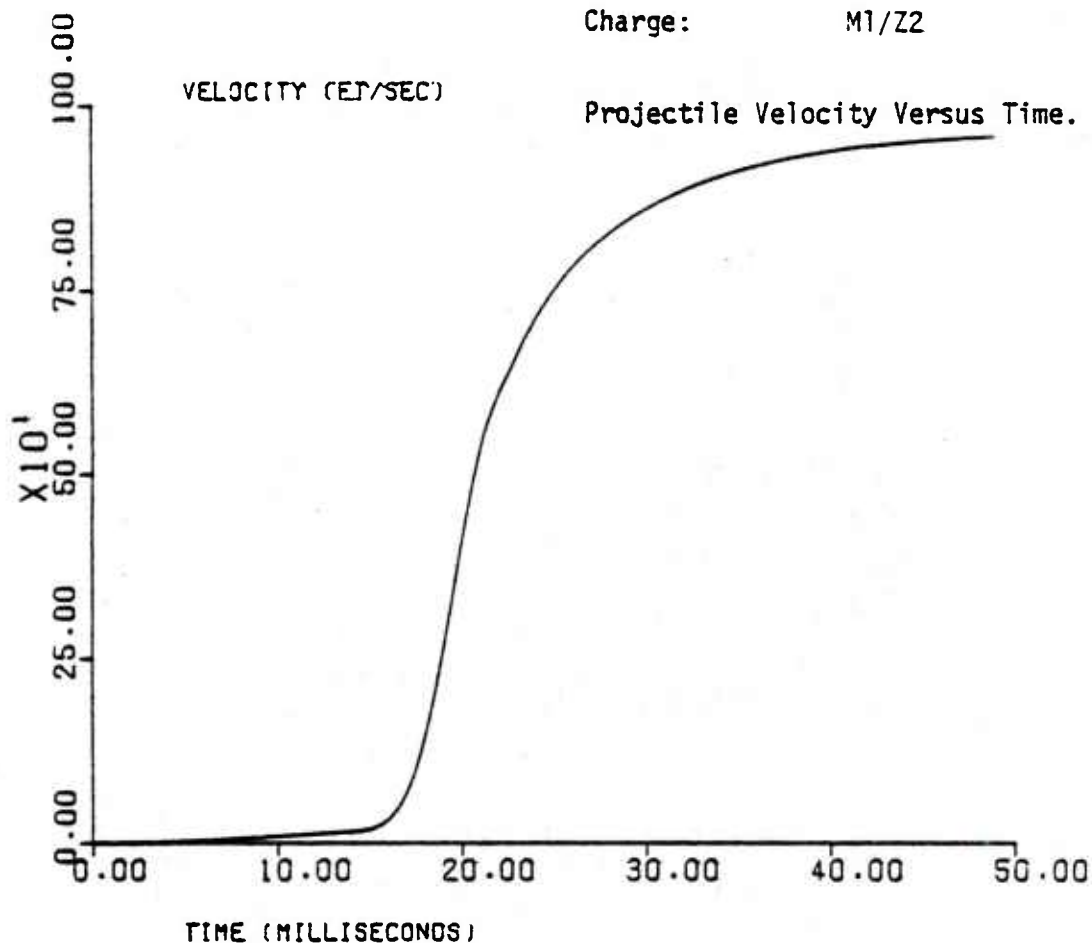Charge: M1/Z2

Mass of Gas Lost Past Obturator Versus Time.

MASS LOSS (LBM)

TIME (MILLISECONDS)

MASS OF GAS (LBM)

Mass of Gas Aft of Projectile Versus Time.

TIME (MILLISECONDS)

100

INTERIOR BALLISTICS WITH FALLBACK

Cannon: M201
Projectile: M106
Charge: M1/Z2

VELOCITY (FT/SEC)   Projectile Velocity Versus Time.

TIME (MILLISECONDS)

INTERNAL ENERGY (FT-LBF)

Internal Energy in Propellant Gas Versus
Time.

TIME (MILLISECONDS)   101

VELOCITY (FT/SEC)

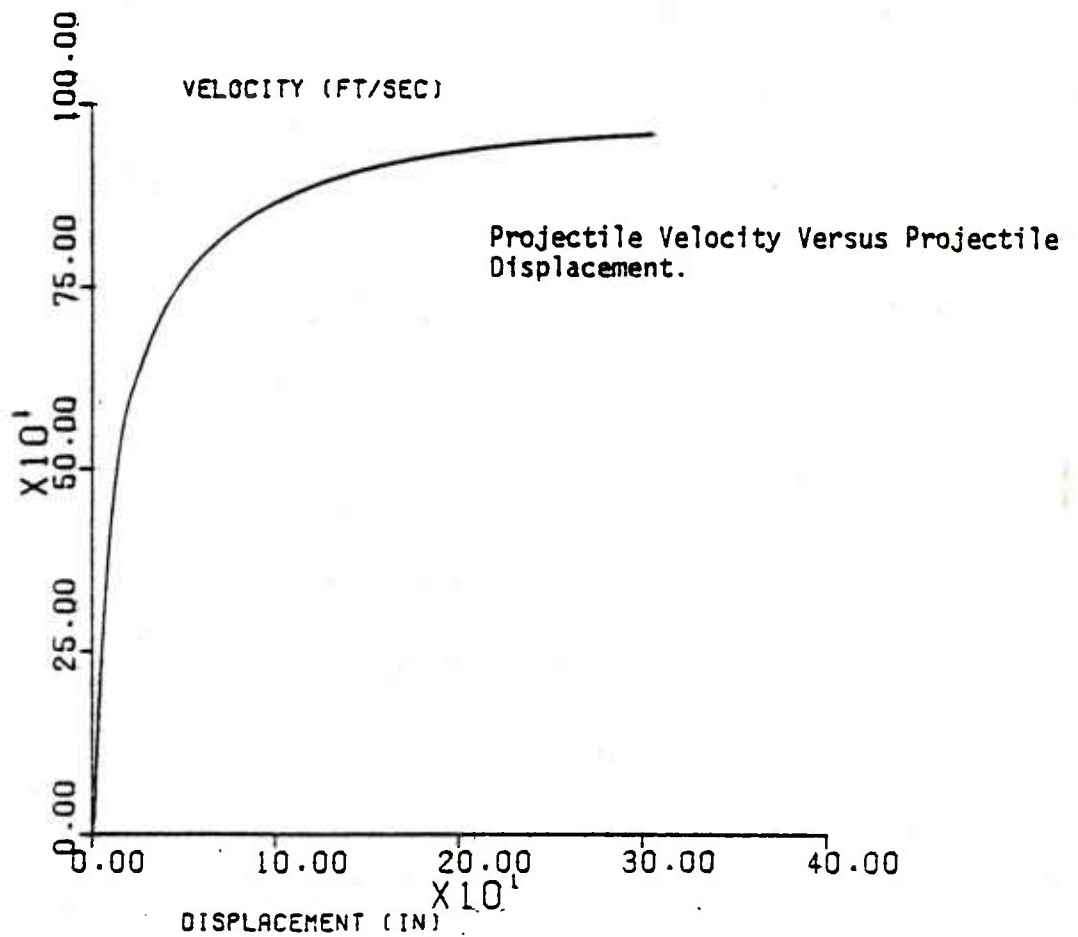INTERIOR BALLISTICS WITH FALLBACK

Cannon: M201
Projectile: M106
Charge: M1/Z2

Projectile Velocity Versus Position of
Base of Projectile Relative to
Reference.

POS RE REF (IN)

VELOCITY (FT/SEC)

Projectile Velocity Versus Projectile
Displacement.

DISPLACEMENT (IN)
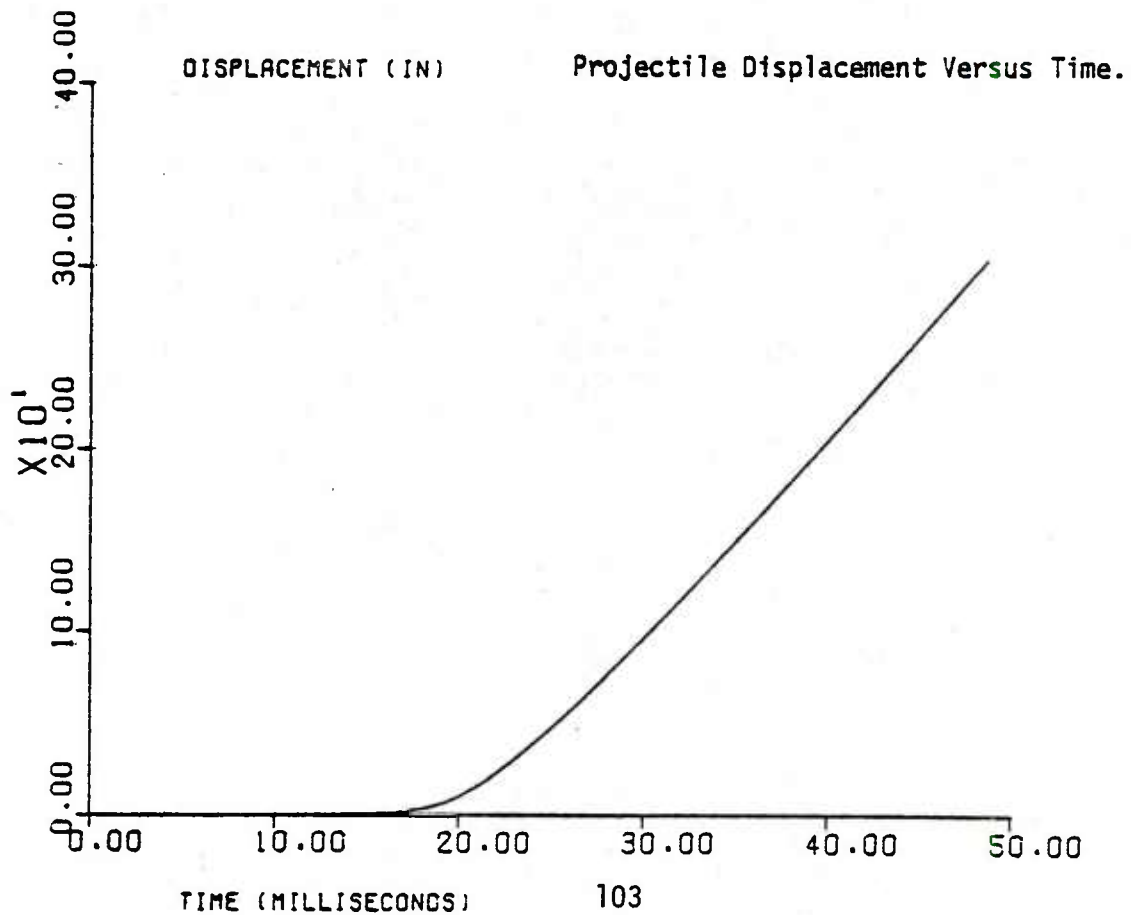
INTERIOR BALLISTICS WITH FALLBACK

Cannon: M201
Projectile: M106
Charge: M1/Z2

POS RE REF (IN)

Position of Projectile Relative to Reference
Versus Time.

TIME (MILLISECONDS)

DISPLACEMENT (IN)   Projectile Displacement Versus Time.

TIME (MILLISECONDS)   103

INTERIOR BALLISTICS WITH FALLBACK
Cannon: M201
Projectile: M106
Charge: M1/Z2

Chamber Wall Surface Temperature Versus Time.

WALL TEMPERATURE (DEG K)

$X10^1$

TIME (MILLISECONDS)

TEMPERATURE (DEG K)

Space-Mean Temperature of Gas Versus Time.

$X10^2$

TIME (MILLISECONDS)

104

Cannon: M201
Projectile: M106
Charge: M1/Z2

SPIN (HZ)   Projectile Spin Rate Versus Time.

TIME (MILLISECONDS)

HEAT LOSS (FT-LBF)

Thermal Loss to Cannon and Projectile
Versus Time.

TIME (MILLISECONDS)

105

Cannon: M201
Projectile: M106
Charge: M1/Z2

SPIN (HZ)

Projectile Spin Rate Versus Position of
Base of Projectile Relative to Reference.
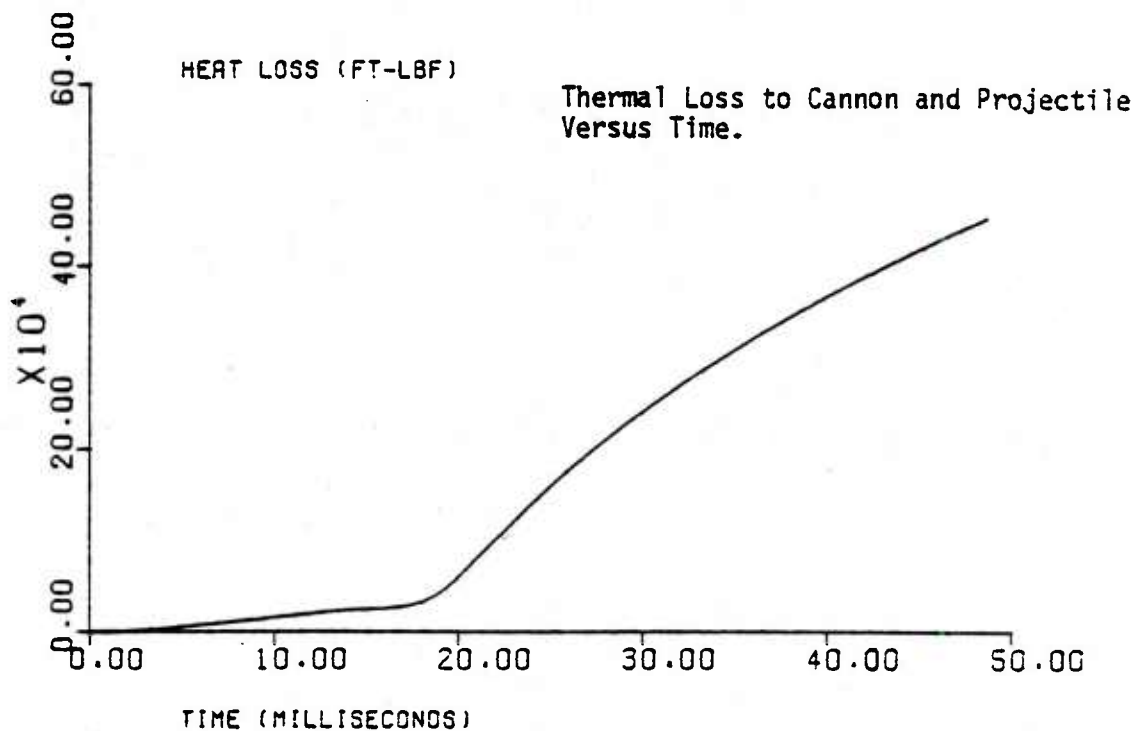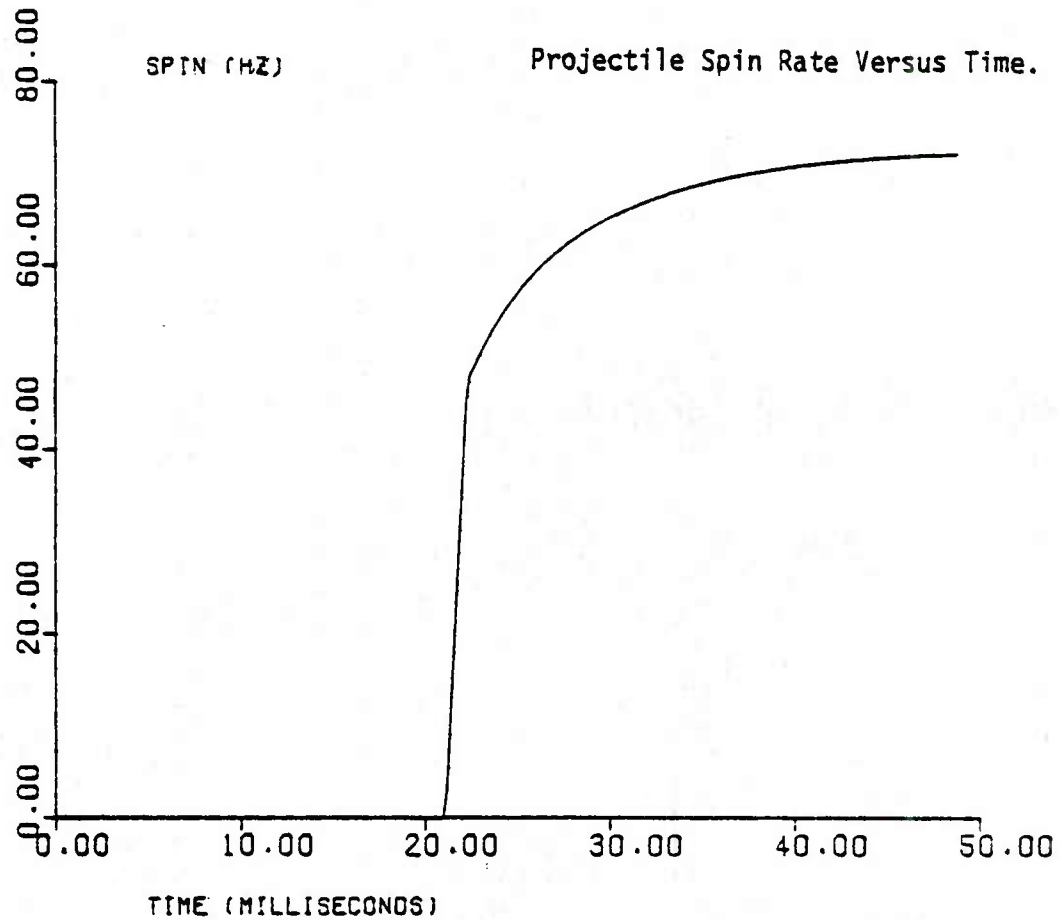
POS RE REF (IN)

PRESSURE (PSI)

INTERIOR BALLISTICS WITH FALLBACK
Cannon: M201
Projectile: M650
Charge: M1/Z2
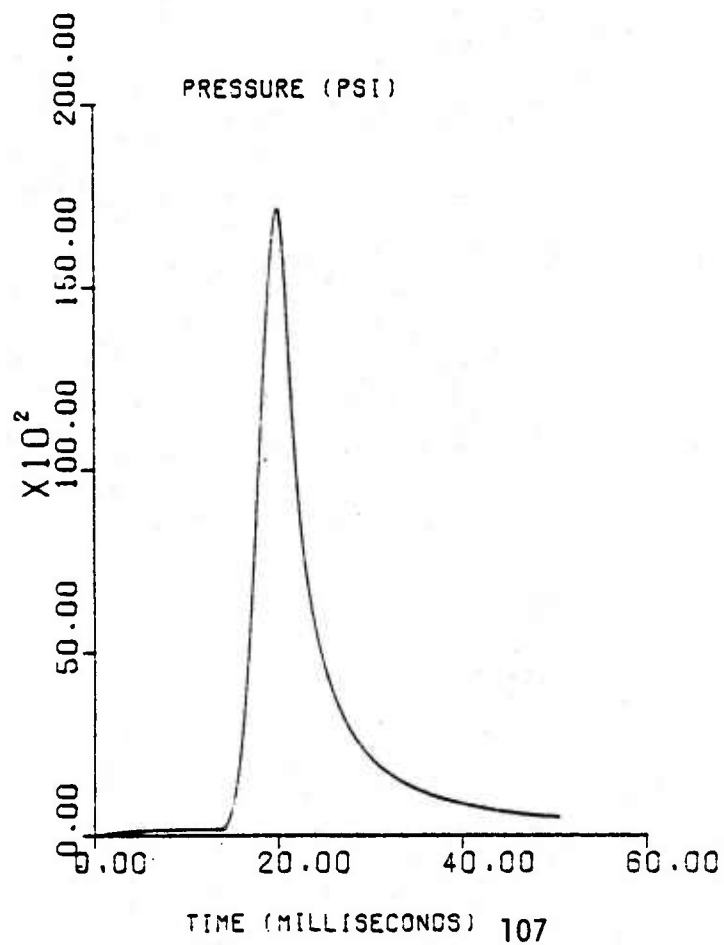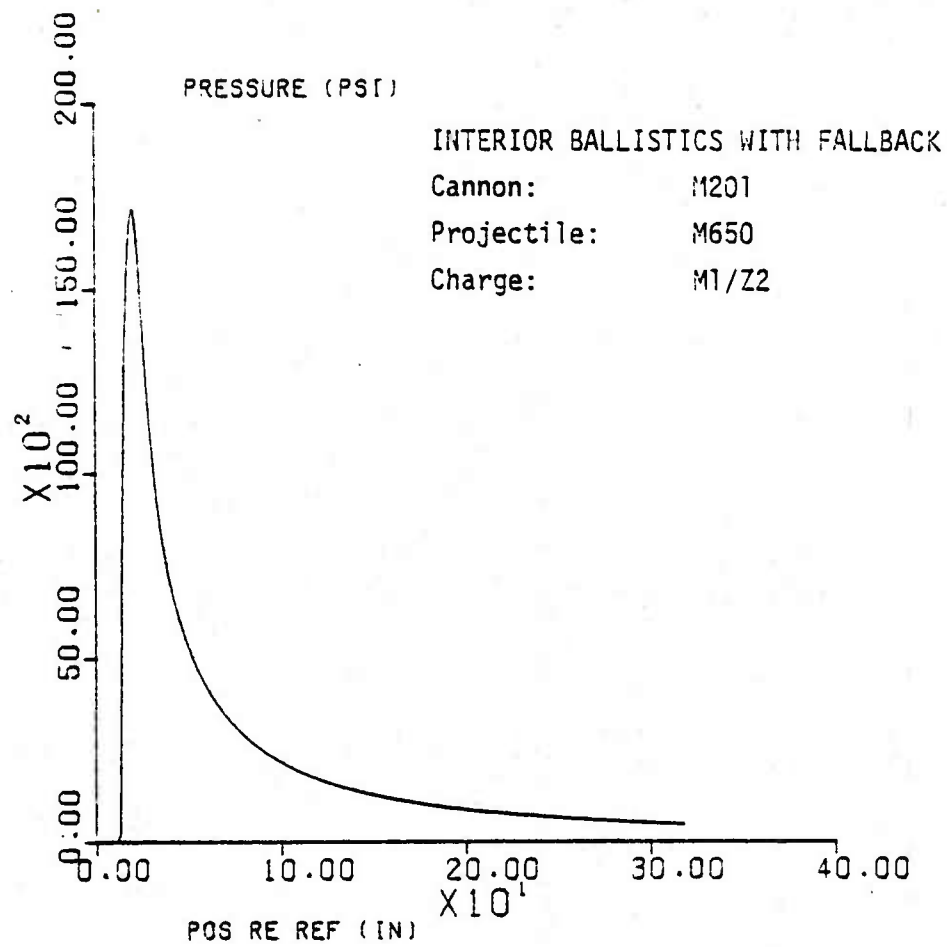
$X10^2$

POS RE REF (IN)

$X10^1$

PRESSURE (PSI)

$X10^2$

TIME (MILLISECONDS) 107

INTERIOR BALLISTICS

OF THE

M509E1 PROJECTILE

IN THE

M110A2 HOWITZER

WHEN FIRED FROM FALLBACK POSITIONS

George Schlenker

MEMORANDUM FOR RECORD

SUBJECT: Interior Ballistics of the M509E1 Projectile in the M110A2
          Howitzer When Fired From Fallback Positions

1. Reference:

     a. MFR, DRSAR-PEL, HQ ARRCOM, 11 Dec 79, subject: Interior Ballistics
of the M106, M650, and M422 Projectiles in the M110A2 Howitzer When Fired
From Fallback Positions.

     b. DF, DRSAR-PE, HQ ARRCOM, 20 Nov 79, subject: Proposed Test Program
Request (TPR) to Investigate Projectile Damage in Firing from Fallback in
the M110A2 SP Howitzer, with inclosures.

2. Background

     This memorandum is a sequel to Reference a. Concern about the consequences
of firing projectiles from a fallback position in the M110A2 howitzer (M201
cannon) extends to all projectiles which can be fired in that system. Although
the original incentive for studying this problem was to understand the cause
and likelihood of cannon damage -- specifically, stripped lands -- a more
recent emphasis of concern is to assess the damage to the projectile fired
from a "hard" fallback position. Hard fallback occurs when the nearly seated
projectile abruptly falls back on the propelling charge during tube elevation.
In this condition the charge is considerably compressed.

3. As indicated in Reference b, the M509 projectile is one of the types of
projectiles whose vulnerability to firing from fallback in the M201 cannon
was to have been examined experimentally. The present analytic study is
intended to support a more extensive study of cannon and projectile damage
and to complement experimental work which may proceed from the Reference b
proposal.

4. Data

     Data relative to the dimensional and inertial characteristics of the
M509E1 were received from DRDAR-LCU-SS, 3 Jan 80, after the Reference a study
had been completed. These data reflect the most recent changes to the aft
main body and boattail. Inferences regarding the parameters used in a computer
simulation of the M509E1 were made from the primitive data. The simulation

DRSAR-PEL
SUBJECT: Interior Ballistics of the M509E1 Projectile in the M110A2
Howitzer When Fired From Fallback Positions

parameters characterizing the M509E1 are found in Table 1.

5. Methodology

The ballistic simulation described in Reference a was used to calculate collision velocity and peak collision force occurring at first major collision between the projectile and gun tube during a fallback trajectory. This event occurs when the forward bourrelet encounters the rifling at the reference position ZCLN. (See Table 1.) Another major collision occurs when the rotating band encounters the rifling.

6. The dynamic behavior of the projectile is not described in detail in the ballistics simulation. Rather an ad hoc semiempirical model is used to characterize the effect of the collision on projectile (Z-) axial and spin motions. See Reference a for details. The computer program reports a variety of measurable variables such as chamber pressure and muzzle velocity as well as many endogenous variables which would be at best difficult to measure. The simulation outputs are displayed graphically for two sample runs in Annex 1. Ballistics are calculated for two conditions: when the projectile starts from a hard fallback position and, second, when the projectile is fully seated. The latter runs are made for the purpose of comparison with the former.

7. Results

A brief summary of results is provided in Table 2 for the fallback case and in Table 3 for the seated case. It is noted that the largest collision velocity using the M509E1 projectile occurs at zone 1 of the M1 propelling charge. This contrasts with the situation using the M106 and M650 projectiles (Reference a) in which the worst-case collision velocity occurs at zone 2. Further, differences are noted in the magnitude of the collision velocity. For the M106 the largest velocity is 558 f/s; for the M650 a comparable value is 486 f/s; and for the M509E1 the largest collision velocity is 421 f/s. Due to its greater inertia and shorter travel to first collision, the M509E1 suffers a less severe impact. Whether even this type of impact would damage the M509E1 is not addressed here. It is also noted that the peak initial collision force for the M509E1 is nearly the same for the first four zones. This fact appears to be due to the combined effects of projectile velocity and acceleration during the collision, notwithstanding the fact that collision velocity declines with increasing zone.

DRSAR-PEL
SUBJECT: Interior Ballistics of the M509E1 Projectile in the M110A2
           Howitzer When Fired From Fallback Positions

8.   One should note from Tables 2 and 3 that the muzzle velocities achieved with the M509E1 are not greatly different between the fallback and seated cases. This is so in spite of the fact that the peak chamber pressure is much larger with fallback, being almost twice as great in fallback as standard at zones 1 and 2. Although combustion occurs at a higher pressure (and with greater thermodynamic efficiency) in the case of fallback, the losses, due principally to blowby, compensate for the gains in this system.

9.   Summary

     This study examines the interior ballistics of the M509E1 projectile fired in the M201 cannon from both fallback and well seated positions. Motivation for the study is a growing concern for the safety of this projectile if it were fired from fallback. The largest axial collision velocity of the M509E1 projectile is 421 f/s, which occurs at zone 1 of the M1 propelling charge. Although this velocity is less than the maximum of 558 f/s produced with the M106 projectile, a velocity of this magnitude may still suffice to damage the projectile. Additional studies are required to evaluate this possibility. Graphs of ballistic variables are presented in Annex 1 to display differences between fallback and standard cases for a typical firing zone.

                                        George Schlenker

1 Incl   GEORGE SCHLENKER
Annex 1   Operations Research Analyst

TABLE 1

PROJECTILE PARAMETERS USED IN THE
INTERIOR BALLISTICS OF FALLBACK PROGRAM

Description of Parameter	Program Name	Value for M509E1
Projectile mass (1bm)	EMP	207.7
Polar radius of gyration	RGRYN	0.3819
Distance from base of proj. to		
max diam. of obturator (in)	ZBOPRB	4.239
Proj. volume aft of obturator (in)	VBOP	209.7
Max diam. of obturator (in)	DIAOBT	8.21
Width of band (in)	WDBAND	2.29
Dist. from obturator to seated		
position (in)	ZRBSET	1.708
Diameter of seat (in)	DIASET	8.186
Dist. from reference end of		
tube to base of seated proj.		
(in) in M201 cannon	ZSEAT	37.74
in M2A2 cannon		29.74
Dist. from reference end of		
tube to base of proj. at		
collision (in)	ZCLN	
in M201 cannon		21.52
in M2A2 cannon		13.52
Plateau pressure (psia) relative		
to base of proj.		
in M201 cannon	PPLAT	450
in M2A2 cannon		400
Peak engraving pressure (psia)	PPEAK	3000

TABLE 2

SUMMARY OF CALCULATED INTERIOR BALLISTICS
IN THE M201 CANNON FOR THE M509E1 PROJECTILE
FIRED FROM HARD* FALLBACK

Simulated conditions are given below

Charge Type	Zone	Peak Press (ksi)	Muzzle Velocity (f/s)	Collision Velocity (f/s)	Axial** Col Force (k lbf)
M1	1	16.7	806	421	109
	2	19.6	900	412	109
	3	22.4	1009	357	109
	4	27.5	1164	232	111
	5	32.5	1380	0	24

* Abrupt drop from the seated position at 1150 mils QE.
** The ratio of axial to cross-axial collision force in the M201 cannon is about 0.4237 under the assumption that the projectile follows the rifling. Values of peak axial force are given.

Conditions:

Propelling charge temperature -- 70 deg F.
Cannon condition -- new.
M1 charge lot no IND 69797.
Position of base of projectile relative to ref. end of tube after fallback (in) at zone:

1	10.8 (in)
2	12.2
3	14.3
4	17.0
5	22.3

TABLE 3

SUMMARY OF CALCULATED INTERIOR BALLISTICS
IN THE M201 CANNON FOR THE M509E1
PROJECTILE FIRED FROM A SEATED* POSITION

Simulated conditions are given below.

Charge Type	Zone	Peak Press (ksi)	Muzzle Vel (f/s)
M1	1G	8.7	808
	2G	10.3	892
	3G	12.5	993
	4G	16.4	1138
	5G	23.9	1358
M2	5W	14.5	1442
	6W	20.9	1676
	7W	30.9	1938

* Projectile is assumed to have been rammed 0.120 (in) beyond the initial contact position.

Conditions:

Propelling charge temperature - 70 deg F.
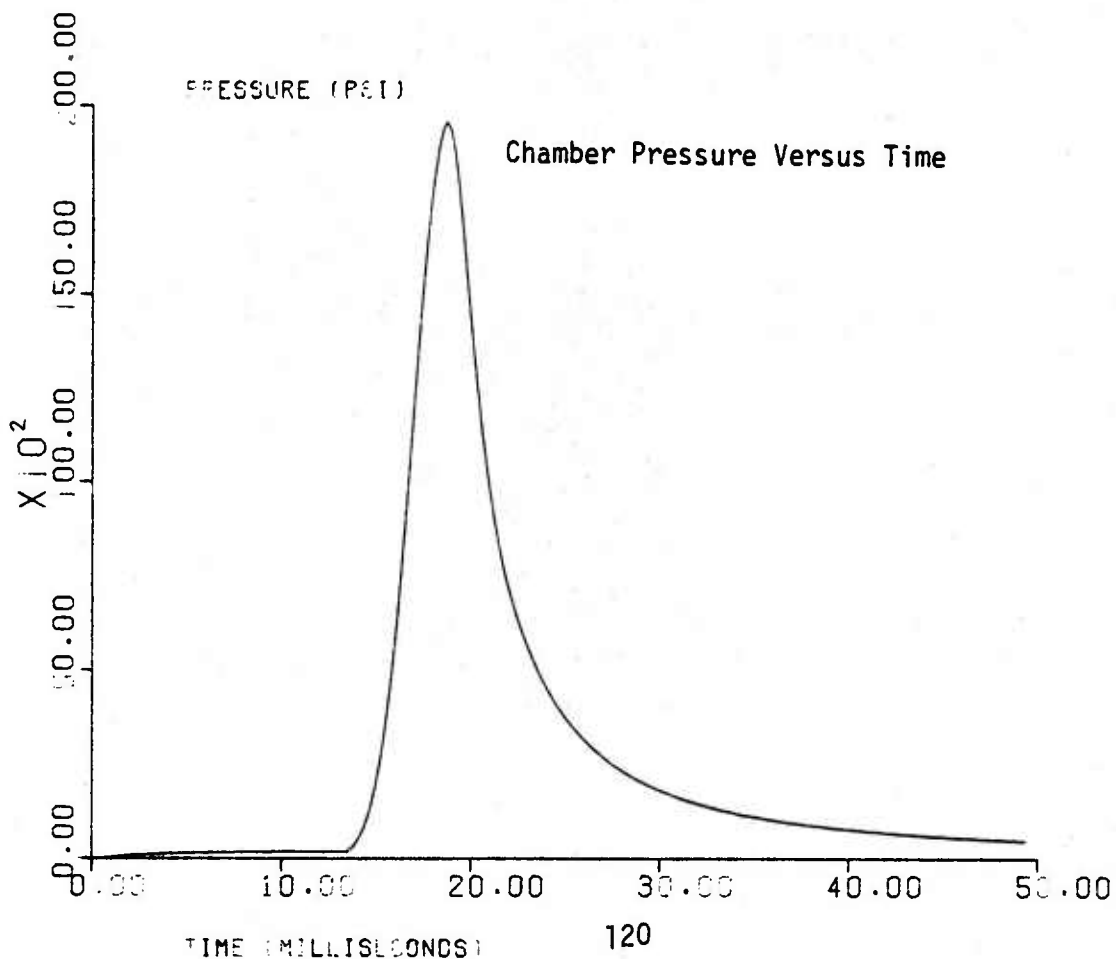Cannon condition - new.
M1 charge lot no IND 69797.
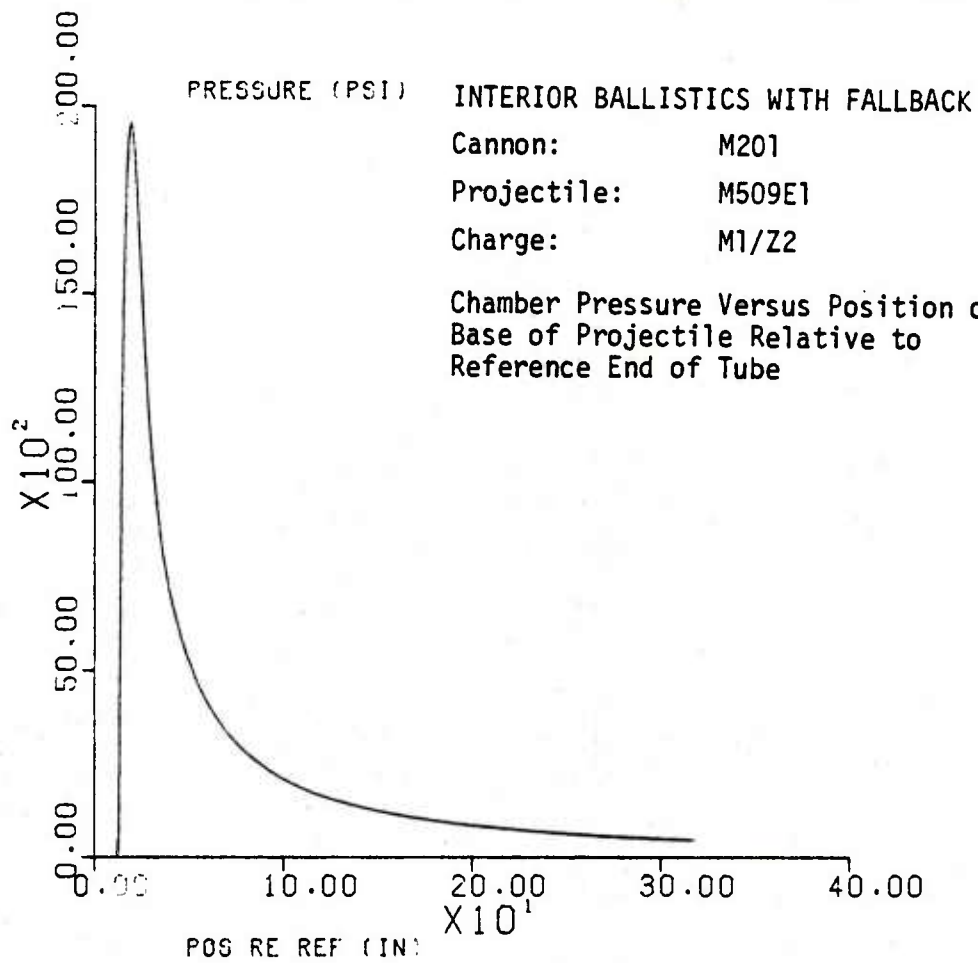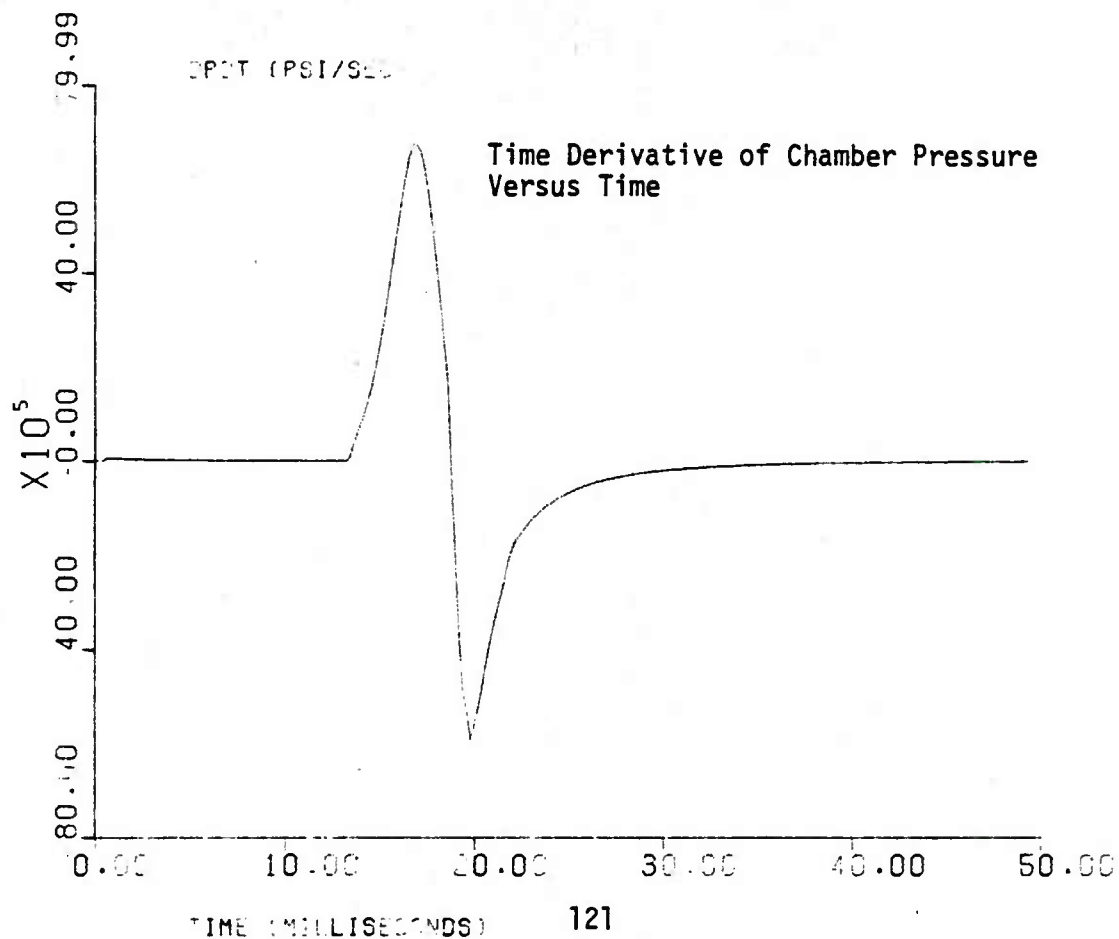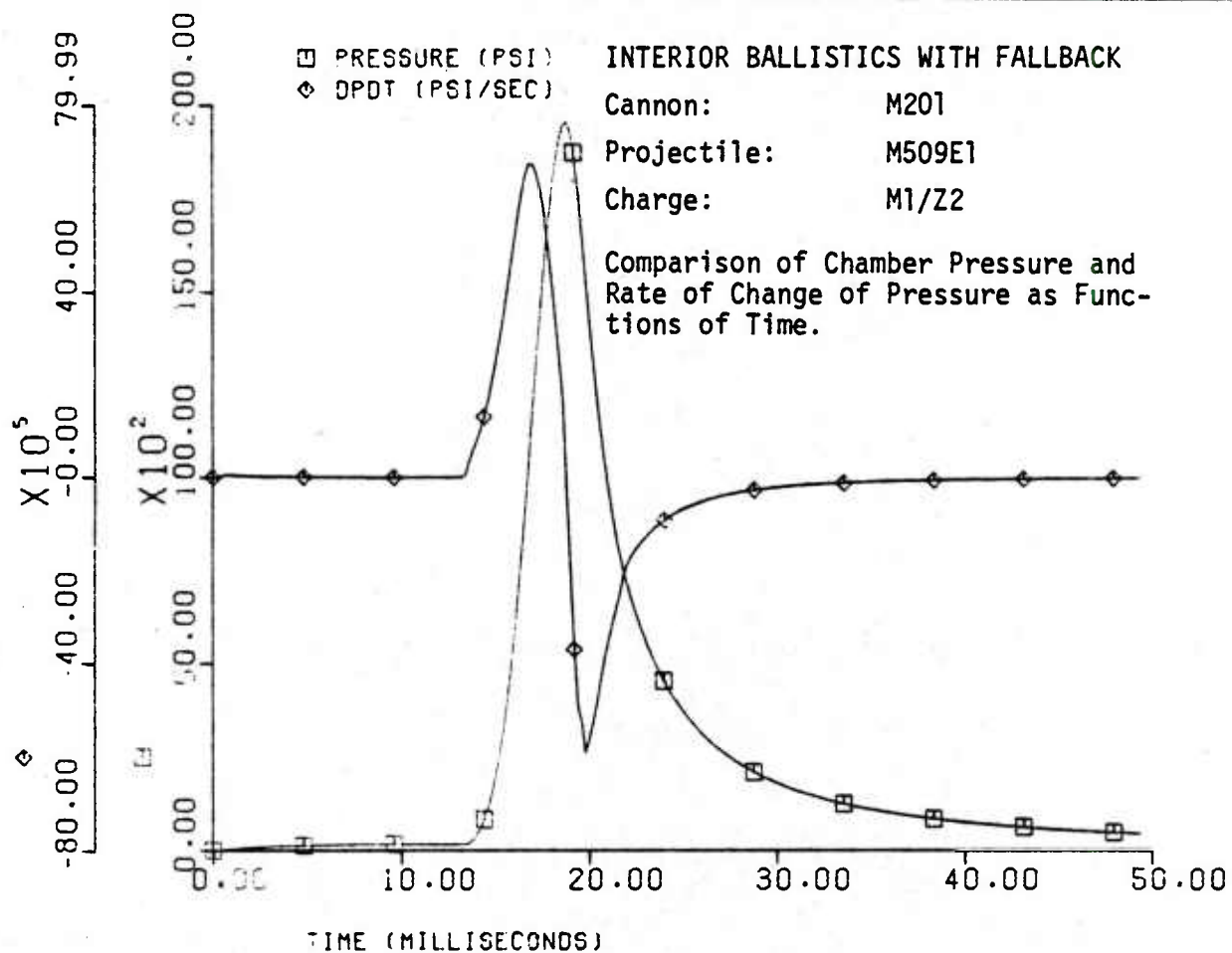M2 charge lot no BAJ 67951.

ANNEX 1

GRAPHICAL RESULTS OF

INTERIOR BALLISTICS FOR THE

M509E1 PROJECTILE FIRED FROM

FALLBACK AND WELL SEATED

POSITIONS IN THE M201 CANNON

TABLE A1

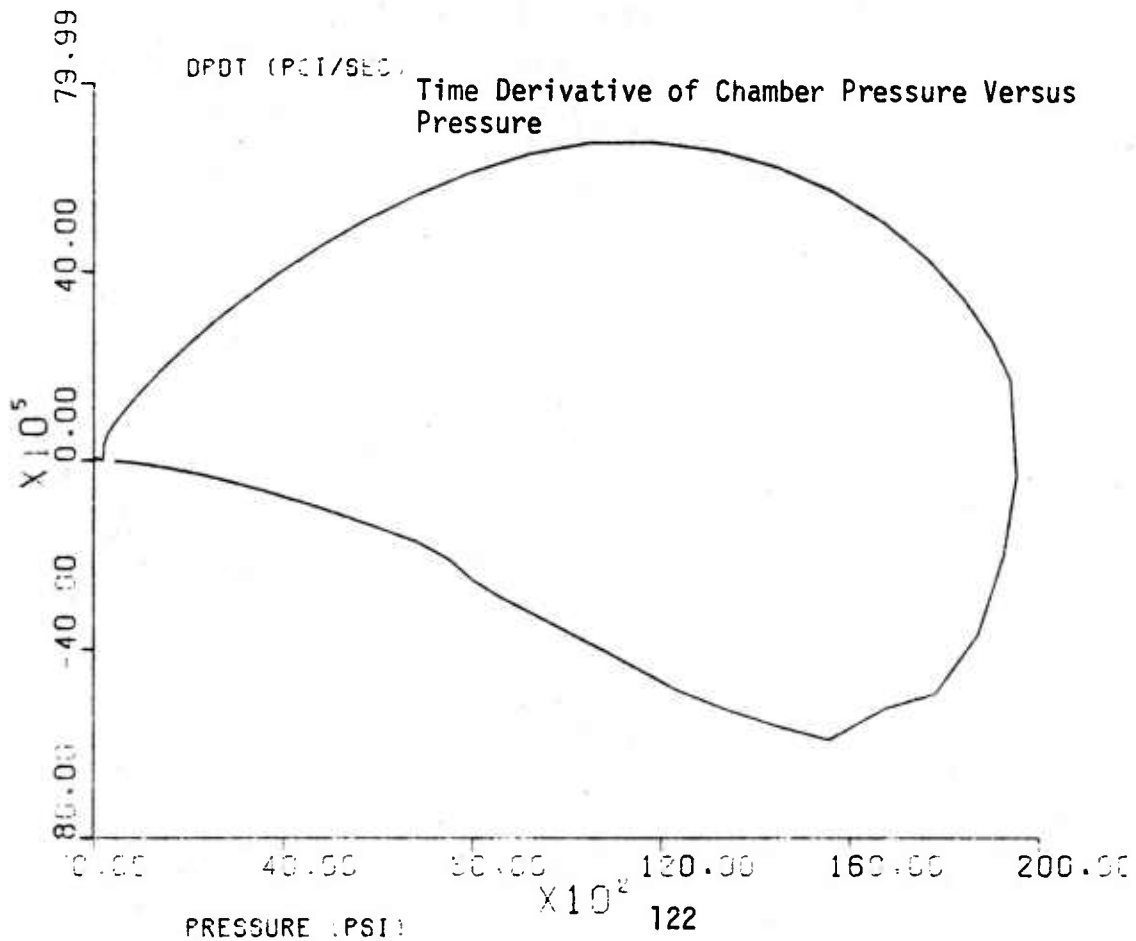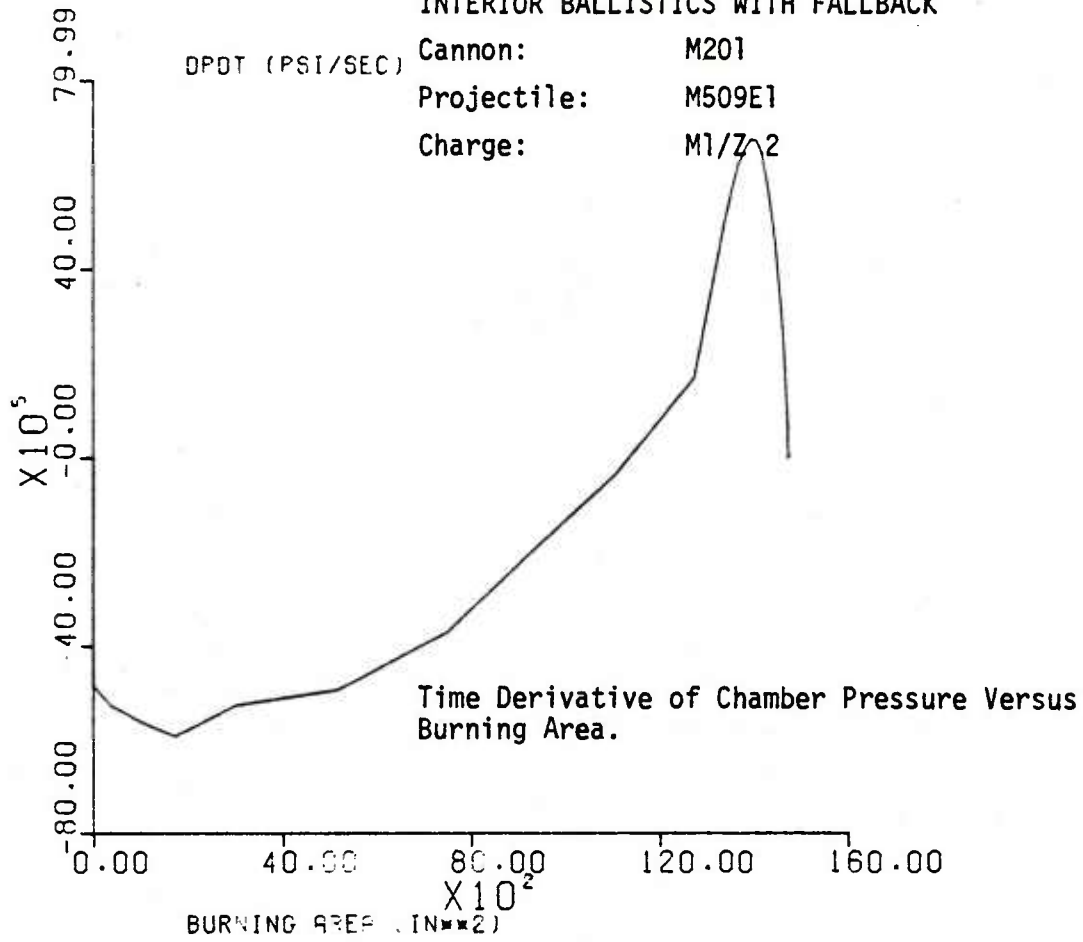## ABBREVIATIONS USED IN PLOTS OF
BALLISTIC SIMULATION OUTPUT

Label on Graph	Description
PRESSURE	Space-mean or "chamber" pressure (psia)
DPDT	Pressure time derivative (psi/s)
ACCELERATION	Projectile axial acceleration (g)
GRAIN ID (ENDS)	Propellant grain inside diam. at the ends of single perf. grain (in)
GRAIN ID (CNTR)	Propellant grain inside diam. at the center of single perf. grain (in)
GRAIN OD	Propellant grain outside diam. (in)
CHG VOLUME	Volume of unburnt propellant in propelling charge (in^3)
BURNING AREA	Area of burning surface of propellant (in^2)
MASS LOSS	Mass of gas lost by escape past obturator (lbm)
MASS OF GAS	Mass of gas remaining behind projectile (lbm)
INTERNAL ENERGY	Internal energy of remaining gas (ft lbf)
VELOCITY	Projectile axial velocity (f/s)
DISPLACEMENT	Axial displacement of projectile relative to initial position (in)
POS RE REF	Position of the base of the projectile relative to the reference end of the tube (in)
WALL TEMPERATURE	Temperature at surface of the chamber wall (deg K)
TEMPERATURE	Space-mean temperature of the gas (deg K)
TOT FWD RESISTANCE	Total resistance to projectile forward motion (lbf)
ENGR RESISTANCE	Resistance to projectile forward motion due to band engraving and friction (lbf)
HEAT LOSS	Thermal loss to cannon and projectile (ft lbf)
FILM COEFFICIENT	Film coefficient of heat transfer (ft lbf/ in^2/s/deg F)
SPIN	Projectile rotational frequency (hz)

INTERIOR BALLISTICS WITH FALLBACK

Cannon: M201

Projectile: M509E1

Charge: M1/Z2

Chamber Pressure Versus Position of
Base of Projectile Relative to
Reference End of Tube

Chamber Pressure Versus Time

120

PRESSURE (PSI)
DPDT (PSI/SEC)

INTERIOR BALLISTICS WITH FALLBACK

Cannon: M201

Projectile: M509E1

Charge: M1/Z2

Comparison of Chamber Pressure and Rate of Change of Pressure as Functions of Time.

TIME (MILLISECONDS)

DPDT (PSI/SEC)

Time Derivative of Chamber Pressure Versus Time

TIME (MILLISECONDS)   121
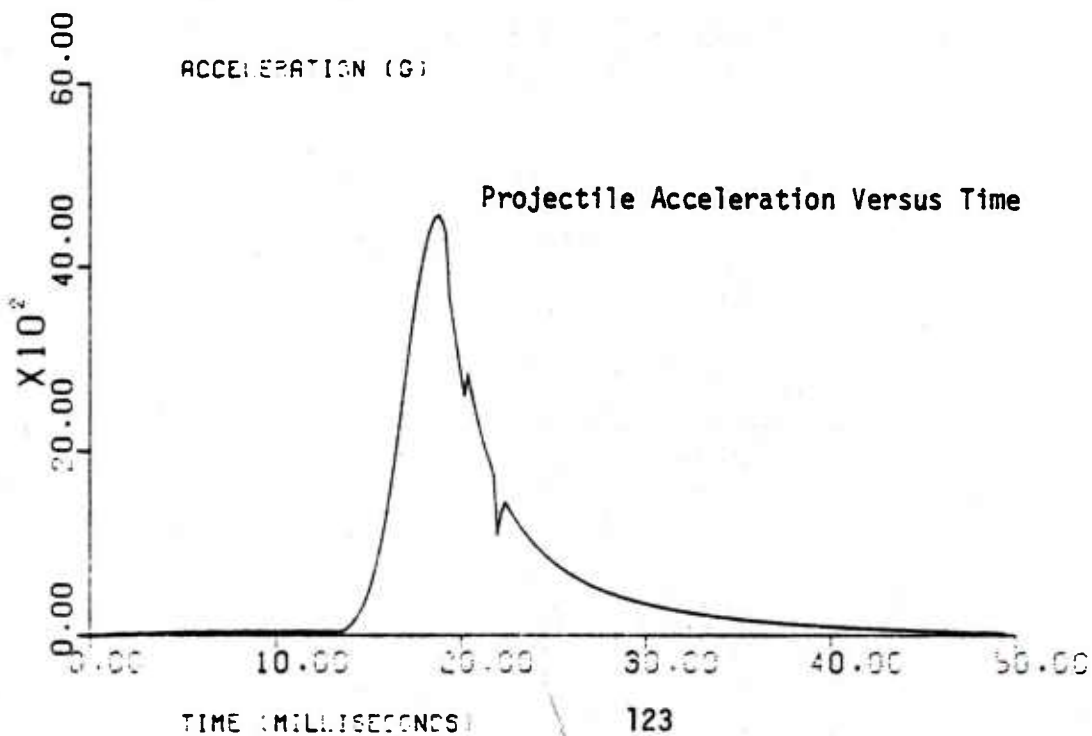
INTERIOR BALLISTICS WITH FALLBACK

Cannon: M201
Projectile: M509E1
Charge: M1/Z^2

DPDT (PSI/SEC)

$\times 10^5$

79.99

40.00

-0.00

-40.00

-80.00

Time Derivative of Chamber Pressure Versus
Burning Area.

0.00   40.00   80.00   120.00   160.00

$\times 10^2$

BURNING AREA (IN**2)

DPDT (PSI/SEC)

$\times 10^5$

79.99

40.00

0.00

-40.00

80.00

Time Derivative of Chamber Pressure Versus
Pressure

0.00   40.00   80.00   120.00   160.00   200.00

$\times 10^2$

PRESSURE (PSI)

122

INTERIOR BALLISTICS WITH FALLBACK
Cannon: M201
Projectile: M509E1
Charge: M1/Z2

Comparison of Chamber Pressure and
Projectile Acceleration as Functions
of Time

Projectile Acceleration Versus Time
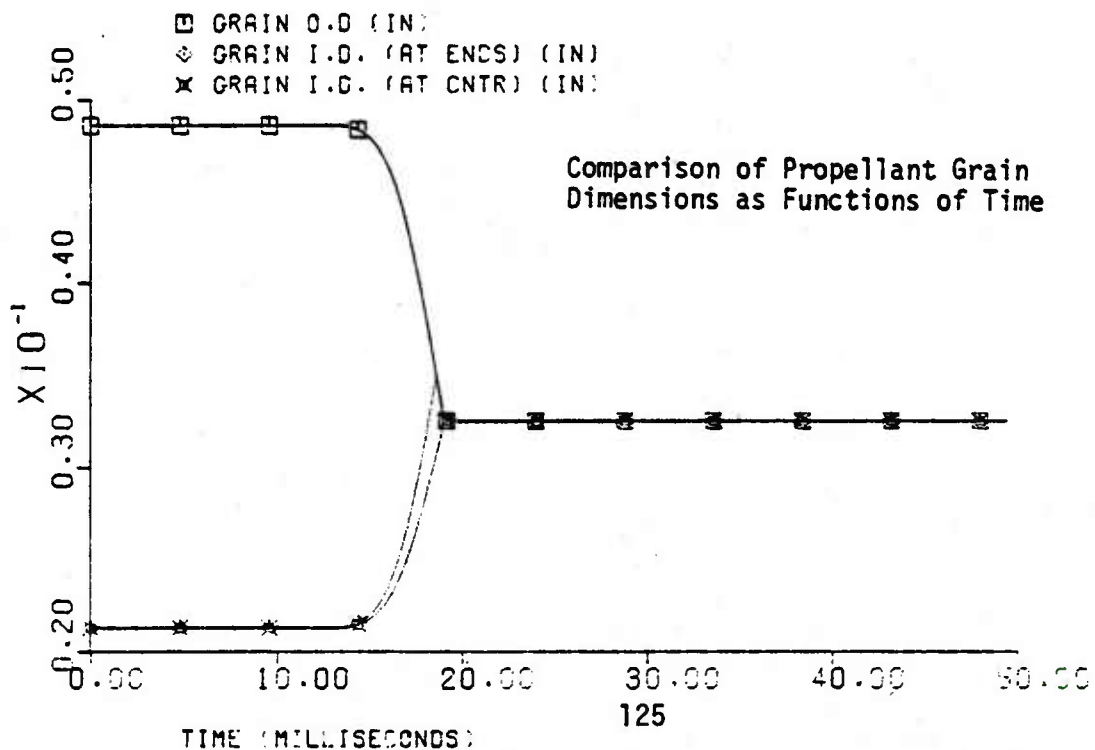
123

GRAIN I.D. (AT ENDS) (IN)

INTERIOR BALLISTICS W/FALLBACK

Cannon: M201

Projectile: M509E1

Charge: M1/Z2

Propellant Grain Inside
Diameter at Grain Ends Versus
Time

X10⁻¹

TIME (MILLISECONDS)

GRAIN O.D (IN)

Propellant Grain Outside
Diameter Versus Time

X10⁻¹

TIME (MILLISECONDS)

124

INTERIOR BALLISTICS W/FALLBACK
Cannon: M201
Projectile: M509E1
Charge: M1/Z2

GRAIN I.D. (AT CNTR) (IN)

Propellant Grain Inside Diameter
at Grain Center Versus Time

X10⁻¹

TIME (MILLISECONDS)

▣ GRAIN O.D (IN)
◇ GRAIN I.D. (AT ENDS) (IN)
✕ GRAIN I.D. (AT CNTR) (IN)

Comparison of Propellant Grain
Dimensions as Functions of Time

X10⁻¹

125

TIME (MILLISECONDS)

INTERIOR BALLISTICS WITH FALLBACK
Cannon: M201
Projectile: M509E1
Charge: M1/Z2

CHG VOLUME (IN**3)

Volume of Unburnt Propellant in Charge
Versus Time

TIME (MILLISECONDS)

BURNING AREA (IN**2)

Burning Area of Charge Versus Time

$X10^2$

TIME (MILLISECONDS)

126

MASS LOSS (LBM)

**Mass of Gas Lost Past Obturator
Versus Time**

TIME (MILLISECONDS)

MASS OF GAS (LBM)

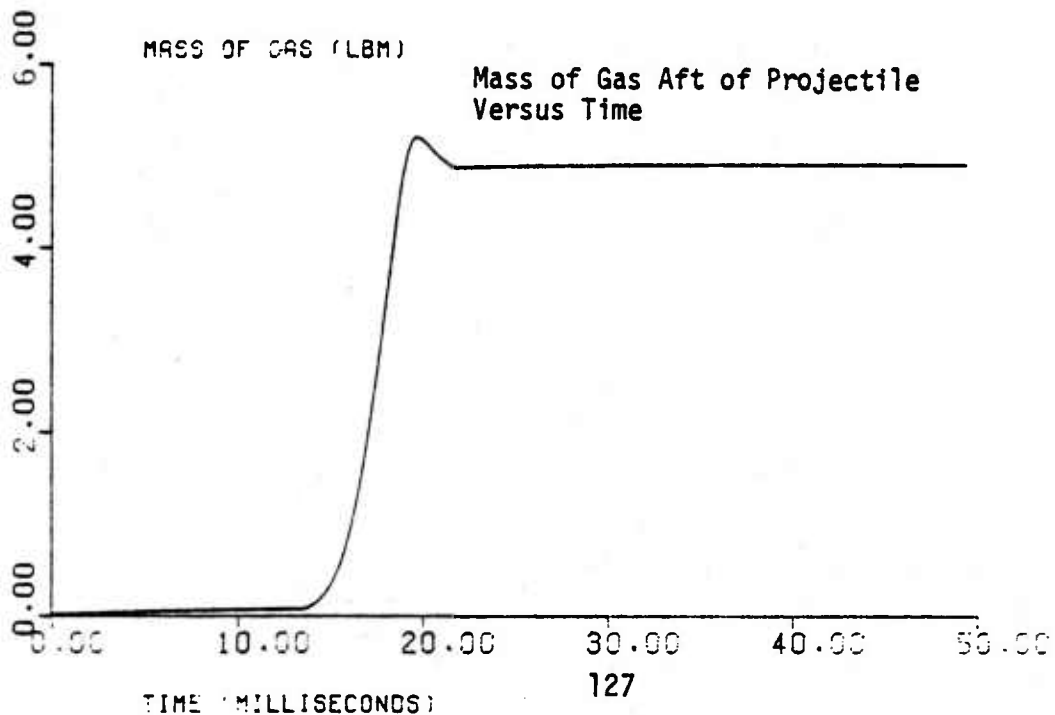**Mass of Gas Aft of Projectile
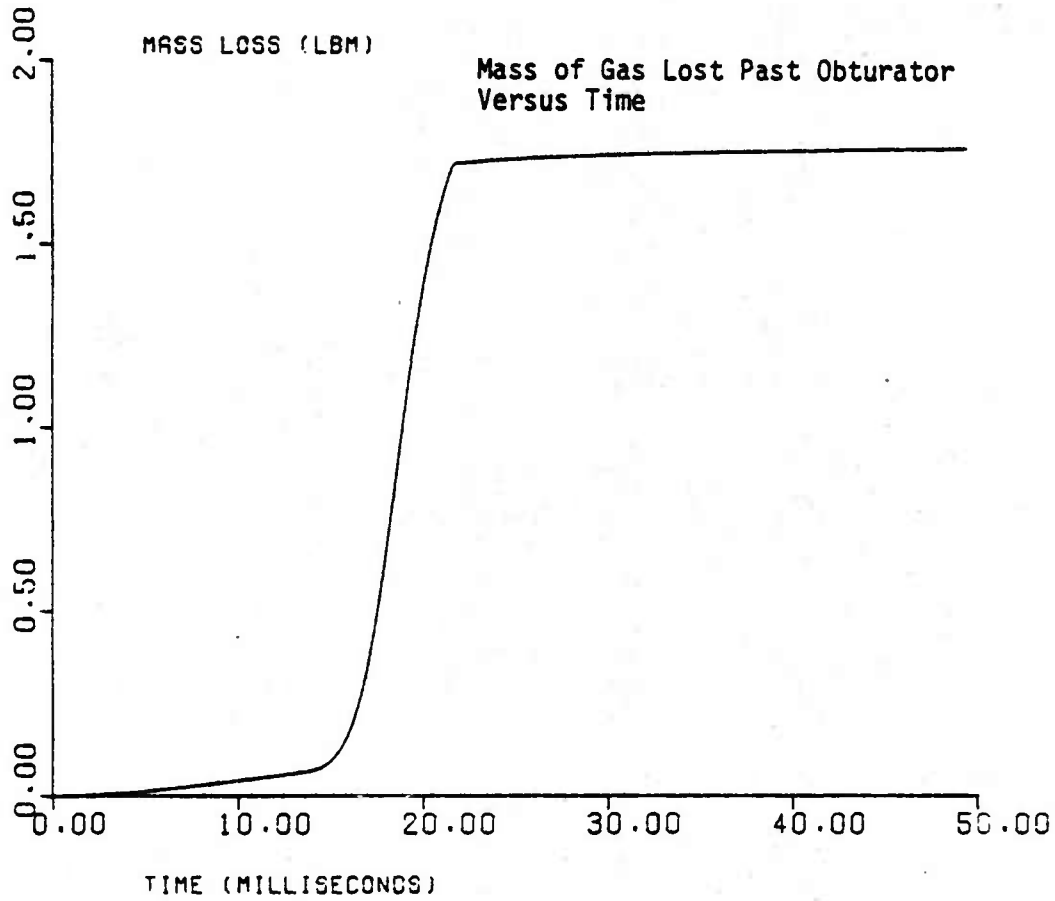Versus Time**

127

TIME (MILLISECONDS)
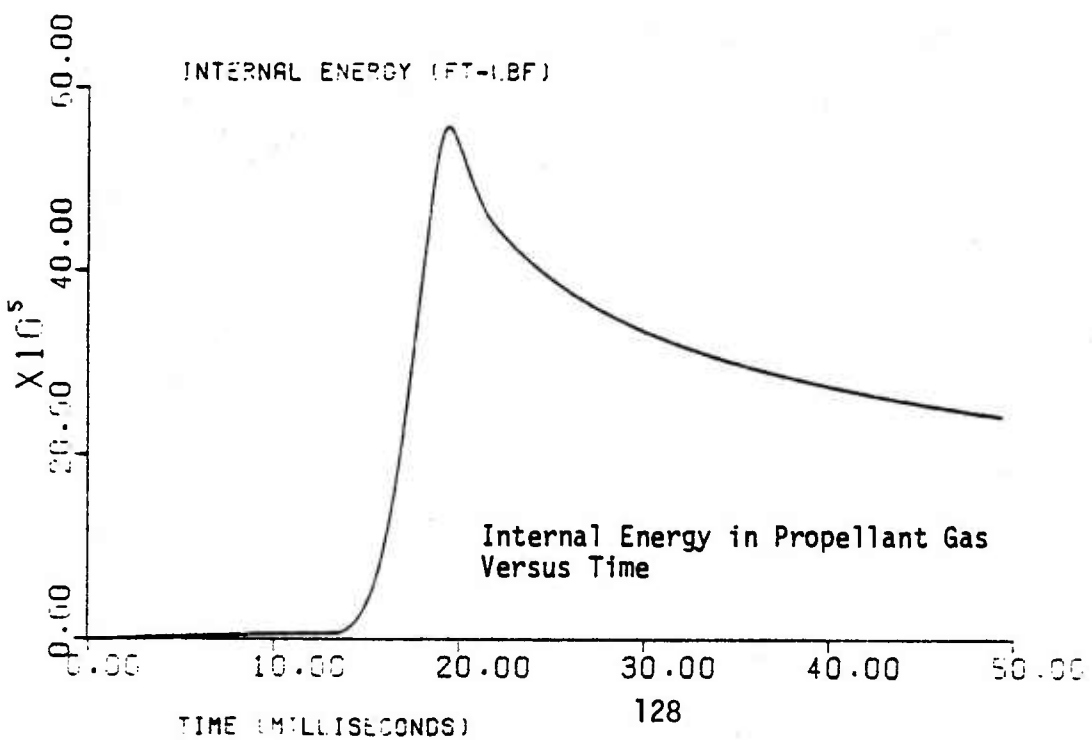
INTERIOR BALLISTICS WITH FALLBACK
Cannon: M201
Projectile: M509E1
Charge: M1/Z2

VELOCITY (FT/SEC)

Projectile Velocity Versus Time

$\times 10^1$

100.00
75.00
50.00
25.00
0.00

0.00   10.00   20.00   30.00   40.00   50.00

TIME (MILLISECONDS)

INTERNAL ENERGY (FT-LBF)

$\times 10^5$

60.00
40.00
20.00
0.00

Internal Energy in Propellant Gas
Versus Time

0.00   10.00   20.00   30.00   40.00   50.00

TIME (MILLISECONDS)

128

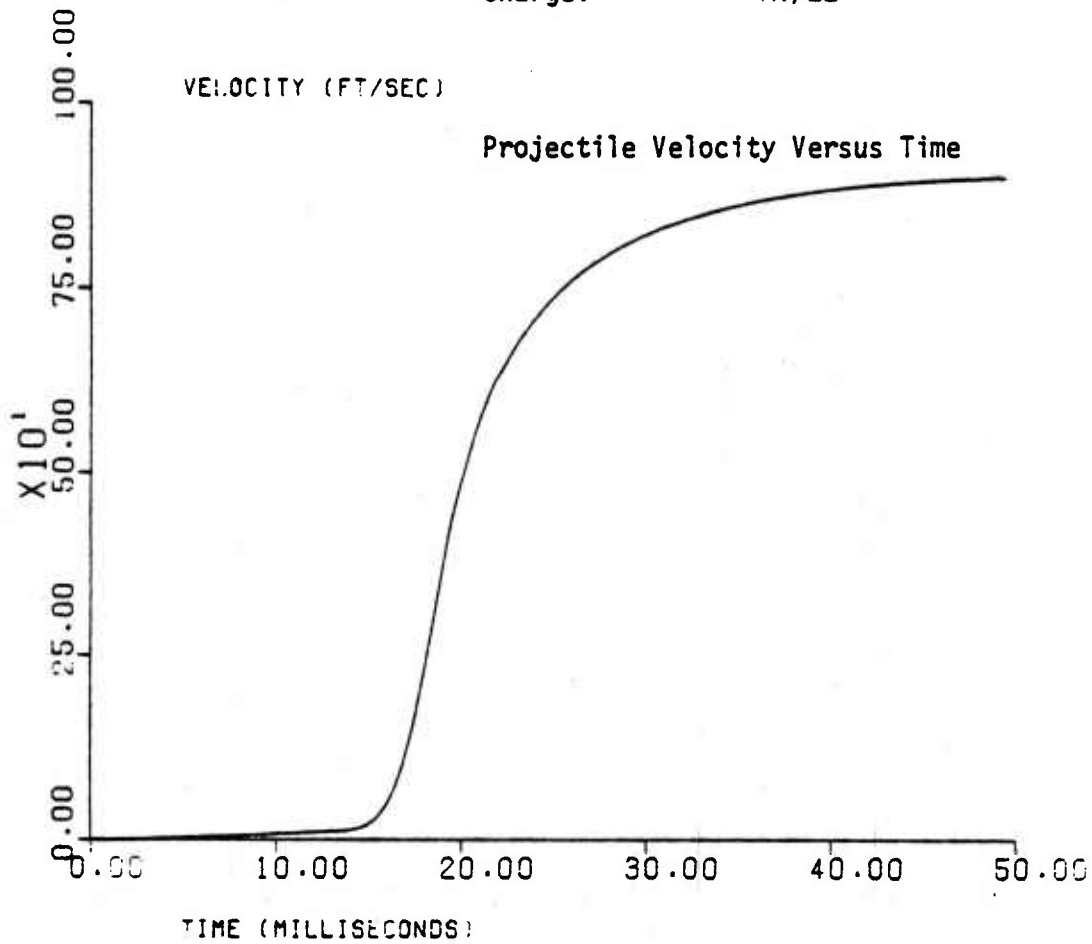VELOCITY (FT/SEC)
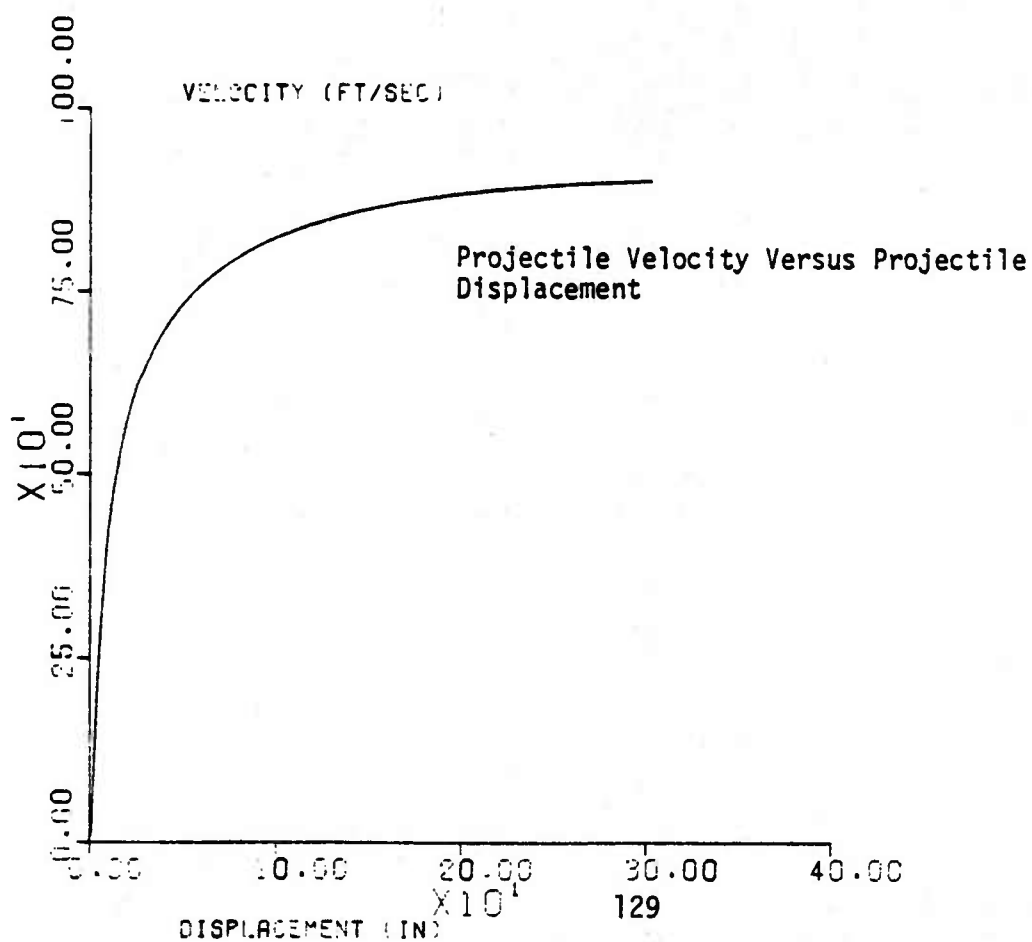
INTERIOR BALLISTICS WITH FALLBACK

Cannon: M201

Projectile: M509E1

Charge: M1/Z2

Projectile Velocity Versus Position of
Base of Projectile Relative to
Reference

POS RE REF (IN)

VELOCITY (FT/SEC)

Projectile Velocity Versus Projectile
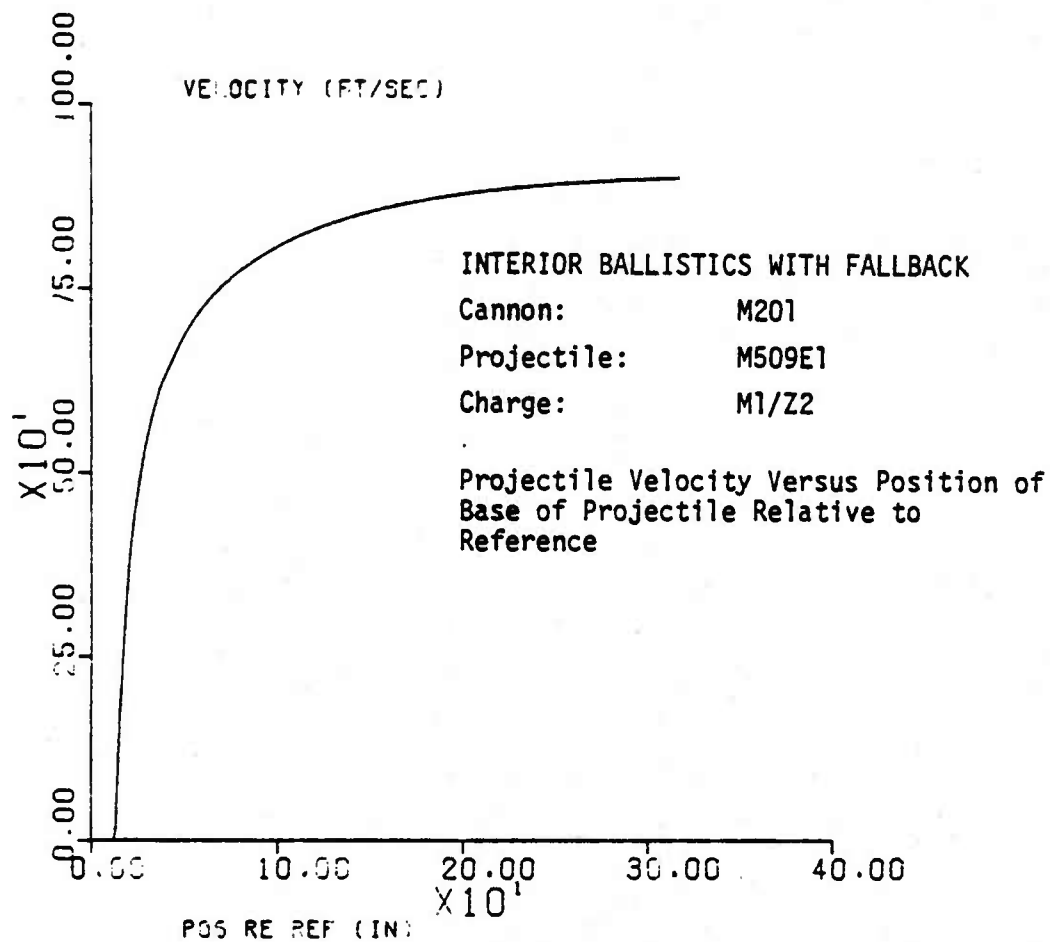Displacement
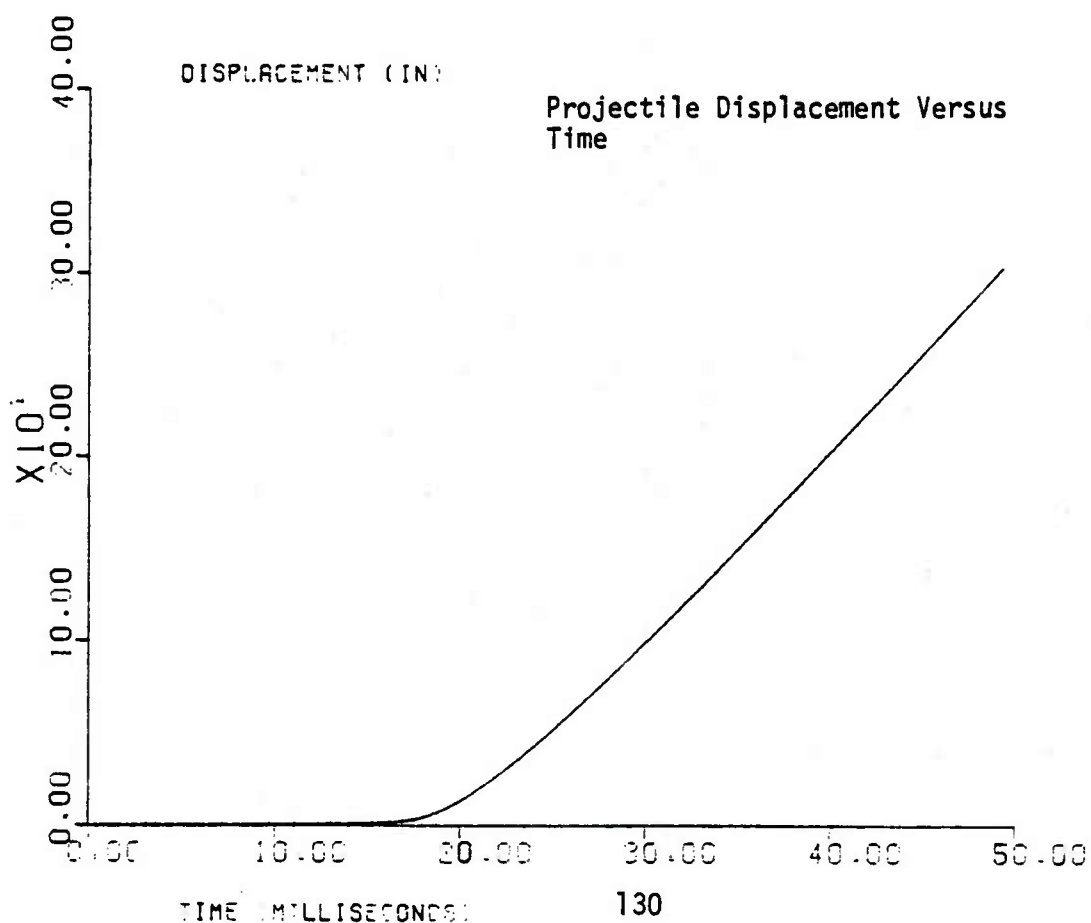
DISPLACEMENT (IN)

129

POS RE REF (IN) INTERIOR BALLISTICS WITH FALLBACK

Cannon: M201
Projectile: M509E1
Charge: M1/Z2

Position of Projectile Relative
to Reference Versus Time

TIME (MILLISECONDS)

DISPLACEMENT (IN)

Projectile Displacement Versus
Time

TIME (MILLISECONDS)   130
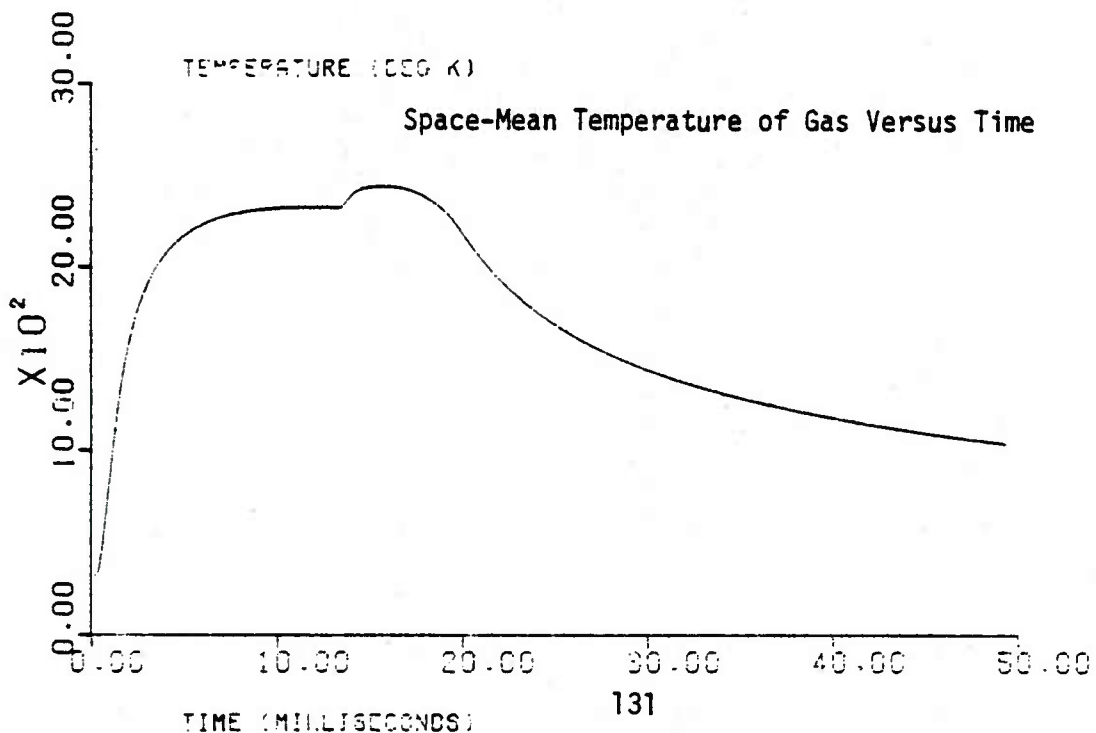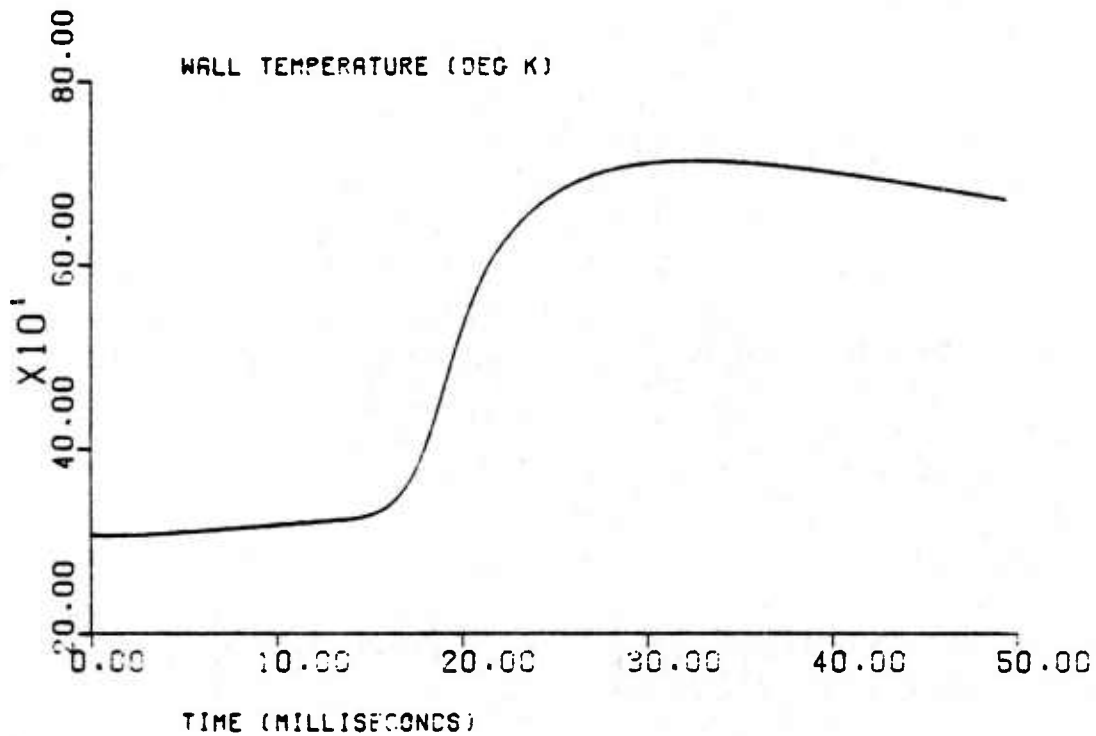
INTERIOR BALLISTICS WITH FALLBACK

Cannon: M201

Projectile: M509E1

Charge: M1/Z2

Chamber Wall Surface Temperature Versus
Time

WALL TEMPERATURE (DEG K)

$X10^1$

TIME (MILLISECONDS)

TEMPERATURE (DEG K)

Space-Mean Temperature of Gas Versus Time

$X10^2$

TIME (MILLISECONDS)

INTERIOR BALLISTICS WITH FALLBACK

Cannon: M201
Projectile: M509E1
Charge: M1/Z2

WALL TEMPERATURE (DEG K)

Chamber Wall Surface Temperature
Versus Displacement

$X10^1$

80.00
60.00
40.00
20.00

0.00   10.00   20.00   30.00   40.00
$X10^1$

DISPLACEMENT (IN)

TOT FWD RESISTANCE (LBF)

Total Forward Resistance Versus Time

$X10^3$

160.00
120.00
80.00
40.00
0.00

0.00   10.00   20.00   30.00   40.00   50.00

132
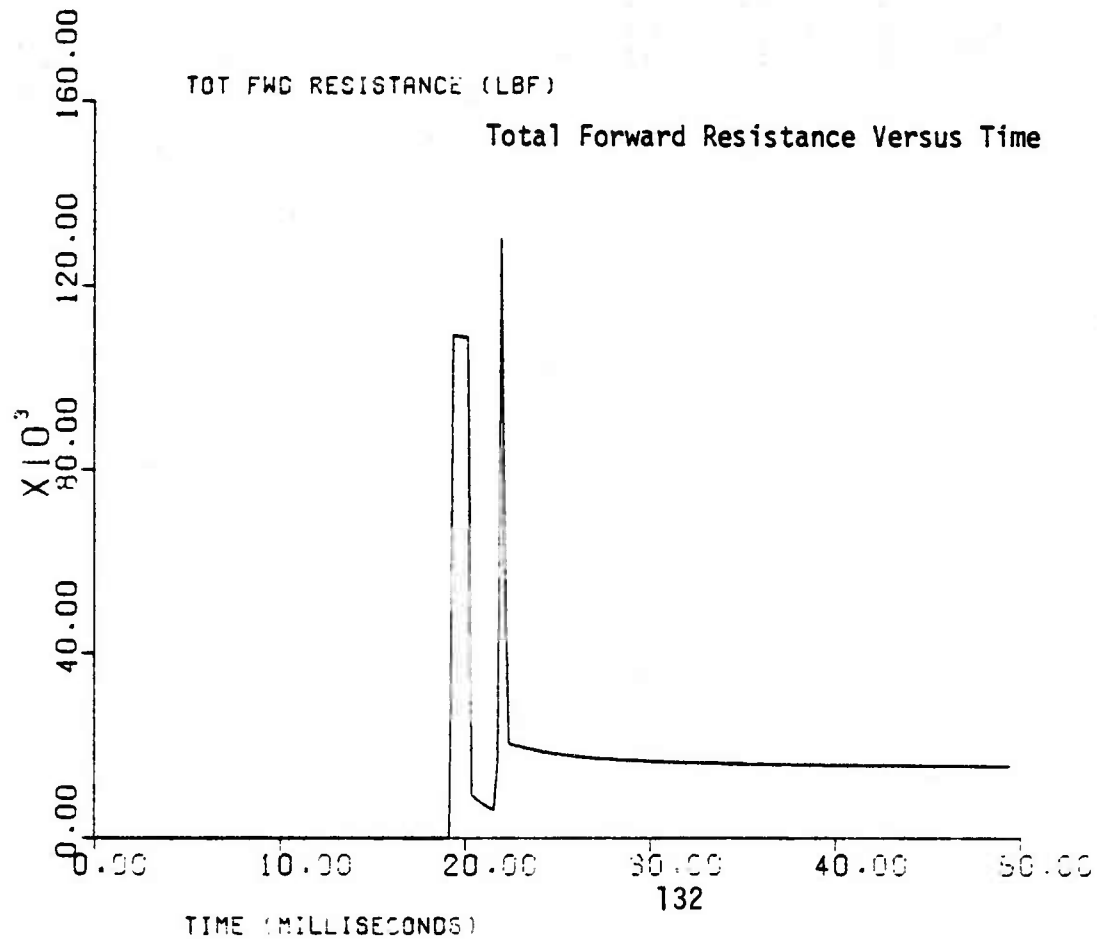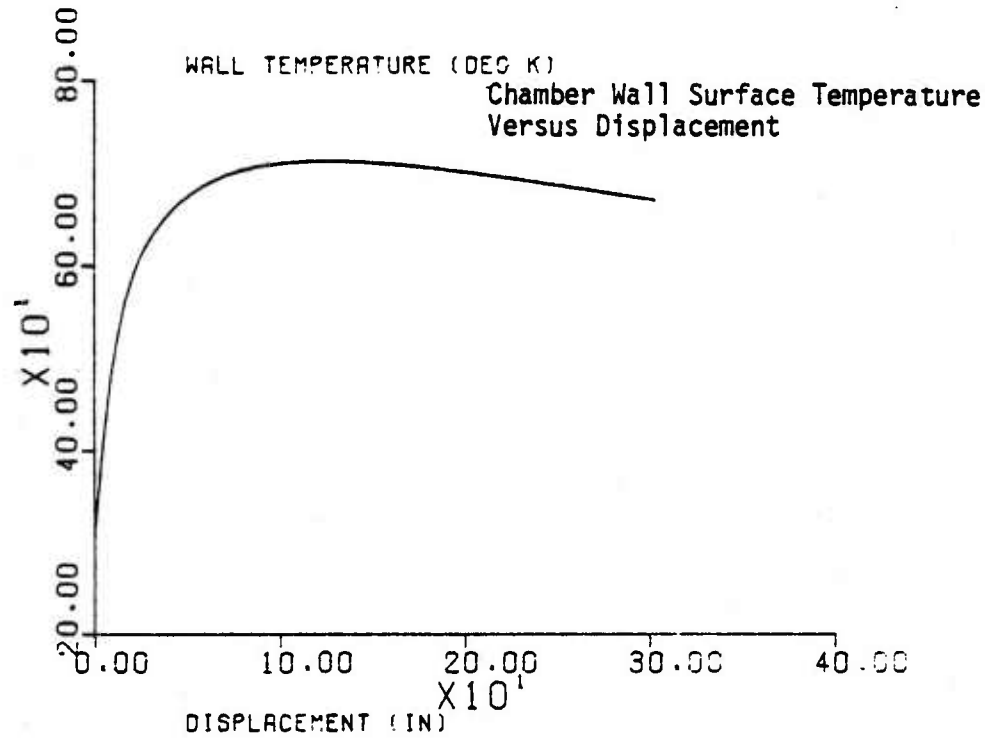
TIME (MILLISECONDS)
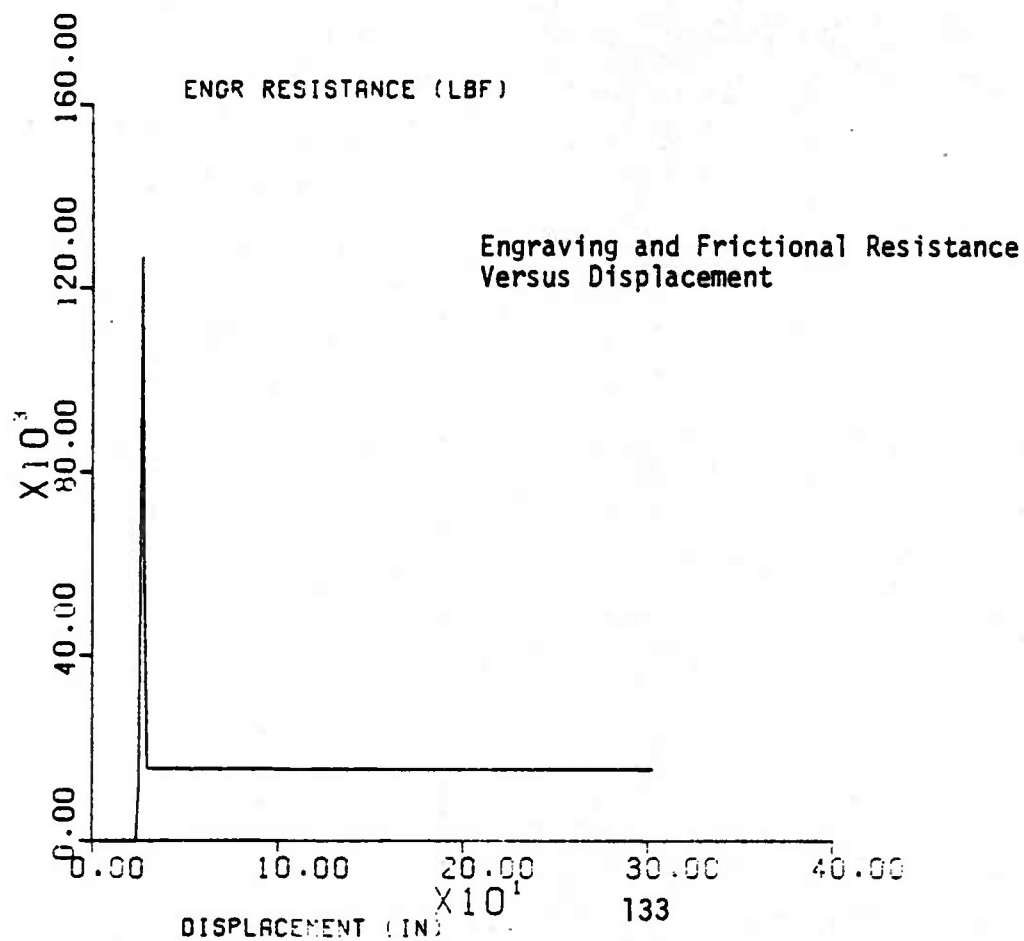
TOT FWD RESISTANCE (LBF)

INTERIOR BALLISTICS WITH FALLBACK

Cannon: M201
Projectile: M509E1
Charge: M1/Z2

Total Forward Resistance to Proj.
Motion Versus Displacement

$X10^3$

160.00

120.00

80.00

40.00

0.00

0.00   10.00   20.00   30.00   40.00

$X10^1$

DISPLACEMENT (IN)

ENGR RESISTANCE (LBF)

Engraving and Frictional Resistance
Versus Displacement

$X10^3$

160.00

120.00

80.00

40.00

0.00

0.00   10.00   20.00   30.00   40.00

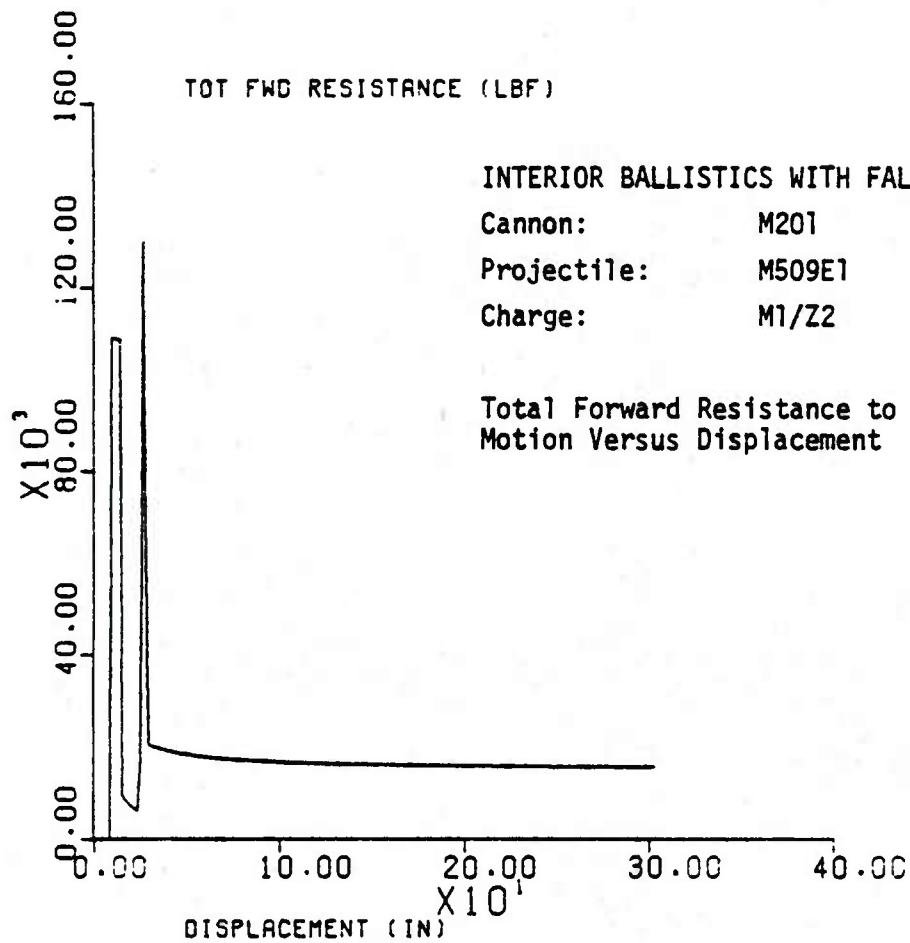$X10^1$

DISPLACEMENT (IN)
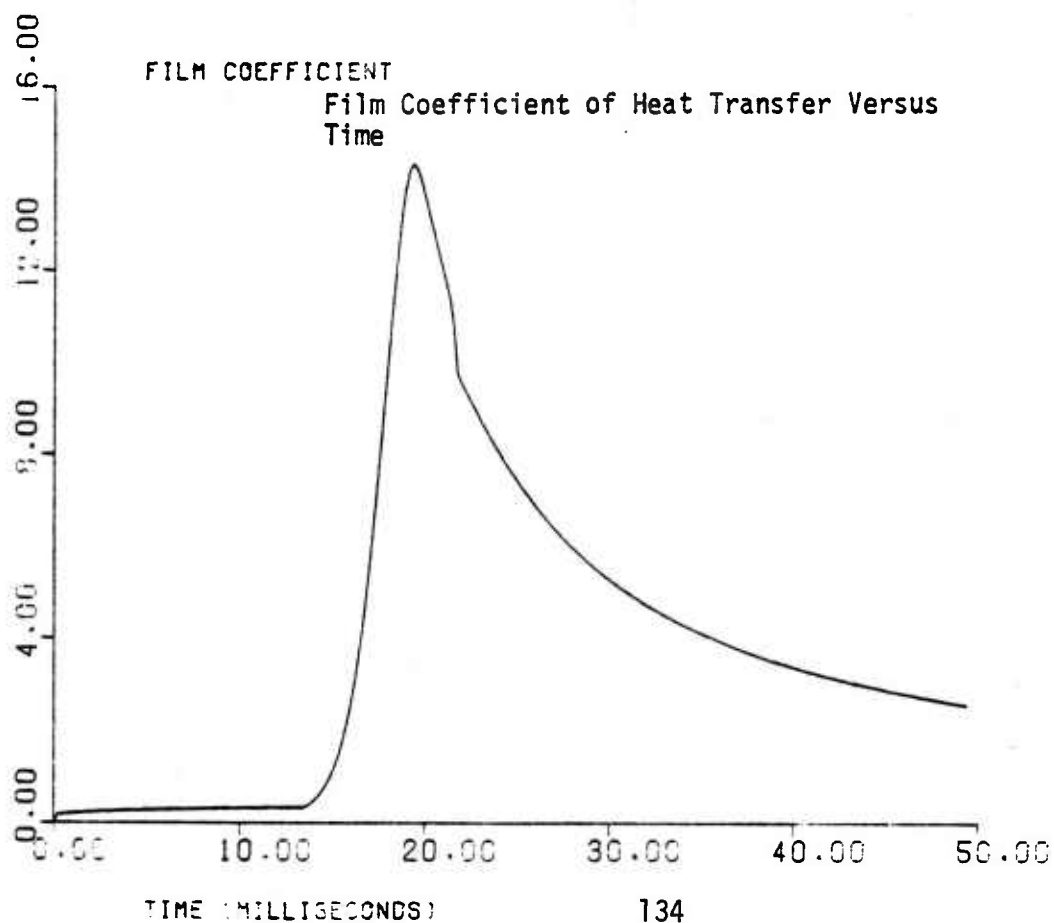
133

INTERIOR BALLISTICS WITH FALLBACK

Cannon: M201
Projectile: M509E1
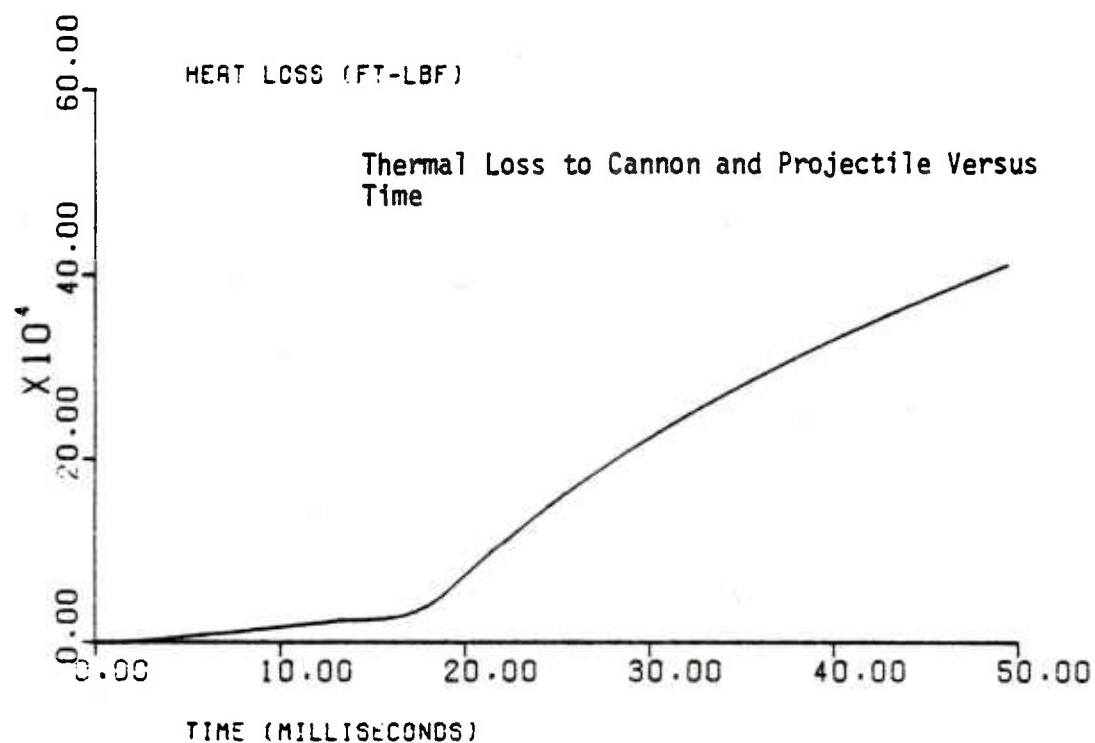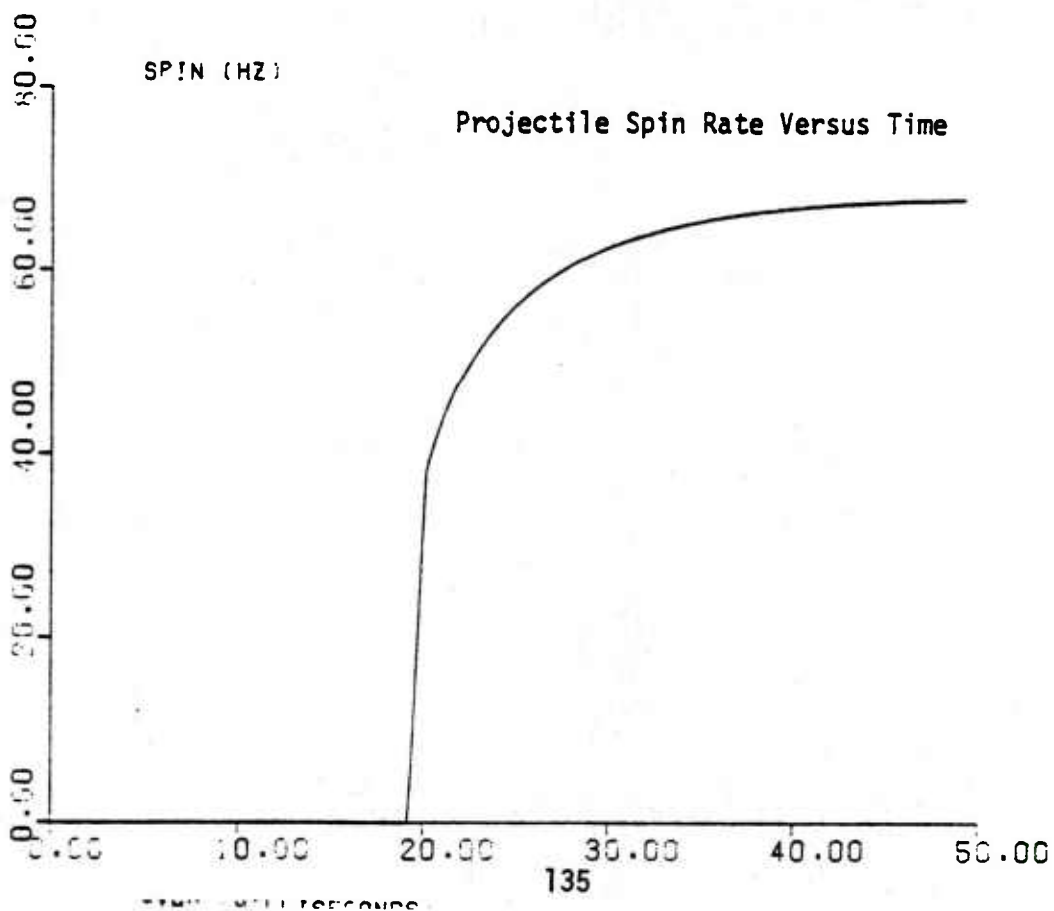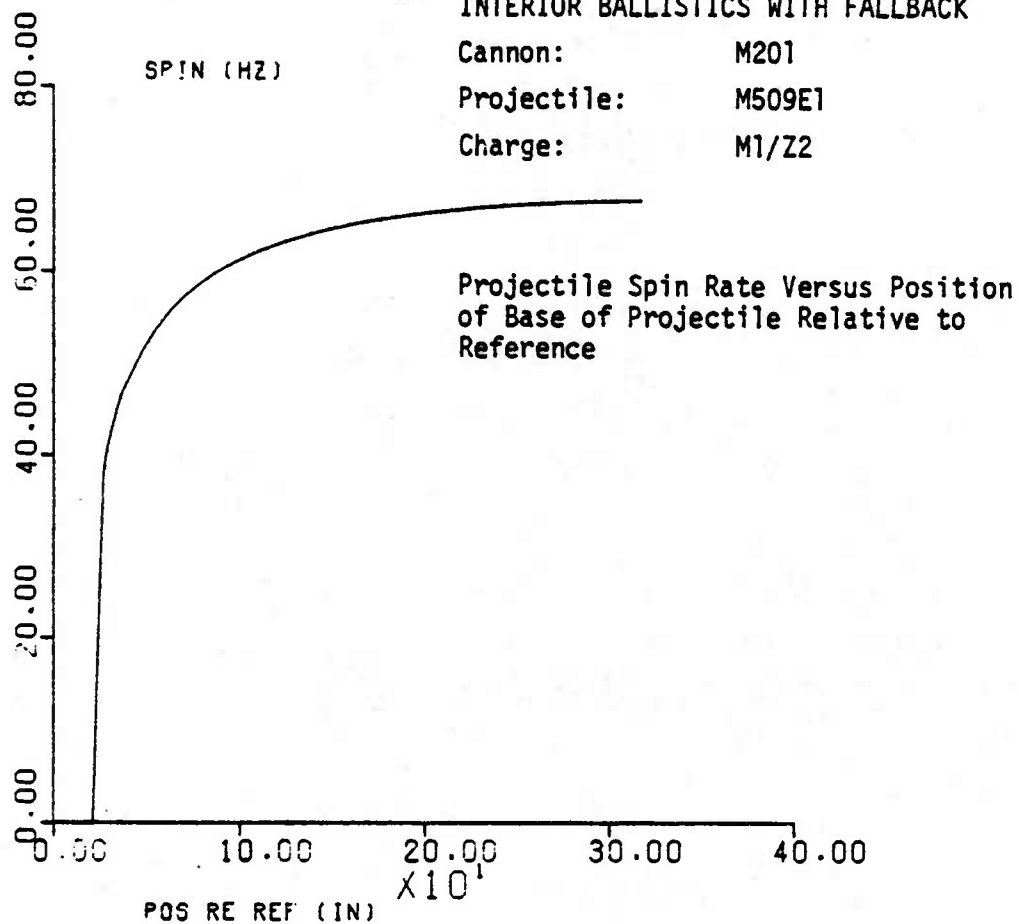Charge: M1/Z2

HEAT LOSS (FT-LBF)

Thermal Loss to Cannon and Projectile Versus
Time

$X10^4$

TIME (MILLISECONDS)

FILM COEFFICIENT

Film Coefficient of Heat Transfer Versus
Time

TIME (MILLISECONDS)   134

INTERIOR BALLISTICS WITH FALLBACK

Cannon:	M201
Projectile:	M509E1
Charge:	M1/Z2

SPIN (HZ)

Projectile Spin Rate Versus Position
of Base of Projectile Relative to
Reference

POS RE REF (IN) $\times 10^1$

SPIN (HZ)

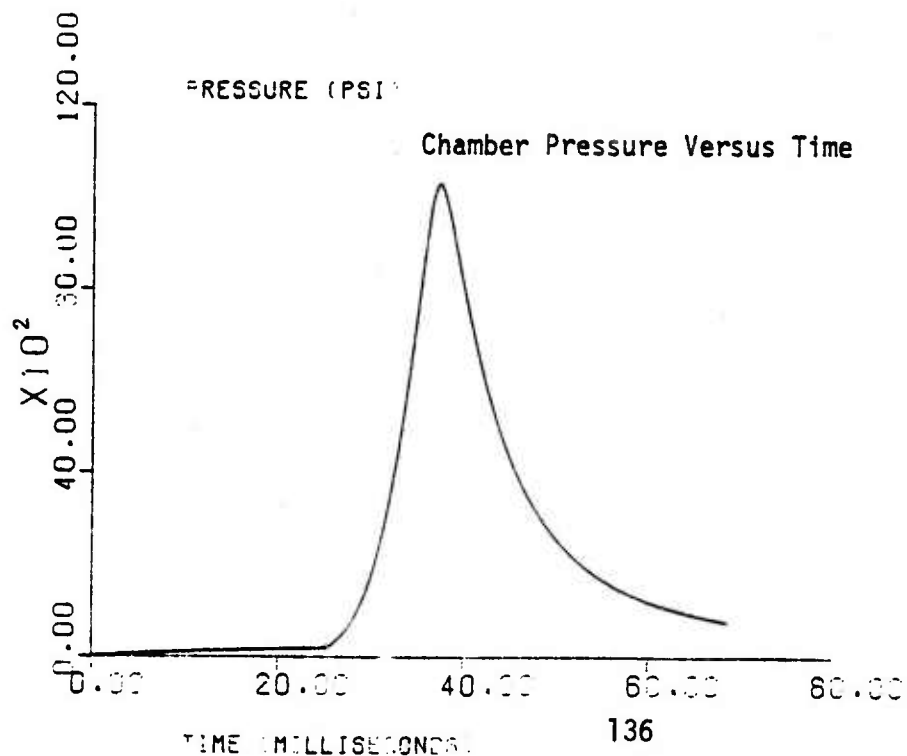Projectile Spin Rate Versus Time

TIME MILLISECONDS

INTERIOR BALLISTICS WITH SEATED PROJECTILE
Cannon: M201
Projectile: M509E1
Charge: M1/Z2

PRESSURE (PSI)

Chamber Pressure Versus Position of
Base of Projectile Relative to Referenced
End of Tube

POS RE REF .IN

PRESSURE (PSI)

Chamber Pressure Versus Time

TIME (MILLISECONDS)
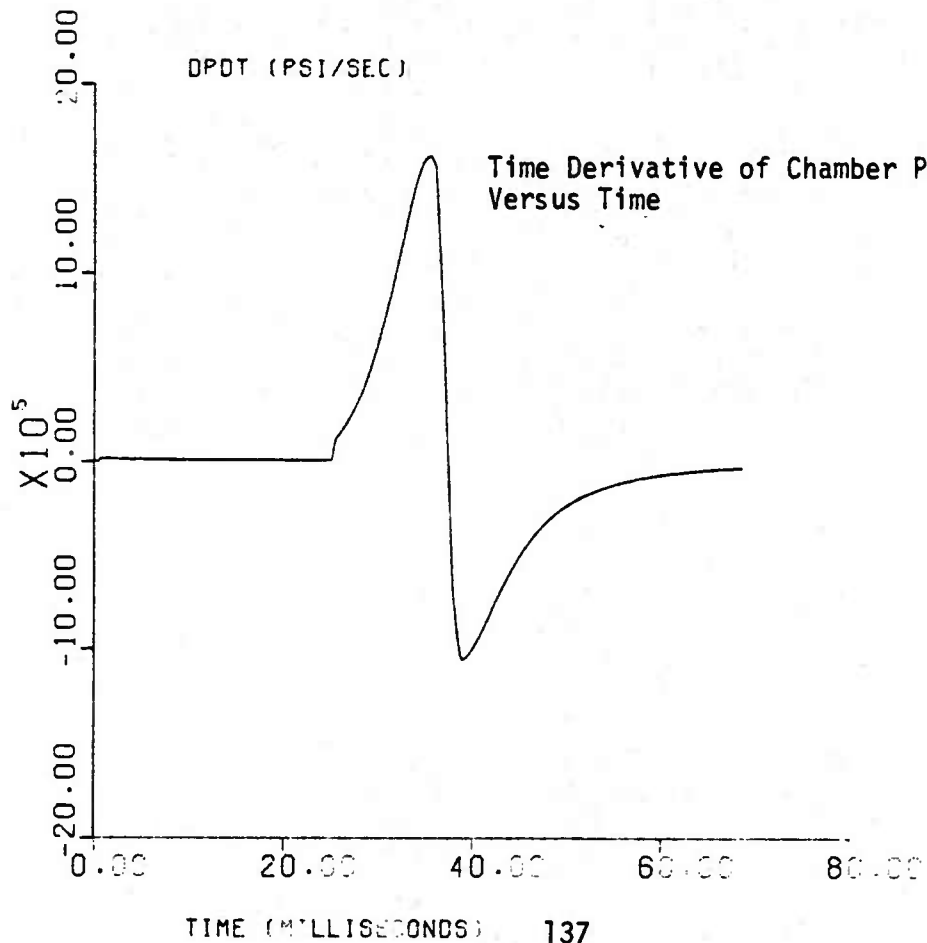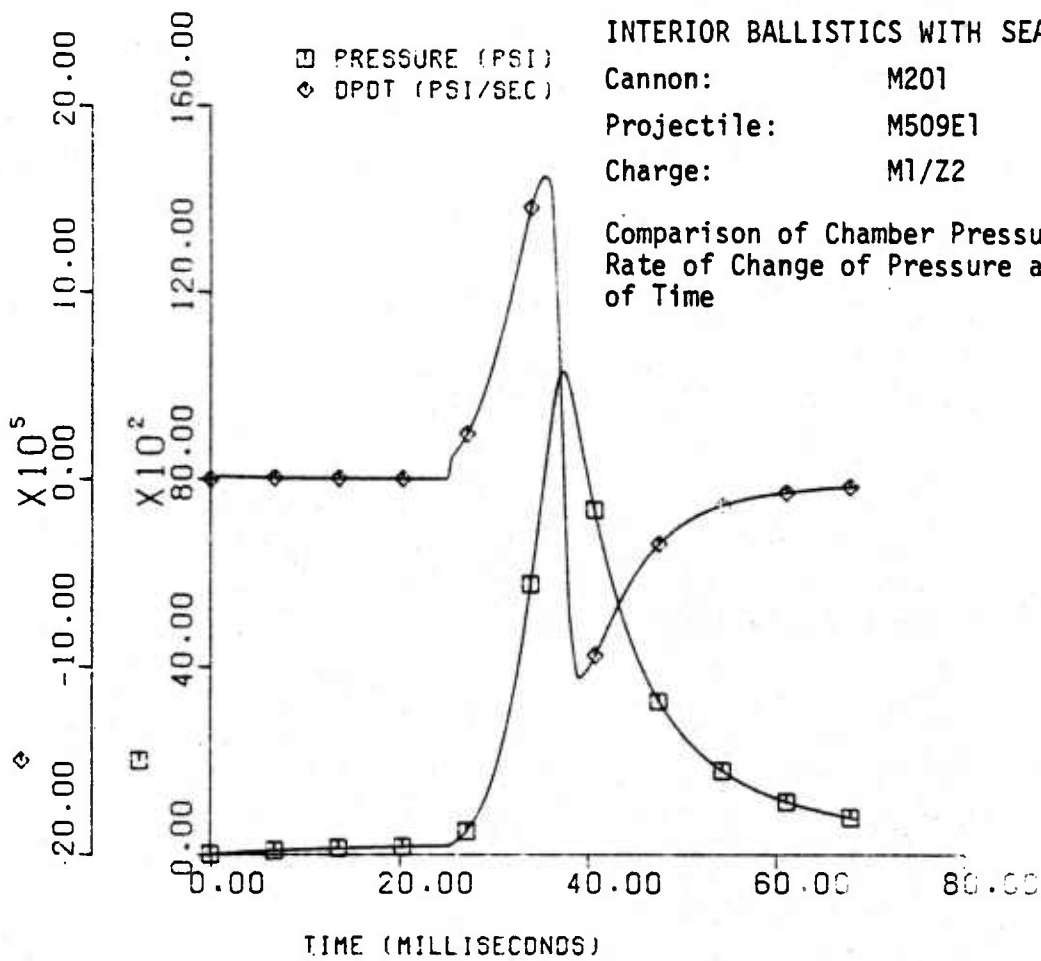
136

INTERIOR BALLISTICS WITH SEATED PROJ.

Cannon: M201
Projectile: M509E1
Charge: M1/Z2

Comparison of Chamber Pressure and
Rate of Change of Pressure as Functions
of Time

Time Derivative of Chamber Pressure
Versus Time

137

INTERIOR BALLISTICS WITH SEATED PROJECTILE

DPDT (PSI/SEC)

Cannon: M201
Projectile: M509E1
Charge: M1/Z2

Time Derivative of Chamber Pressure Versus
Burning Area

$X10^5$

$X10^2$

BURNING AREA (IN**2)

DPDT (PSI/SEC) Time Derivative of Chamber Pressure Versus
Pressure

$X10^5$

$X10^2$

PRESSURE (PSI)

138

INTERIOR BALLISTICS WITH SEATED PROJECTILE

Cannon: M201
Projectile: M509E1
Charge: M1/Z2

☐ ACCELERATION (G)
◇ PRESSURE (PSI)

Comparison of Chamber Pressure and Projectile Acceleration as Functions of Time

TIME (MILLISECONDS)

ACCELERATION (G)

Projectile Acceleration Versus Time

TIME (MILLISECONDS)   139

GRAIN I.D. (AT ENDS) (IN)

INTERIOR BALLISTICS WITH SEATED PROJ.

Cannon: M201
Projectile: M509E1
Charge: M1/Z2

Propellant Grain Inside Diameter at
Grain Ends Versus Time

$X10^{-1}$

TIME (MILLISECONDS)

GRAIN O.D. (IN)

Propellant Grain Outside Diameter
Versus Time

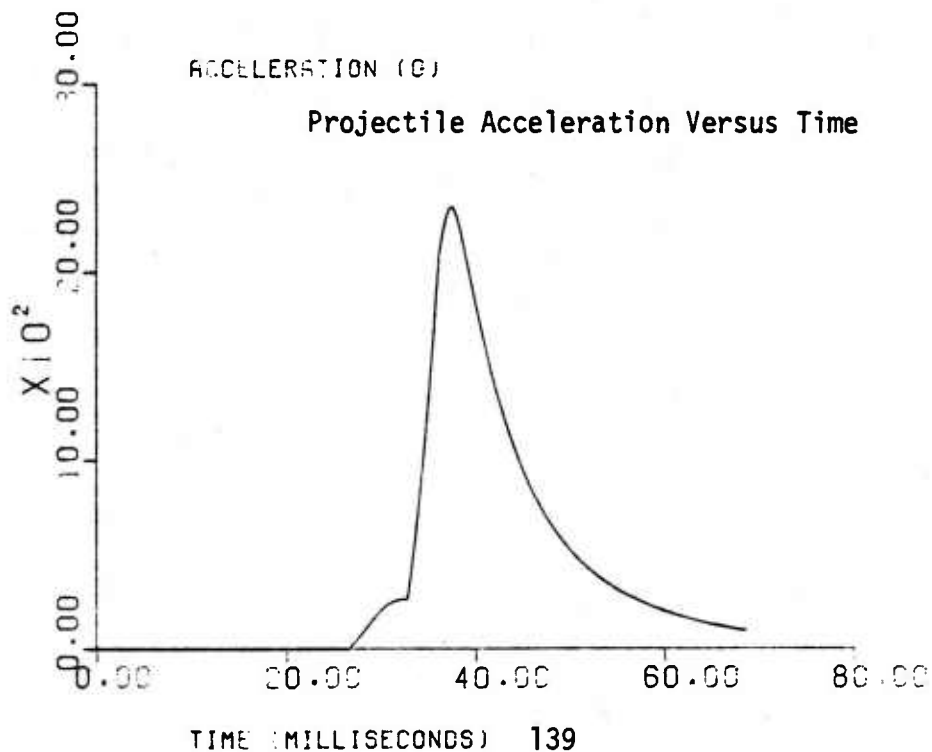$X10^{-1}$

TIME (MILLISECONDS) 140

INTERIOR BALLISTICS WITH SEATED PROJECTILE

Cannon: M201

Projectile: M509E1

Charge: M1/Z2

GRAIN I.D. (AT CNTR) (IN)

Propellant Grain Inside Diameter at Grain
Center Versus Time

TIME (MILLISECONDS)

□ GRAIN O.D (IN)
◇ GRAIN I.D. (AT ENDS) (IN)
✕ GRAIN I.D. (AT CNTR) (IN)

Comparison of Propellant Grain Dimensions
as Functions of Time

TIME (MILLISECONDS)   141

INTERIOR BALLISTICS WITH SEATED PROJECTILE

Cannon: M201
Projectile: M509E1
Charge: M1/Z2

CHG VOLUME (IN**3)

Volume of Unburnt Propellant in Charge
Versus Time

TIME (MILLISECONDS)

BURNING AREA (IN**2)

Burning Area of Charge Versus Time

$\times 10^2$

TIME (MILLISECONDS)

142

INTERIOR BALLISTICS WITH SEATED PROJECTILE
Cannon: M201
Projectile: M509E1
Charge: M1/Z2

MASS LOSS (LBM)

Mass of Gas Lost Past Obturator Versus Time

TIME (MILLISECONDS)

MASS OF GAS (LBM)

Mass of Gas Aft of Projectile Versus Time

TIME (MILLISECONDS)   143

INTERIOR BALLISTICS WITH SEATED PROJ.

VELOCITY (FT/SEC) Cannon: M201

Projectile: M509E1

Charge: M1/Z2

Projectile Velocity Versus Time

TIME (MILLISECONDS)

INTERNAL ENERGY (FT-LBF) Internal Energy in Propellant Gas Versus Time

TIME (MILLISECONDS)

144
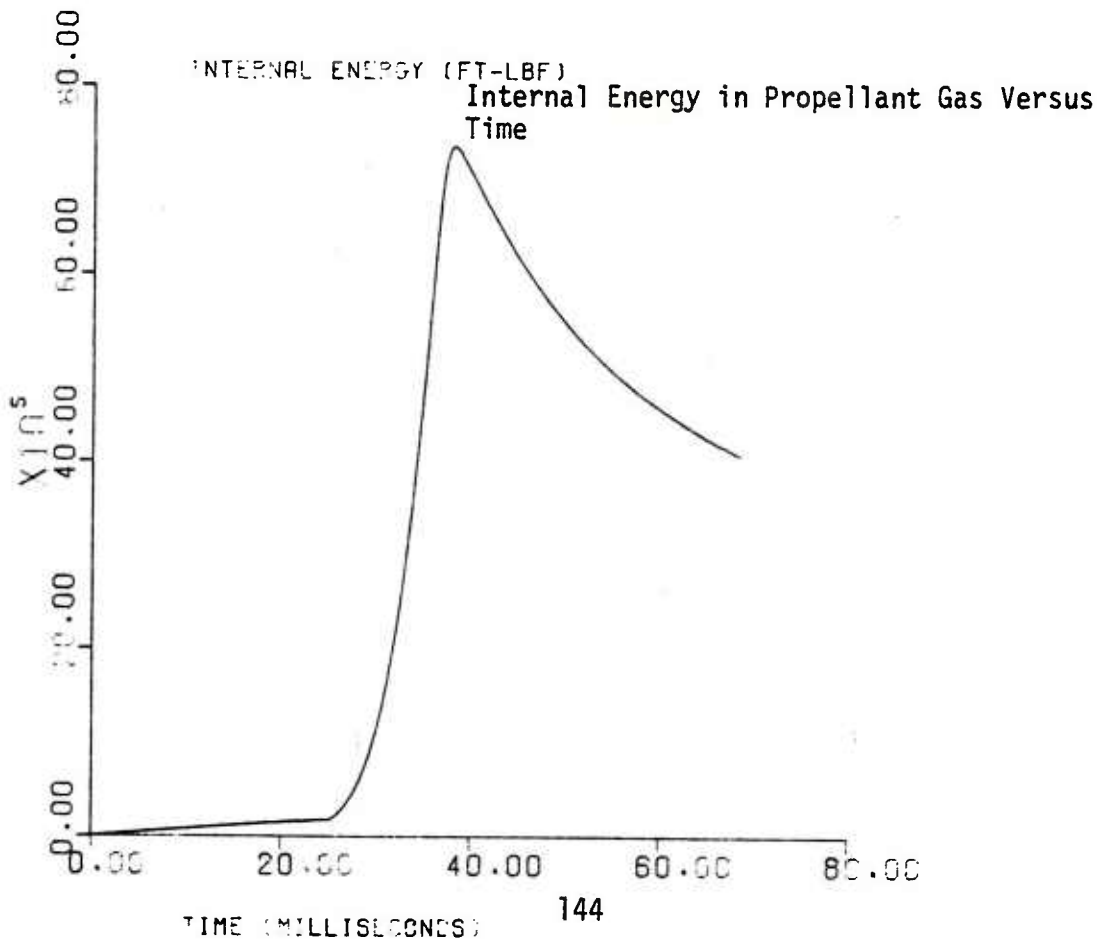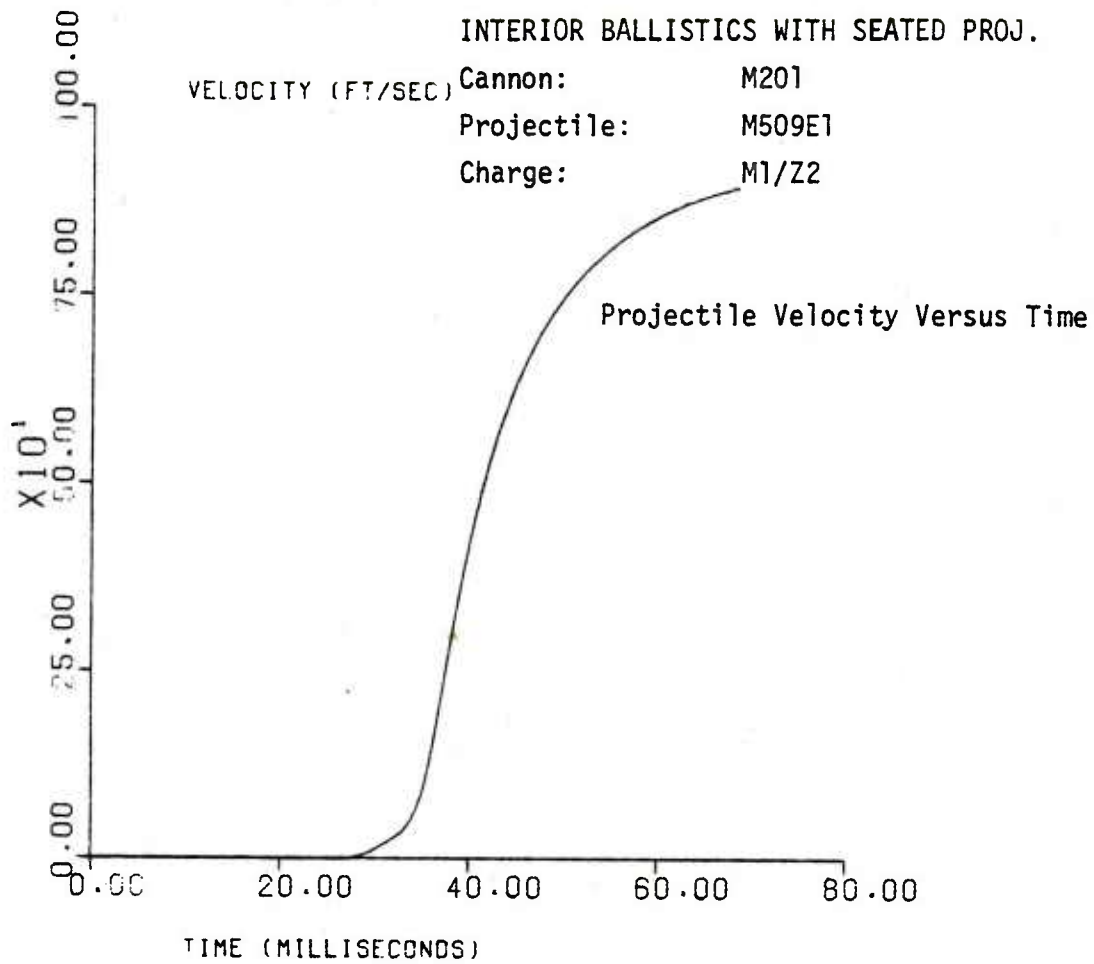
INTERIOR BALLISTICS W/SEATED PROJECTILE

Cannon: M201
Projectile: M509E1
Charge: M1/Z2

VELOCITY (FT/SEC)
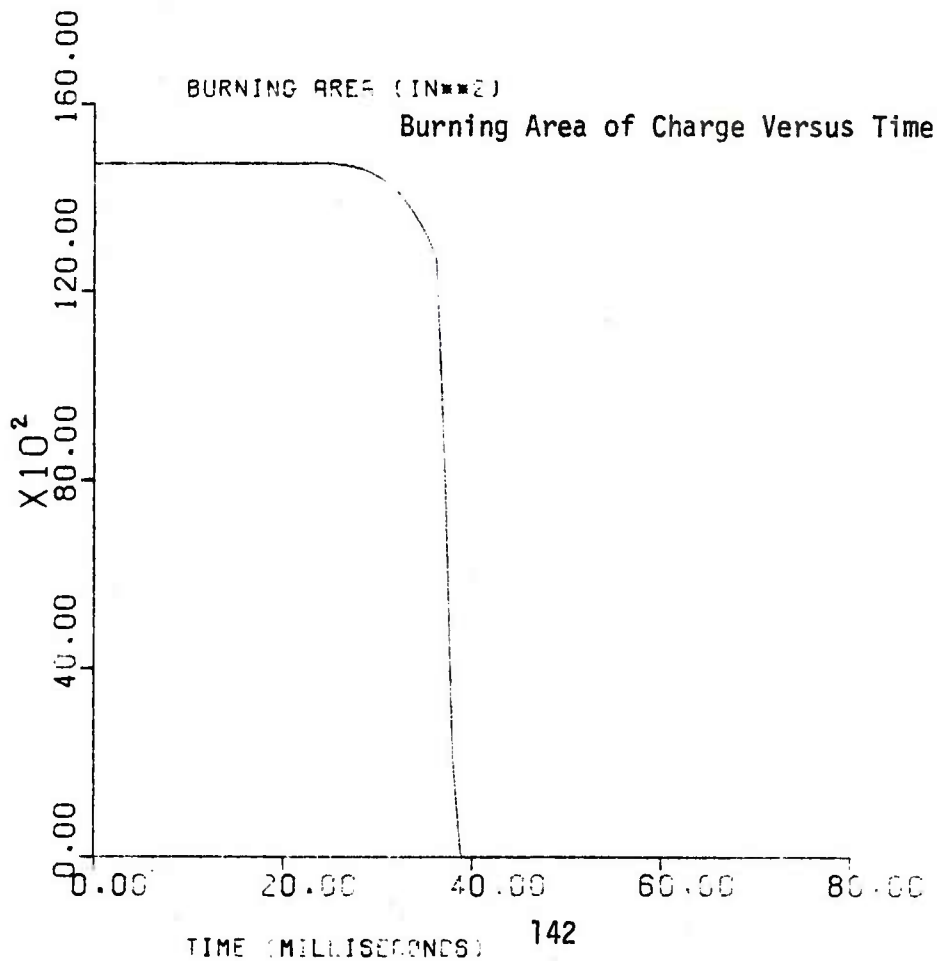
Projectile Velocity Versus Position of
Base of Projectile Relative to Reference

X10¹

POS RE REF (IN)

VELOCITY (FT/SEC)

Projectile Velocity Versus Projectile
Displacement

X10¹

DISPLACEMENT (IN)

145
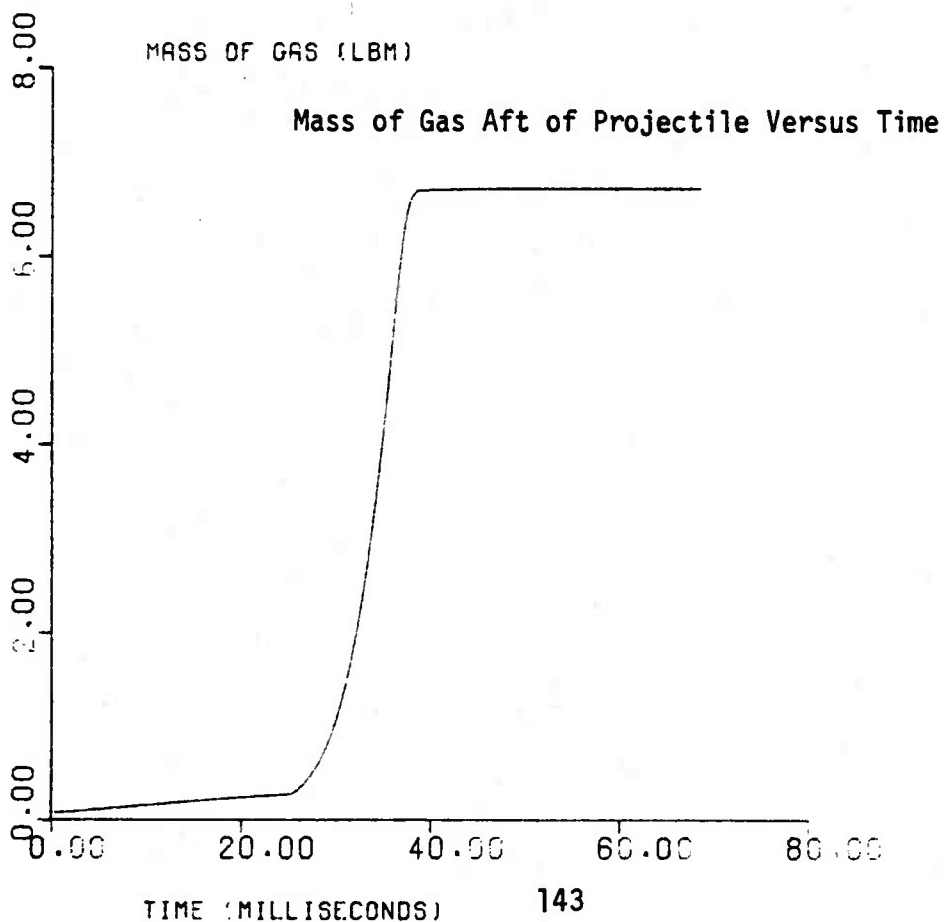
INTERIOR BALLISTICS WITH SEATED PROJECTILE

Cannon: M201

Projectile: M509E1

Charge: M1/Z2

POS RE REF (IN)

Position of Projectile Relative to Reference
Versus Time

TIME (MILLISECONDS)

DISPLACEMENT (IN)

Projectile Displacement Versus Time
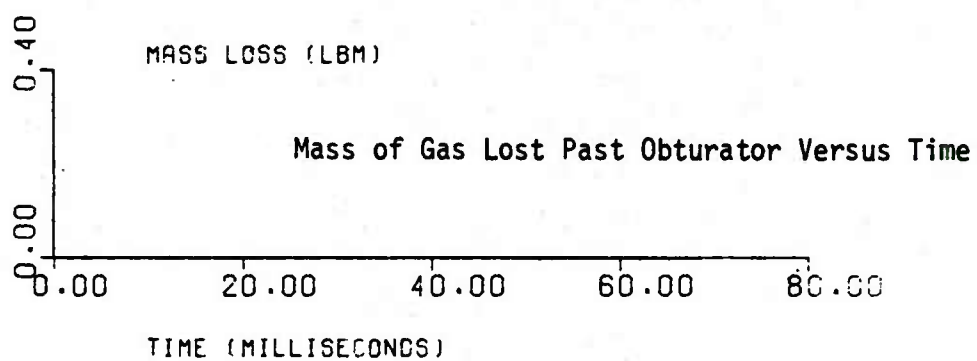
TIME (MILLISECONDS)   146

INTERIOR BALLISTICS WITH SEATED PROJECTILE
Cannon: M201
Projectile: M509E1
Charge: M1/Z2

WALL TEMPERATURE (DEG K)

Chamber Wall Surface Temperature Versus Time.

TEMPERATURE (DEG K)

Space-Mean Temperature of Gas Versus Time.

147

INTERIOR BALLISTICS WITH SEATED PROJECTILE

Cannon: M201
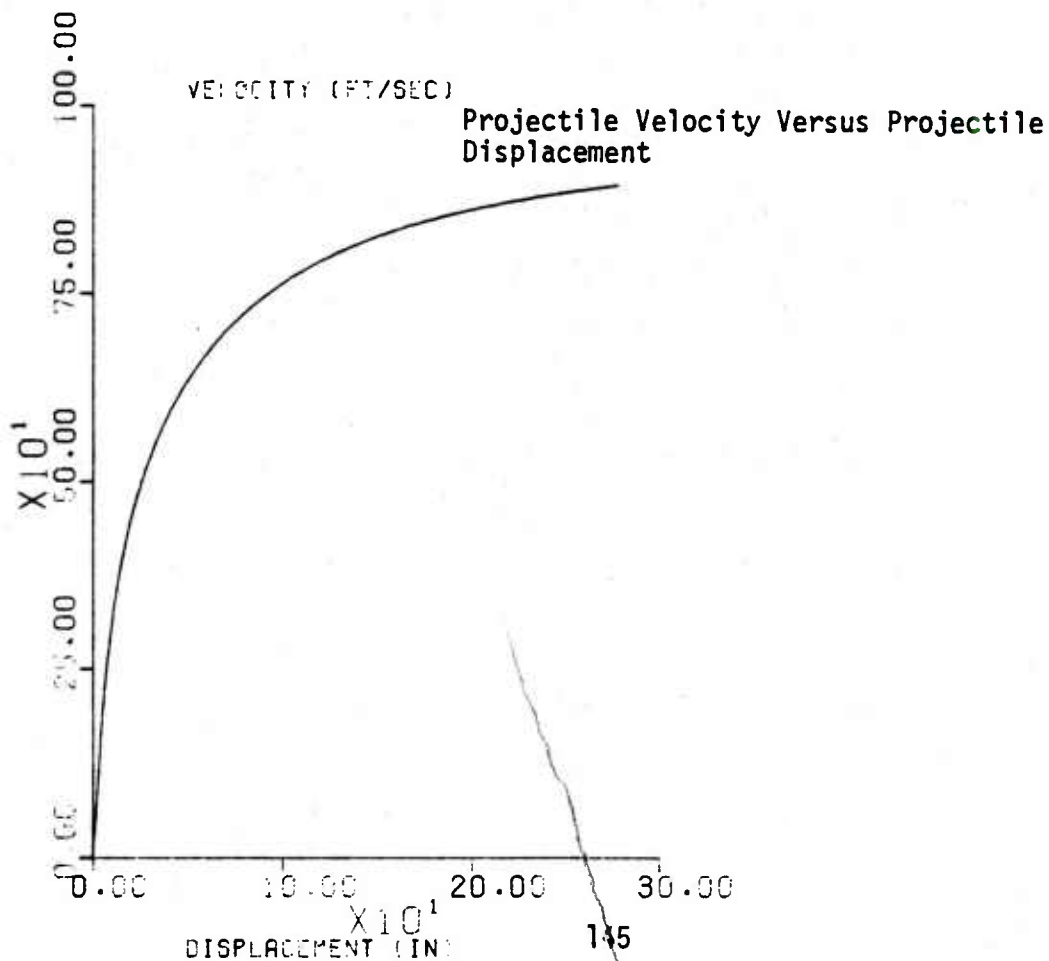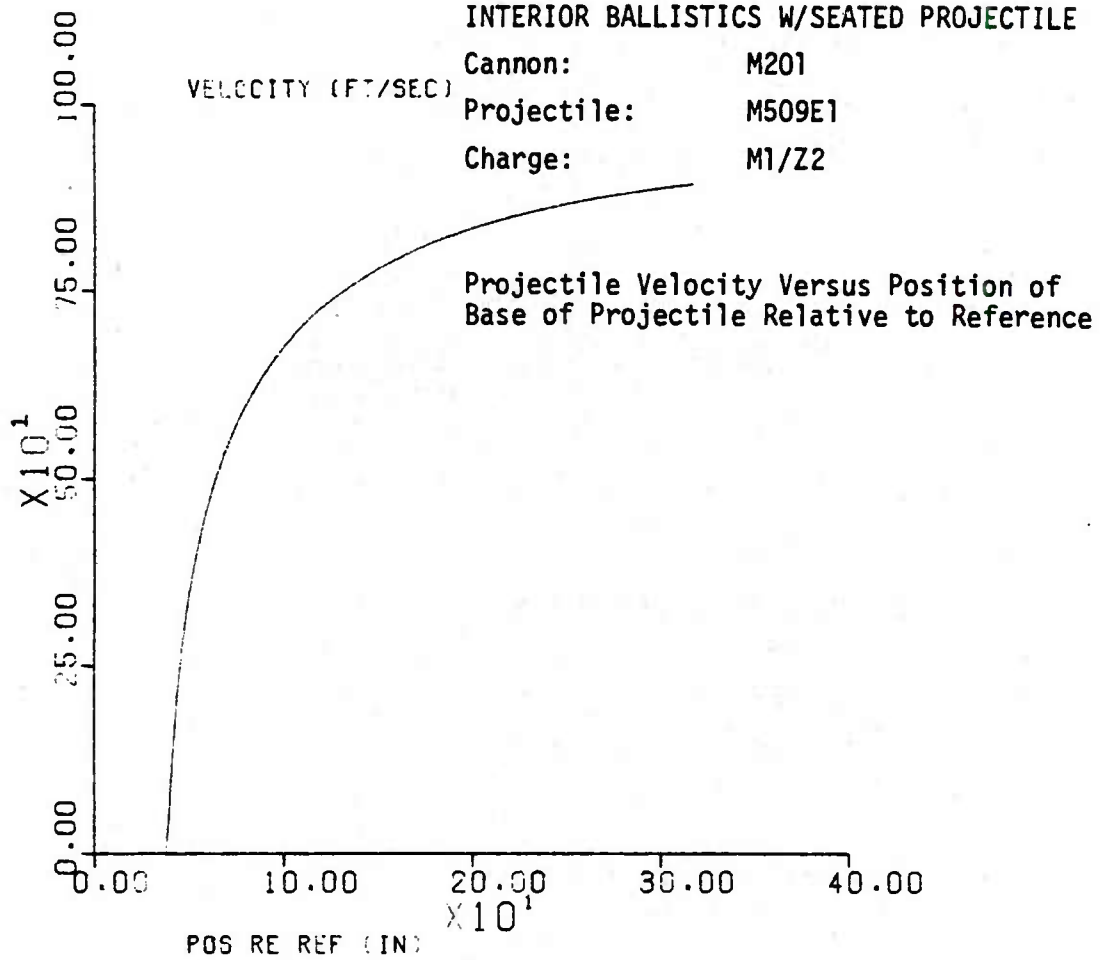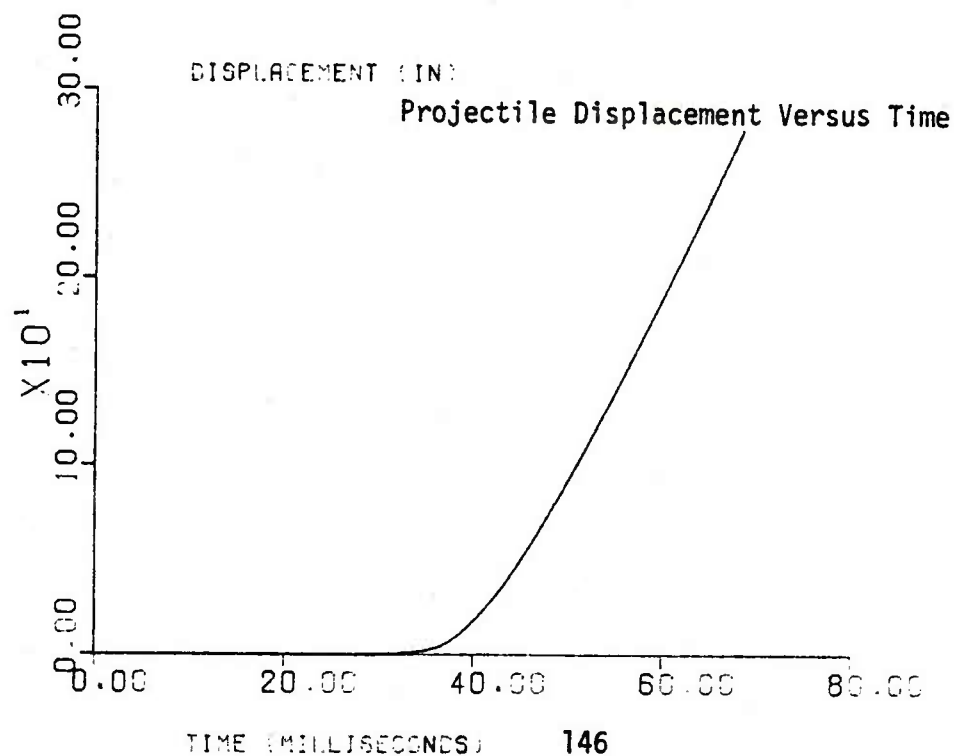
Projectile: M509E1

Charge: M1/Z2

WALL TEMPERATURE (DEG K)

Chamber Wall Surface Temperature Versus
Displacement

$\times 10^1$

$\times 10^1$

DISPLACEMENT (IN)

TOT FWD RESISTANCE (LBF)

Total Forward Resistance Versus Time

$\times 10^3$

TIME (MILLISECONDS)   148

INTERIOR BALLISTICS WITH SEATED PROJECTILE

HEAT LOSS (FT-LBF)

$\times 10^4$

Cannon: M201
Projectile: M509E1
Charge: M1/Z2

Thermal Loss to Cannon and
Projectile Versus Time

TIME (MILLISECONDS)

FILM COEFFICIENT

Film Coefficient of Heat Transfer
Versus Time

TIME (MILLISECONDS)   149

INTERIOR BALLISTICS WITH SEATED PROJECTILE

SPIN (HZ)

Cannon: M201
Projectile: M509E1
Charge: M1/Z2
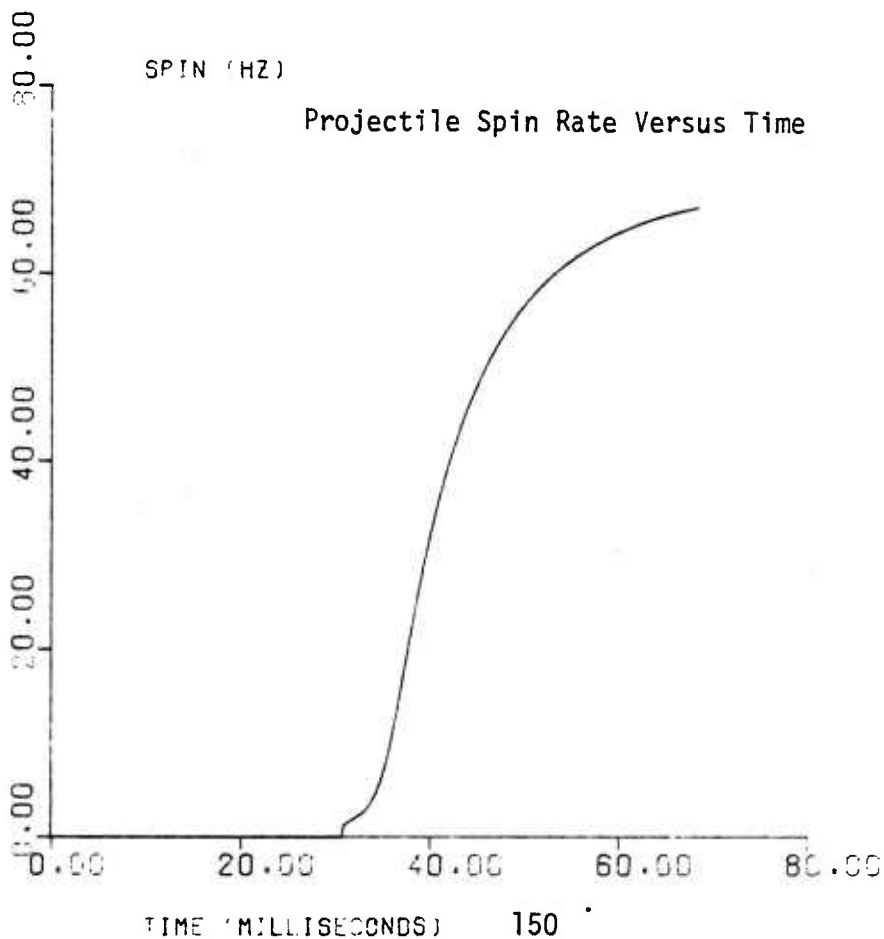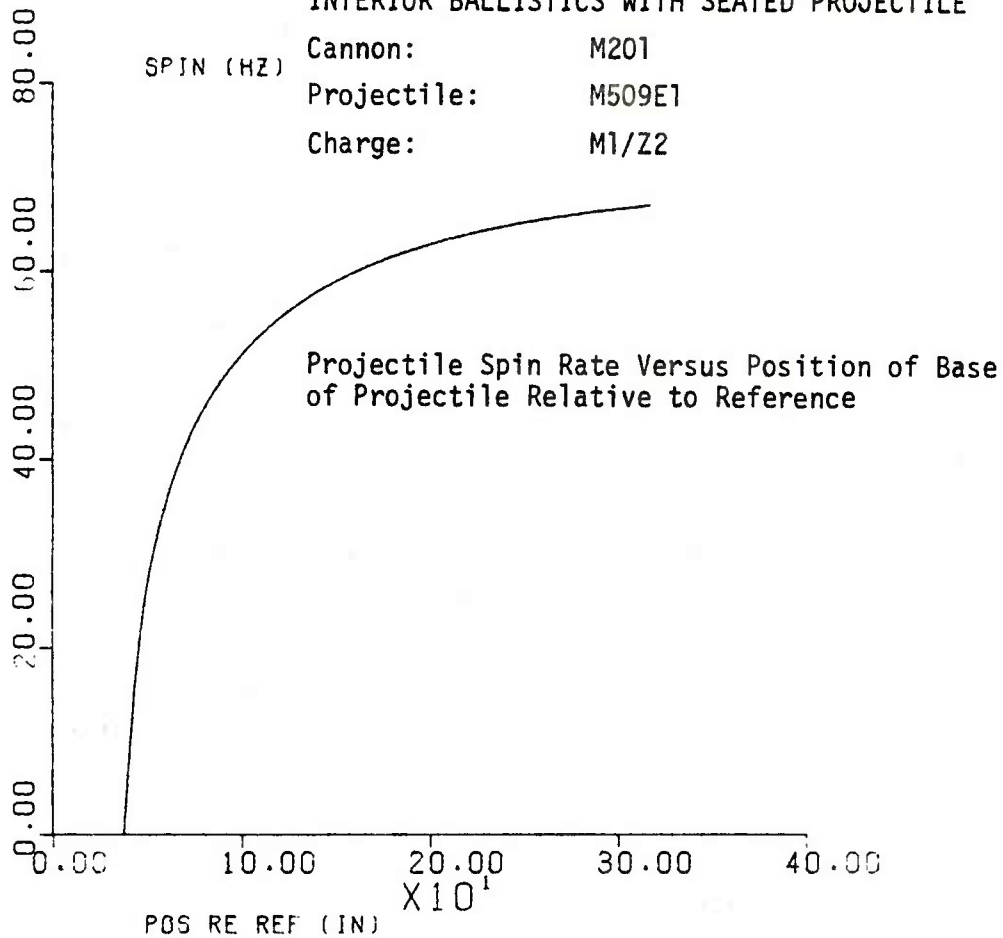
Projectile Spin Rate Versus Position of Base
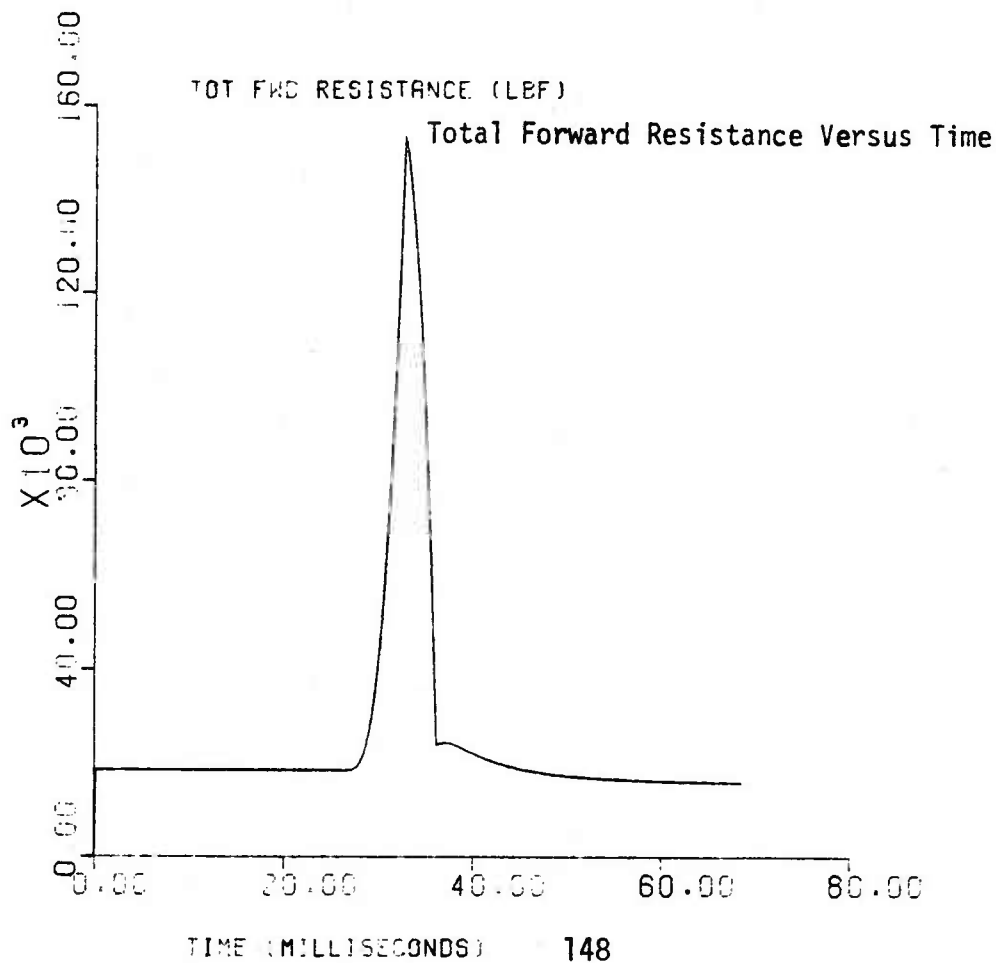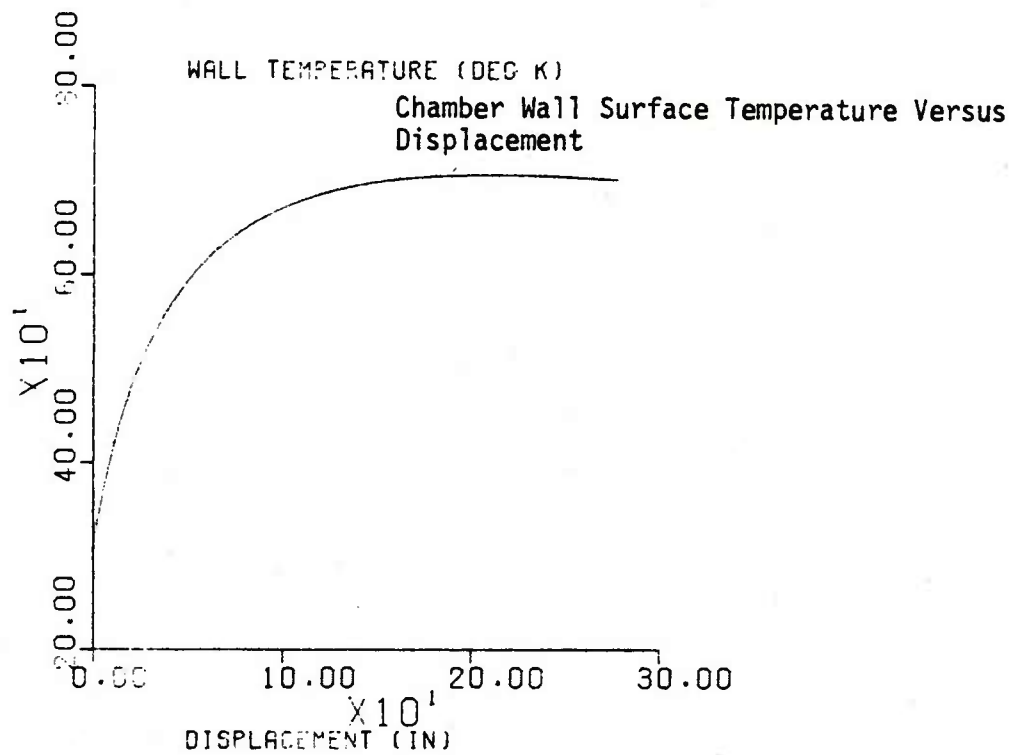of Projectile Relative to Reference

POS RE REF (IN)

SPIN (HZ)

Projectile Spin Rate Versus Time

TIME (MILLISECONDS)   150

APPROXIMATION

FOR THE

STANDARDIZED

CUMULATIVE PRODUCTION COST

USING

LEARNING THEORY

George Schlenker

DRSAR-PEL   2 November 1979

MEMORANDUM FOR RECORD

SUBJECT: Approximation for the Standardized Cumulative Production Cost
          Using Learning Theory

1. Reference:

    a. Handbook ALM-63-3126-H2, US Army Logistic Management Center (ALMC),
issued first by Directorate of Procurement and Production, USAMICOM, title:
Alpha and Omega and the Experience Curve.

    b. CEE Course Handout ALM-63-3126-H1C, US ALMC, title: Learning Curve
Summary.

2. Background

    I recently had the opportunity to attend a course offered by ALMC which
was concerned with cost estimation. During the course, materials were pre-
sented concerning the theory of learning or experience related to product
manufacturing cost. This MFR was stimulated by that course.

3. Where applicable, learning theory is useful in predicting the relation
of manufacturing unit cost (or man hours) of a product to the number of
units produced. Manufacturing experience with missiles and with tanks
and automotive vehicles has shown that the specific reduction of unit cost
with units produced is commodity dependent. However, for a variety of pro-
ducts and over a considerable range of production quantity, the expected
direct cost of manufacturing the 2n th unit is proportional to the unit
cost for the n th unit for n an integer up to some limit, where the constant
of proportionality, s, is called the "slope" of the learning curve and is
frequently expressed as a percentage.* Thus, the unit cost for the n th
unit, u(n), is given by

$$u(2n) = s\,u(n), \quad 0 < s \leq 1 \quad . \tag{1}$$

This result implies

$$u(n) = An^B, \tag{2}$$

_____

*Production experience with missiles indicates a 79 to 84% slope and with
 automotive and tank vehicles a 92 to 96% slope.

153

with A the first unit cost and

$$B = \log(s)/\log(2) \quad . \tag{3}$$

From (2) the expected total cost of manufacturing a lot of products starting with the n_1 th and proceeding through the n_2 th is given by

$$\text{total lot cost} = \sum_{n_1}^{n_2} u(n) \tag{4}$$

or

$$= A[\sum_{n=1}^{n_2} n^B - \sum_{n=1}^{n_1-1} n^B] \quad . \tag{5}$$

The sum terms on the right in equation (5) have been named cumulative total factors for the n_2 th and $n_1 - 1$ th quantities. Because the term

$$Q(n) = \sum_{n=1}^{N} n^B \tag{6}$$

represents the cumulative production cost from the first through the N th unit standardized by division by the first unit cost, it is here called the standardized cumulative cost. With this notation equation (5) becomes

$$\text{total lot cost}/A = Q(n_2) - Q(n_1-1) \quad . \tag{7}$$

4. Applications

A variety of applications of (7) are possible. For example, one may have prior estimates of A and B and wish to calculate the total lot cost or average lot cost --

$$\text{total lot cost}/(n_2 - n_1 + 1) \quad .$$

Alternatively, one may have a total lot cost and an estimate of B from prior experience and wish to estimate A. Finally, one may wish to estimate the learning slope B from values of total lot cost and first unit cost. Additionally, the "algebraic lot midpoint", i.e., the value of n (=K) such that

$$AK^B$$

is the average lot cost, is obtained from (7) via the equation

$$K^B = \frac{Q(n_2) - Q(n_1-1)}{n_2 - n_1 + 1} = \frac{\Delta Q}{n_2 - n_1 + 1} \quad . \tag{8}$$

154

5. Because of the significance of the standardized cumulative cost and the effort to calculate it directly from (6), this quantity has been tabulated for a large set of the parameters B (or s) and n. Some examples of tables are given in Reference a. Without recourse to tables or a computer, one can calculate Q(n) using a numerical approximation.

6. Approximations for Q(n)

One approximations for Q(n) is obtained directly from the approximation for the algebraic lot midpoint, K_1, proposed by ALMC in Reference b:

$$K_1 = \frac{F + L + 2\sqrt{FL}}{4} ,$$ (9)

with

F = first unit in the lot

L = last unit in the lot.

With F = 1 and L = n and using the definition of algebraic lot midpoint, the ALMC approximation for Q(n) is

$$\hat{Q}_1(n) = nK_1^B$$

$$= n[(1 + n + 2\sqrt{n})/4]^B .$$ (10)

7. Another approximation, proposed by the author, is derived by treating n as a continuous variable and by solving the integral analog of equation (6). This approximation, designated $Q_2(n)$, has the form

$$\hat{Q}_2(n) = (B + 1)^{-1}[(n + 0.5)^{B+1} - 0.5^{B+1}] .$$ (11)

The presence of the term 0.5 as a correction to n is motivated by the need for a symmetric integral approximation to a discrete variable in the same spirit as the gaussian distribution function approximates a binomial distribution.

8. Using the approximation $\hat{Q}_2(n)$, the standardized cumulative cost of manufacturing a product from the n_1 th through the n_2 th units is given approximately by

$$\Delta Q \cong (B + 1)^{-1}[(n_2 + 0.5)^{B+1} - (n_1 - 0.5)^{B+1}] .$$ (12)

155

SUBJECT: Approximation for the Standardized Cumulative Production Cost
           Using Learning Theory

In the limit as B approaches zero, i.e., as no learning occurs,

$\Delta Q \Rightarrow n_2 - n_1 + 1$,

which is exactly what would be expected. Further, the standardized average unit cost of manufacturing n units from the n_1 th through the n_2 th:

$n_2 = n_1 + n - 1$

is given by

$$\text{lot std avg unit cost} \cong \frac{(n_2 + 0.5)^{B+1} - (n_1 - 0.5)^{B+1}}{(B + 1)(n_2 - n_1 + 1)} \quad . \quad (13)$$

9. Numerical Comparisons of Accuracy

With the availability of scientific calculators the two approximations given in (10) and (11) can be easily carried out. Some numerical examples are provided in Table 1. The range of slope values shown there is representative of a variety of products. Although lot sizes, n, may exceed 1000 units, Table 1 does not display $Q(n)$ for larger values since the theoretical or ideal learning may have leveled off by that point. Note that for values of n less than about 20, $\hat{Q}_1$ and $\hat{Q}_2$ are equally good approximations. However, for $n \gtrsim 100$, $\hat{Q}_2$ is distinctly superior to the ALMC approximation, $\hat{Q}_1$. Note also that the error in $\hat{Q}_1(100)$ is about 2.4% whereas that of $\hat{Q}_2(100)$ is only 0.02% for a 90% slope. The approximation $\hat{Q}_2(n)$ improves as n increases, while $\hat{Q}_1(n)$ becomes a progressively poorer approximation with increasing n. The foregoing results are generally valid for learning slopes above 80%.

10. Summary and Recommendations

It has been shown that application of learning theory requires the use of the standardized cumulative cost (sometimes called the cumulative total). To retain tables of this quantity is unnecessary if one has use of a presently commonplace, scientific calculator. The use of an approximation for $Q(n)$ seems justified since the error of the approximation for the best approximation $\hat{Q}_2(n)$ is quite small relative to other errors. Since $\hat{Q}_2$ is just as

SUBJECT: Approximation for the Standardized Cumulative Production Cost
           Using Learning Theory

easy to calculate as $\hat{Q}_1$, and since it is generally more accurate, $\hat{Q}_2$ is recommended. Further, $\hat{Q}_1$ is to be avoided for n in excess of 200 because of a sizeable error of approximation.

GEORGE SCHLENKER
Operations Research Analyst

1 Incl
Table 1

TABLE 1. COMPARISON OF APPROXIMATIONS FOR THE STANDARDIZED CUMULATIVE MFG COST WITH THE EXACT VALUE FOR SEVERAL LEARNING CURVES

Percent Learning Slope	B*	Number of Units	Cumulative Cost Approx (1) $\hat{Q}_1$	(2) $\hat{Q}_2$	Exact Value	(3)
80	-0.321928	5	3.67	3.76	3.74	
		10	6.24	6.34	6.32	
		20	10.46	10.51	10.48	
		50	20.36	20.15	20.12	
		100	33.37	32.68	32.65	
		200	54.32	52.75	52.72	
		1000	165.70	158.70	158.67	
85	-0.234465	5	3.99	4.05	4.03	
		10	7.09	7.13	7.12	
		20	12.48	12.42	12.40	
		50	25.99	25.53	25.51	
		100	44.96	43.77	43.75	
		200	77.40	74.81	74.79	
		1000	270.04	257.94	257.91	
90	-0.152003	5	4.32	4.35	4.34	
		10	8.00	8.00	7.99	
		20	14.73	14.62	14.61	
		50	32.72	32.15	32.14	
		100	59.56	58.15	58.14	
		200	108.08	104.98	104.96	
		1000	427.95	412.18	412.17	
95	-0.0740009	5	4.66	4.67	4.66	
		10	8.97	8.96	8.95	
		20	17.23	17.14	17.13	
		50	40.67	40.23	40.22	
		100	77.70	76.59	76.58	
		200	148.22	145.70	145.69	
		1000	661.53	647.45	647.42	

Notes:

*$B = \log_{10}(\text{slope})/\log_{10}(2)$

(1) Cumulative using the ALMC algebraic lot midpoint is $n[\frac{1 + n + 2\sqrt{n}}{4}]^B$

(2) $\hat{Q}_2 = (B + 1)^{-1}[(n + 0.5)^{B+1} - 0.5^{B+1}]$

(3) $Q = \Sigma_{i=1}^{n} i^B$

Incl 1

DISTRIBUTION LIST

1	HQDA(DAMO-ZA) WASH DC 20310
1	HQDA(DAMA-CSZ-A) WASH DC 20310
1	HQDA(DALO-SMZ) WASH DC 20310

Commander
US Army Materiel Development and Readiness Command

1	ATTN: DRCRE
1	DRCPA-S
1	DRCDMR/LTG H. F. Hardin, Jr.

5001 Eisenhower Avenue
Alexandria, VA 22333

Commander
US Army Armament Materiel Readiness Command

1	ATTN: DRSAR-CG
1	DRSAR-DCG
1	DRSAR-LC
1	DRSAR-LE
1	DRSAR-LEP-L (Tech Library)
1	DRSAR-CP
10	DRSAR-PE
1	DRSAR-DA
1	DRSAR-HA
1	DRSAR-PC
1	DRSAR-PD
1	DRSAR-IR
1	DRSAR-OP
1	DRSAR-QA
1	DRSAR-IS
1	DRSAR-MA
1	DRSAR-MM
1	DRSAR-AS
1	DRSAR-SF

Rock Island, IL 61299

1	Commander US Army Materiel Development and Readiness Command Washington Field Office ATTN: DRSAR-AA 5001 Eisenhower Avenue Alexandria, VA 22333

Commander
US Army Armament Research and Development Command

1	ATTN: DRDAR-SEA
1	DRDAR-SCS-M
1	DRDAR-LCS-E

Dover, NJ 07801

159

NO. OF COPIES	
1	Commander US Army Development and Readiness Command Office of the Project Manager for Selected Ammunition ATTN: DRCPM-SA Dover, NJ 07801
1	DIVAD Manager Logistic Support Office ATTN: DRCPM-ADG Rock Island, IL 61299
1	Product Manager for Production Base Modification and Expansion ATTN: DRCPM-PBM Dover, NJ 07801
1	Product Manager for Advanced Attack Helicopter Systems US Army Aviation Systems Command St. Louis, MO 63166
1	Product Manager for AH-1 Cobra Series Aircraft US Army Development and Readiness Command P.O. Box 209 St. Louis, MO 63166
1	Commander Rock Island Arsenal ATTN: SARRI-CO Rock Island, IL 61299
1	Commander Watervliet Arsenal ATTN: SARWV-CO Watervliet, NY 12189
1	Commander Human Engineering Laboratories ATTN: DRXHE-D Aberdeen Proving Ground, MD 21005
1 1	Director US Army Materiel Systems Analysis Activity ATTN: DRXSY-DL/Mr. Gilbert DRXSY-MP/Mr. Cohen Aberdeen Proving Ground, MD 21005

DISTRIBUTION LIST (Cont)

1   Commander
           US Army Communications and Electronics Materiel Readiness Command
           ATTN: DRSEL-PL-SA
           Fort Monmouth, NJ 07703

1   Commander
           US Army Electronics Research and Development Command
           ATTN: DRDEL-ST-SE
           Adelphi, MD 20783

           Commander
           US Army Missile Command
1   ATTN: DRSMI-D
1   DRSMI-DS (R&D)
           Redstone Arsenal, AL 35809

1   Commander
           US Army Communications Research and Development Command
           ATTN: DRDCO-PPA-SA
           Fort Monmouth, NJ 07703

1   Commander
           US Army Operational Test and Evaluation Agency
           ATTN: CSTE-ED
           5600 Columbia Pike
           Falls Church, VA 22041

1   Commander
           US Army Tank-Automotive Materiel and Readiness Command
           ATTN: DRSTA-S
           Warren, MI 48090

1   Commander
           US Army Tank-Automotive Research and Development Command
           ATTN: DRDTA-V
           Warren, MI 48090

1   Commander
           US Army Troop Support and Aviation Materiel Readiness Command
           ATTN: DRDAV-BC
           P.O. Box 209
           St. Louis, MO 63120

1   Project Manager for Cannon Artillery Weapons Systems
           ATTN: DRCPM-CAWS
           Dover, NJ 07801

DISTRIBUTION LIST (Cont)

1	Commander US Army Mobility Equipment Research and Development Command ATTN: DRDME-O Fort Belvoir, VA 22060
1	Commandant US Army Field Artillery Center Fort Sill, OK 73503
1	Commandant US Army Infantry School Fort Benning, GA 31905
1	Commander US Army Missile and Munitions Center and School Redstone Arsenal, AL 35809
1	Commandant US Army Air Defense School Fort Bliss, TX 79916
1	Director US Army Management Engineering Training Agency ATTN: DRXOM-QA Rock Island, IL 61299
2	Director US Army TRADOC Systems Analysis Activity ATTN: ATAA-SL (Tech Lib) White Sands Missile Range White Sands, NM 88002
1	Director Advanced Research Projects Agency 1400 Wilson Boulevard Arlington, VA 22209
1	Commander Defense Logistics Studies Information Exchange Fort Lee, VA 23801
1	Commander US Army Logistics Center ATTN: ATCL-S Fort Lee, VA 23801
1	Director US Army Materiel Development and Readiness Command Ammunition Center ATTN: SARAC-DO Savanna, IL 61074

DISTRIBUTION LIST (Cont)

1
Commander
US Army Test and Evaluation Command
ATTN: DRSTE-SY
Aberdeen Proving Ground, MD 21005

1
Director
US Army Inventory Research Office
ATTN: DRXMC-IRO
Room 800, Custom House
2nd & Chestnut Streets
Philadelphia, PA 19106

12
Defense Documentation Center
Cameron Station
Alexandria, VA 22314